~~ARR No. 5C01~~

NATIONAL ADVISORY COMMITTEE FOR AERONAUTICS

WARTIME REPORT

ORIGINALLY ISSUED

July 1945 as
Advance Restricted Report 5C01

AN EXPERIMENTAL INVESTIGATION OF THE EFFECT OF PROPELLERS USED AS AERODYNAMIC BRAKES ON STABILITY AND CONTROL

By Victor I. Stevens, George B. McCullough,
and Frederick H. Hanson

Ames Aeronautical Laboratory
Moffett Field, California

NACA

WASHINGTON

NACA ARR No. 5C01

NATIONAL ADVISORY COMMITTEE FOR AERONAUTICS

ADVANCE RESTRICTED REPORT

AN EXPERIMENTAL INVESTIGATION OF THE EFFECT ON PROPELLERS USED AS AERODYNAMIC BRAKES ON STABILITY AND CONTROL

By Victor I. Stevens, George B. McCullough, and Frederick H. Hanson

SUMMARY

Tests were made of a model representative of a single-engine tractor-type airplane for the purpose of determining the stability and control effects of a propeller used as an aerodynamic brake. The tests were made with single- and dual-rotation propellers to show the effect of type of propeller rotation, and with positive thrust to provide basic data with which to compare the effects of negative thrust. Four configurations of the model were used to give the effects of tilting the propeller thrust axis down 5°, raising the horizontal tail, and combining both tilt and raised tail. Results of the tests are reported herein.

The effects of negative thrust were found to be significant. The longitudinal stability was increased because of the loss of wing lift and increase of the angle of attack of the tail. Directional stability and both longitudinal and directional control were decreased because of the reduced velocity at the tail. These effects are moderate for moderate braking but become pronounced with full-power braking, particularly at high values of lift coefficient.

The effects of model configuration changes were small when compared with the over-all effects of negative-thrust operation; however, improved stability and control characteristics were exhibited by the model with the tilted thrust axis. Raising the horizontal tail improved the longitudinal

characteristics, but was detrimental to directional characteristics. The use of a dual-rotation propeller reduced the directional trim charges resulting from the braking operation.

A prototype airplane was assumed and handling qualities were computed and analyzed for normal (positive thrust) and braking operation with full and partial power. The results of these analyses are presented for the longitudinal characteristics in steady and accelerated flight, and for the directional characteristics in high- and low-speed flight. It was found that by limiting the power output of the engine (assuming the constant-speed propeller will function in the range of blade angles required for negative thrust) the stability and control characteristics may be held within the limits required for safe operation. Braking with full power, particularly at low speeds, is dangerous, but braking with very small power output is satisfactory from the standpoint of control. The amount of braking produced with zero power output is equal to or better than that produced by conventional spoiler-type brakes.

INTRODUCTION

Modern aerial combat experience has demonstrated the need of a device to produce rapid deceleration of certain tactical-type aircraft for the following purposes: (1) to allow more time for aiming and shooting at a slow-moving target after it has been overtaken; (2) to reduce the time required to slow down for torpedo launching; and (3) to limit the maximum speed in a dive. Although not covered in this report, a fourth possible use of a powerful decelerating device is to shorten the landing run of an airplane after it has made contact with the ground.

Previous tests of a model equipped with flap- or spoiler-type aerodynamic brakes have shown this type to be subject to several undesirable features: (1) change of trim of the airplane resulting from application of the brakes, thus spoiling the pilot's aim on the target; (2) tail buffeting resulting from the turbulent wake of the drag-producing flaps impinging on the tail, (3) loss of effectiveness with decreasing speed, and (4) increased complications of the wing structure and difficulties of producing a smooth exterior surface on the wing.

Wind-tunnel tests have been made to determine the effectivemess of a propeller as a brake (reference 1). It was found that negative thrust could be more effective in slowing down the airplane than the increased drag caused by flap-type brakes. Curves showing the computed variations of airplane speed with time are shown in figure 1 for both types of braking. No measurements were made, however, of the effects of negative thrust of a propeller on the stability and control characteristics of the model.

It is the purpose of the tests reported herein to determine the effects of a braking propeller, as it might be used in actual service, on the stability and control characteristics of a wind-tunnel model. The tests were made in the Ames 7- by 10-foot wind tunnel. The model used for the tests is not a scale model of a particular airplane, but rather is representative of a general type of highly loaded, highly powered, single-engine, tractor-type military aircraft. The scope of the tests was intended to be sufficient to cover the use of the propeller as a brake in level and diving flight. No tests to simulate the landing condition were made.

Some brief preliminary tests made with another model indicated that the use of negative thrust produced significant changes in the stability and control characteristics. For this reason the scope of the present test was expanded to include configuration changes which it was hoped would result in improved characteristics with negative thrust, and also to provide a basis for estimating the characteristics of airplanes of different conformations. The configuration changes include tilting the propeller thrust axis, raising the horizontal tail, and a combination of both. The model in all configurations was tested with both single- and dual-rotation propellers.

MODEL

The model used is representative of a midwing single-engine airplane of a type requiring additional means of speed control because of its tactical purpose. The fuselage lines have been simplified and do not include a canopy. For convenience, the model is referred to as the stability model. A three-view drawing is given in figure 2 and complete

dimensions in table I. Photographs of the model installed in the wind tunnel are given in figure 3.

The horizontal tail could be mounted in two positions: 4.26 inches (basic configuration), and 12.77 inches above the fuselage reference line. Also, the thrust axis of the propeller, which normally coincided with the fuselage reference line, could be inclined in a vertical plane about a point approximately midway between the two propeller disks. A sketch showing the relation of the propeller and horizontal tail to the center of gravity is given in figure 4. A key to the configuration notation used is given in the appendix.

Both the single- and dual-rotation propellers were mounted in the dual-rotation spinner. The front hub was keyed to the motor shaft, and drove the rear hub through reversing gears. Four blades were used in both the single- and dual-rotation propellers. For single rotation, four blades were placed in the rear hub. Since the rear hub will accept left-hand blades only left-hand rotation was used for all tests with the single-rotation propeller. The propeller diameter was 2.52 feet. The blades used were models of Hamilton Standard blade forms Nos. 3155-6 and 3156-6.

A prototype airplane was assumed in order that the wind-tunnel data could be applied in terms of handling qualities of a full-scale airplane. The dimensions of the prototype were such that the model tested became a 3/16-scale replica of an airplane possessing the following characteristics: (1) weight, 14,700 pounds (W/S = 39.2 lb/sq ft), and (2) power, 2100 brake horsepower at 1350 rpm of propeller.

POWER CONDITIONS

In order to convert the wind-tunnel data into airplane operating conditions, relationships between thrust coefficient T_C and lift coefficient C_L are required for the various constant-power outputs to be considered. To achieve a constant-power output with negative thrust, the propeller-blade-angle actuating mechanism must be capable of functioning in the negative blade-angle range in the same manner as in the normal positive blade-angle range for positive thrust. To avoid overspeeding the engine, the blade-angle actuating mechanism

must be capable of rapid motion through the windmilling range. It may be well to review the operational states of a propeller as the blade angle is changed from positive to negative.

Assume for simplicity that the propeller operates at a constant value of V/nD (constant speed of the airplane and constant rpm). At a large positive blade angle, the propeller produces positive thrust and absorbs power from the engine. As the blade angle is progressively reduced, the propeller absorbs less power and produces less thrust until it no longer absorbs power and is furnishing a small amount of negative thrust because of its own rotational losses. This is the beginning of the windmilling state, and the propeller now tends to drive the engine and will cause it to overspeed unless a brake is used to hold the revolutions per minute constant. The negative thrust produced is progressively increasing. A blade angle, however, will be reached at which the propeller no longer tends to drive the engine. This is the zero-power condition and is accompanied by a substantial amount of negative thrust. Further reduction of the blade angle will cause the propeller to windmill backward unless power is supplied by the engine to keep it turning in the normal direction. This is the beginning of the power-on negative-thrust state; the amount of negative thrust may be increased by increasing the engine power.

The relationships of T_c to C_L (fig. 5) were computed from the data of reference 1. A rate power of 2100 brake horsepower at a propeller speed of 1350 rpm and a wing loading of 39.2 pounds per square foot were assumed. Curves for zero power at 1350 and 1000 rpm are also shown in figure 5. It will be noted that, for low values of C_L (corresponding to high values of V/nD), only a small increase of negative thrust results from the use of full power. An infinite number of families of T_c versus C_L curves may be obtained by varying the power and revolutions per minute, and it should be possible to find a power condition which will satisfy the operational requirements for negative thrust.

TESTS

The wind-tunnel tests were made of the model in the following configurations:

(1) Model in basic configuration

(2) Model in basic configuration with thrust axis tilted down 5°

(3) Model with raised horizontal tail

(4) Model with raised horizontal tail, thrust axis tilted down 5°

Tests were also made with the tail removed.

In addition to tests with negative thrust, tests were made with the propeller removed and with positive thrust to serve as bases of comparison for the effects of negative thrust. Tests made with the single-rotation propeller were duplicated with the dual-rotation propeller to give the effect of type of propeller rotation. All tests with power were made at constant thrust.

Some preliminary negative-thrust tests were made with propeller-blade angles of -5°, -10°, and -15° (measured at the 0.75 radius station). The effect of blade angle on the stability characteristics of the model proved to be inappreciable, and, since a blade angle of -15° gave the best conditions for tunnel operation, all further negative-thrust tests were made with this blade setting. Tests with positive thrust were made with a blade angle of 25°. Experimentally determined T_c versus V/nD relations for these blade angles are shown in figure 6.

Longitudinal Tests

To determine longitudinal-stability and longitudinal-control characteristics of the model, tests in pitch were made of the model in all four configurations with various elevator deflections.

Directional Tests

Tests in yaw to provide directional-stability and directional-control characteristics were made of the model in the basic configuration and with the thrust axis tilted down 5° with various rudder deflections. The model with raised horizontal tail, thrust axis untilted and tilted, was tested

with the rudder undeflected only. The tests in yaw were made at two angles of attack, $\alpha_u = -2^\circ$ and $\alpha_u = 9^\circ$.

COEFFICIENTS AND CORRECTIONS

The data are presented in NACA standard coefficient form and are corrected for tunnel-wall effects. The corrections were applied to the negative-thrust data in the same manner as for positive thrust because of lack of information on tunnel-wall effects with negative thrust. No corrections were applied for strut-tare and interference effects. Previous experience with similar models has shown that the corrections are small and have no appreciable influence on stability and control characteristics. The dimensions on which the coefficients are based and the tunnel-wall corrections applied are given in the appendix.

Moment coefficients were computed for a center of gravity located fore and aft by the 25-percent point of the mean aerodynamic chord and 1-percent mean aerodynamic chord vertically above the fuselage reference line.

RESULTS

Tests to Determine Longitudinal Characteristics

The large number of figures involved makes it impractical to present all of the constant-thrust data for the four model configurations tested. Instead, complete constant-thrust data for the basic configuration of the model, single-rotation propeller, are presented. However, longitudinal characteristics corresponding to various power conditions obtained by cross-plotting the fundamental data are given for all model configurations.

The wind-tunnel data obtained with the model in the basic configuration, single-rotation propeller with positive and negative thrust, are given in figures 7 to 13. Data obtained with the tail removed are given in figures 14 and 15. Data obtained with the propeller removed, tail on and off, are given in figure 16.

Longitudinal characteristics for the four model configurations are presented in figures 17 to 32. For each configuration, rated power was simulated with single- and dual-rotation propellers for positive and negative thrust. Summary plots of the variations of C_m and C_{h_e} with C_L to show the effects of model configuration with either single- or dual-rotation propellers are presented in figures 33 to 36. The effects of a change in incidence of the horizontal tail for the basic configuration are given in figure 37.

In order to show the effect of power on the longitudinal-stability characteristics of the model with basic configuration, a summary plot for various power conditions is given in figure 38.

To investigate the effects of the slipstream on the horizontal tail, velocity surveys were made in a vertical plane containing the elevator hinge line. The data, plotted in the form of contours of equal values of the ratio $\frac{q_{tail}}{q_{free\ stream}}$ are presented in the following figures:

Fig. no.	Configuration	α_u (deg)	T_c
39(a)	SP_S^{-15}-HV	0	-0.1
39(b)	SP_S^{-15}-HV	0	-.2
40(a)	SP_S^{-15}-HV	9	-.1
40(b)	SP_S^{-15}-HV	9	-.3
40(c)	SP_S^{-15}-HV	9	-.5

For the purpose of gaining further insight into the stability and control effects of negative thrust, the ratio

$\frac{q_{\text{effective at the tail}}}{q_{\text{free stream}}}$ and the angle of attack at the tail α_t were computed as follows:

$$\frac{q_t}{q} = \frac{(dC_m/d\delta_e)_{\alpha_u \text{power on}}}{(dC_m/d\delta_e)_{\alpha_u \text{power off}}}$$

$$\alpha_T = \frac{C_{m_t}}{(dC_m/di_t)} \quad \text{(subscript t denotes tail)}$$

These results for rated-power operation are compared in figure 41 for the four model configurations.

The computed variations of elevator angle and stick force with indicated airspeed in steady flight are presented in figure 42 for all four model configurations, rated-power operation.

The longitudinal characteristics corresponding to zero power at a propeller speed of 1000 rpm for the model in the basic configuration, single-rotation propeller, are presented in figure 43. The longitudinal characteristics with elevator deflected for the other configurations of the model will not be presented, because almost identical elevator effectiveness and hinge-moment characteristics were found. However, longitudinal characteristics for all model configurations with the elevator undeflected are presented in figures 44 and 45. Computed variations of elevator angle and stick force with indicated airspeed in steady flight proved to be nearly identical for all model configurations with this power condition, and are presented for the basic configuration of the model only in figure 46.

The computed variation of elevator angle and stick force with normal acceleration in a dive pull-out (T_C = -0.13, TAS = 310 mph) is presented in figure 47. To serve as a basis of comparison, the variation of elevator angle and stick force with normal acceleration in steady turning flight for positive-thrust operation is presented in the same figure. Since all configurations gave similar stick-force gradients, results obtained with the model in basic configuration only are presented.

Tests to Determine Directional and Lateral Characteristics

The tests at $\alpha_u = -2^\circ$ with positive thrust were made at $T_c = 0.03$ to give characteristics corresponding to high-speed flight with rated power, and with negative thrust at $T_c = -0.19$ to give characteristics corresponding to diving flight with rated-power braking. Results obtained with the rudder deflected are presented in figures 48 to 52.

Tests at $\alpha_u = 9^\circ$ with positive thrust were made at $T_c = 0.32$ to give characteristics corresponding to climbing flight with rated power. To obtain characteristics corresponding to slow-speed decelerating flight, tests with negative thrust were made at $T_c = -0.19$ and $T_c = -0.38$. The maximum negative thrust available with rated power corresponds approximately to $T_c = -0.38$, and $T_c = 0.19$ was selected arbitrarily as corresponding to one-half the available negative thrust.

Characteristics of the model with rudder deflected, single-rotation propeller, are presented in figures 53 to 59. The rudder effectiveness obtained with the dual-rotation propeller was similar.

For the purpose of showing the effects of changes in model configuration and type of propeller rotation on the directional-stability characteristics, results of tests with the rudder undeflected, $\alpha_u = -2^\circ$ and $\alpha_u = 9^\circ$, are presented in the summary plots of figures 60 to 69.

Comparisons of the effectiveness of the rudder are made in figures 70(a) and (b), in which the ratio

$$\frac{(dC_n/d\delta_r)_{\text{power on}}}{(dC_n/d\delta_r)_{\text{power off}}}$$

is given for the basic model configuration.

The effect of power on the lateral characteristics of the model, basic configuration, is presented for the high-speed condition in figure 71. Since the effects are small the variation of C_l with ψ only is presented. For the low-speed condition the effects are considerable, and the variations of C_L, C_m, C_Y, and C_l with ψ are

presented in figures 72 and 73 for the model with the tail on and off. To give an indication of the effect of power on lateral-directional correspondence, the ratio of $dC_n/d\psi$ to $dC_l/d\psi$ is plotted as a function of T_c in figure 74.

DISCUSSION

Longitudinal Characteristics

To facilitate presentation and analysis the longitudinal characteristics are discussed under the headings: Steady flight with full power, Steady flight with partial power, and Accelerated flight. Handling requirements for a fighter or torpedo bomber are used as a basis for judgment of satisfactory steady-flight characteristics. Elevator control in a dive pull-out would be critical for a dive bomber and is therefore used as a basis for judgment of satisfactory accelerated-flight characteristics. Because of the similarity of results obtained with single- and dual-rotation propellers, all unqualified statements apply to the model equipped with either propeller type operating at negative thrust.

It will be noted that a large part of this discussion is devoted to comments on the handling qualities of this model. This is considered justifiable since it is typical of the existing highly powered, single-engine airplanes and its characteristics are probably representative. On the other hand these characteristics may be altered by either a movement of center of gravity (which would translate the moment curves and cause different sections of the curves to be utilized for trim) or by a change in tail plan form (which would cause the tail to respond differently to the influence of q_t and α_t). For this reason, due regard should be given to q_t, α_t, and the tail-off characteristics which indicate the more fundamental effects of a propeller producing negative thrust.

Steady flight with full power.- Application of full power to a braking propeller produces very high deceleration by reducing the air velocity through the propeller disk. When the thrust coefficient T_c becomes greater than -0.4, the mean velocity through the disk is less than half the free-stream velocity, and the propeller wake is necessarily much larger

than the propeller diameter. The results of velocity surveys in the tail region (figs. 39 and 40) show that the wake intensity and size are a function of T_c, and the wake location is a function of α. Similar surveys were made with the propeller thrust axis tilted, but are not presented because the results were essentially the same. Consideration of these velocity effects alone would probably lead a designer to expect the following results, which are partially substantiated by experiment: (1) a loss in wing effectiveness $(dC_L/d\alpha)$, (2) a loss in elevator effectiveness $(dC_m/d\delta_e)$, and (3) loss in tail load for a given model attitude.

Basic configuration.- As expected, the value of $dC_L/d\alpha$ (tail off) with negative thrust applied by a single-rotation propeller is 51 percent of the value obtained with propellers removed and 43 percent of the value obtained with positive thrust (figs. 16, 17, and 18). A change to dual rotation produces an unexplained change in $dC_L/d\alpha$ which raises the foregoing fraction to 60 and 47 percent, respectively. (See figs. 16, 19, and 20.) These lift-curve slopes are not unreasonable when it is considered that one-third the wing area is behind the propeller disk, and that at $C_L = 0.8$ $(T_c = -0.4)$ the mean-velocity flow through the propeller is less than half the free-stream velocity. Also, as the velocity over the wing is reduced, the wing of aspect ratio 5.4 is giving the effect of two smaller wings of aspect ratio 2. The loss in lift-curve slope probably could be minimized by lowering the wing with respect to the thrust line, by decreasing wing taper, or by increasing aspect ratio.

Applying negative thrust to the model with the tail removed produces a negative increment in C_m. This increment grows with C_L and, at the higher attitudes, the model with tail off exhibits a negative dC_m/dC_L. A small part of this stability change is due to the negative-thrust moment, and the remainder must be caused by propeller normal force and the propeller wake effect on wing and fuselage. Evidence given later in this discussion indicates that moments produced by the normal force are small when the propeller is producing negative thrust.

The complete model operating with negative thrust possesses moderate stability at low lift coefficients and very high stability at the higher lift coefficients. The high stability is largely a result of a tendency toward stability with the tail off and the very low $dC_L/d\alpha$. With dual rotation the stability is not so great because $dC_L/d\alpha$ is higher than with single rotation. Contrary to expectation there is no consistent reduction in $dC_{m_t}/d\alpha$ with application of negative thrust, although the loss in elevator effectiveness can be seen by comparing figures 16, 18, and 20.

The cause for the maintenance of $dC_{m_t}/d\alpha$ which is as great as or greater than that observed with propeller off may be found in the variations of q_t/q and α_t (fig. 41) and their subsequent effect on $dC_{m_t}/d\alpha$. It can be shown that the following is true:

$$\frac{-dC_{m_t}}{d\alpha} = \alpha_t \left(\frac{dq_t/q}{d\alpha}\right) + \frac{q_t}{q}\left(\frac{d\alpha_t}{d\alpha}\right)$$

At low angles of attack the stability contributed by the first term of the foregoing equation and the high $d\alpha_t/d\alpha$ are nearly sufficient to compensate for the low q_t/q. At the higher angles of attack ($\alpha>4^\circ$) the stabilizer moves out of the low-velocity core of the wake (figs. 41 and 42), and $d\alpha_t/d\alpha$ increases sharply to increase further the stability contributed by the tail. The generally high value of $d\alpha_t/d\alpha$ can be attributed to the loss in wing downwash behind the propeller. The sharp increase in $d\alpha_t/d\alpha$ between $\alpha = 4^\circ$ and $\alpha = 6^\circ$ is probably a result of the stabilizer moving into the wake upwash which is present in the lower half of high-intensity wakes (reference 2). The same trends of q_t and α_t can be observed in the hinge-moment curves, but, since hinge moments are subject to secondary effects, they do not lend themselves to a direct analysis.

The variation of elevator angle and stick force with speed for the assumed airplane shows adequate stick-fixed and stick-free stability for negative-thrust operation (fig. 42). For positive thrust both the stick-free and stick-fixed

stability are marginal which is not unusual for a highly powered airplane of this type.

The minimum trim speed is about 160 miles per hour due to the very high stick-fixed stability (high dC_m/dC_L and low $dC_m/d\delta_e$) in the low-speed range. Since this speed is approximately the speed for torpedo launching, such a limitation would be objectionable for a torpedo bomber. At first it might appear that a compromise in stabilizer incidence would satisfactorily lower the minimum trim speed, but at best only 5 to 10 miles per hour could be gained because of the extremely high stability (dC_m/dC_L).

On a fighter-type airplane it would be desirable to change from positive to negative thrust without a change in trim. The change in elevator required for trim at a given speed is small in high-speed flight where the braking propeller would be used. The untrimmed stick forces differ by 30 or 40 pounds. Proper location of a trim tab relative to the propeller wake and slipstream probably could reduce this difference when the tab is set for trim in positive-thrust operation.

Propeller tilt.- By tilting a propeller nose down, the thrust line is raised relative to the center of gravity, and the thrust-line angle of attack is decreased for a given attitude or lift coefficient. It has been shown that for positive thrust the resulting increments of propeller-thrust and normal-force moments will increase the stability. It can be similarly reasoned that with negative thrust the opposite effect would be realized; that is, the stability would be decreased.

As anticipated, the sole effect of propeller tilt is to shift the rotate the pitching-moment curves for either tail on or off (figs. 34 and 36). The variations of q_t/q and α_t with α presented in figure 41 show no significant change due to propeller tilt. Within the experimental accuracy the change in moment characteristics can be justified by the thrust moment which indicates that normal forces are insignificant.

Except for possible effects of stalled portions of the blade, a much reduced normal force should be expected from a propeller developing negative thrust. The cause for normal force on a propeller developing positive thrust can be explained

by sketch (a) below which shows a propeller-blade element with its rotational and forward velocity vectors.

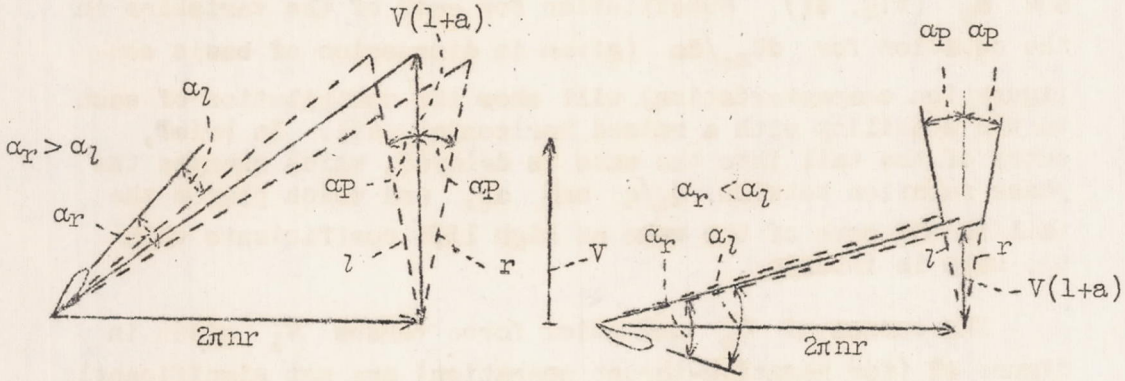

(a) Positive thrust (b) Negative thrust

When the propeller axis is tilted $\alpha_p{}^o$, the vector $V(1+a)$ rotates relative to the propeller plane assuming the position r and l for blades on the right and left half of the propeller. The difference between the resulting α_r and α_l produces unbalanced torque forces between right and left sides of the propeller disk. The difference between the torque forces is known as propeller normal force. As shown in sketch (b), for a propeller delivering negative thrust the vector $V(1+a)$ is much smaller because a is negative. The resulting normal force is very small and in the opposite direction.

The change in trim and loss in stick-fixed stability resulting from propeller tilt reduce the minimum trim speed by 5 miles per hour (fig. 42). This is a step in the right direction but still leaves much to be desired. The effects of propeller tilt realized with negative thrust, combined with the increased stability for positive thrust, reduce the trim changes between positive- and negative-thrust operation. Use of a trim tab at high speeds might increase the difference in stick forces because of a change in tab effectiveness between positive- and negative-thrust operation. Lack of definite criteria specifying allowable trim changes for a fighter makes final judgment of trim characteristics impossible.

Raised horizontal tail.- The change in horizontal tail position from low to high resulted in the following stability increments: (1) an increase at low lift coefficients, (2) a large decrease at $C_L = 0.4$ to 0.6, and (3) a slight to large decrease at high lift coefficients depending upon whether a single- or dual-rotation propeller was used (figs. 34 and 36).

The cause for these increments which produce an S-shape C_m versus C_L curve can be traced to the variations of q_t/q and α_t (fig. 41). Substitution for each of the variables in the equation for $dC_{m_t}/d\alpha$ (given in discussion of basic configuration characteristics) will show the contribution of each to the stability with a raised horizontal tail. In brief, entry of the tail into the wake is delayed, which changes the phase relation between q_t/q and α_t, and which places the tail in the core of the wake at high lift coefficients when the wake is intense.

The curves of δ_e and stick force versus V_i given in figure 42 (for negative-thrust operation) are not significantly different from those for the basic configuration. Even though the stability is lower, the minimum trim speed is greater by 5 or 10 miles per hour because of the very low elevator effectiveness. For positive thrust there is a definite improvement in stability as would be predicted from results of tests on similar models.

Raised horizontal tail and tilted propeller.- Within a fair degree of accuracy, the pitching-moment characteristics of the model with raised stability and tilted propeller are the pitching-moment characteristics of the basic configuration with the individual effects of raised horizontal tail and tilted propeller superimposed (figs. 34 and 36). The trim characteristics cannot be obtained by simple superposition, because raising the horizontal tail removes any semblance of linearity in the C_m versus C_L curves, and tilting the propeller rotates the curves bringing a different section of the curves across the $C_m = 0$ axis.

The stability of the model as indicated by the variation of δ_e and stick force with speed is reduced for negative thrust and increased for positive thrust. The resulting trim changes from positive- to negative-thrust operation are small for any speed greater than 200 miles per hour. The minimum trim speed is reduced to 150 miles per hour. Of the four configurations tested this configuration yields the best longitudinal characteristics in steady flight; however, it is apparent that the effects of configuration are relatively small when compared to the basic effects of a propeller producing negative thrust.

Steady flight with partial power.- To check on possible tail buffeting as a result of high negative thrust, a grid of yarns, located in a vertical plane at the tail, was observed as the thrust coefficient was varied. At a T_c of -0.2 the tufts began oscillating badly, and at a T_c of -0.3 the disturbance increased so that the tufts oscillated through an included angle of about 45°. For $T_c = -0.4$ and -0.5 the flow near the fuselage reversed and the oscillation was so severe that it would appear unsafe to operate in this range. Such a test is not necessarily a quantitative measure of buffeting; however, it seems likely that full power should not be used for braking at low speed.

An obvious solution to the difficulties experienced with full-power braking is to reduce the power output. By properly selecting the power and propeller speed it is possible to obtain a great variety of T_c versus C_L relationships (fig. 5). The longitudinal-stability characteristics of the model in the basic configuration are compared in figure 38 for several power conditions. Only 25 percent power produces half the stability change (dC_m/dC_L) between zero power and full power. Zero power appears to be the best operating condition, since it produces good braking and yet does not cause large changes in pitching-moment characteristics.

With zero power the longitudinal-stability characteristics for the four configurations tested are nearly the same (figs. 44 and 45). Most of the effects noted with full power are still present but to a lesser extent. Both stick-fixed and stick-free stability as shown by figure 46 are satisfactory for the basic configuration, and, although not presented, were satisfactory for all configurations tested. The elimination of extreme stability at low speed and the increase in elevator effectiveness remove the serious limitation of minimum trim speed existing with full power. The $\Delta\delta_e$ required to maintain a given speed upon application of the brake is small. The stick-force increments required to maintain a given speed show no consistent improvement. However, stick-force characteristics are a function of many variables and if $\Delta\delta_e$ is small the increments could probably be held within the desired limits by adjustment of these variables.

Accelerated flight.- One of the flight conditions for which the use of the propeller as a brake is considered is that of

limiting the maximum speed in a dive. It is assumed the pilot will use a predetermined amount of power to hold the desired speed in the dive and then pull out without changing the power output of the engine. This maneuver may prove to be the critical cause of the stick force required of the pilot to produce the desired amount of normal acceleration. (A steady turn possibly would require more stick force, but this is not considered to be a normal maneuver with negative thrust.)

The condition selected for analysis is a 70° dive at a speed of 310 miles per hour. The thrust coefficient required to limit the airplane to this speed is -0.13 for an assumed drag coefficient of 0.025. The variation of δ_e and stick force with normal acceleration for the basic configuration of the model is presented in figure 47. In order to give a basis of comparison, the variations of δ_e and stick force with normal acceleration in steady turning flight with rated power and positive thrust at the same speed as the dive pull-outs are shown in the same figure. The stick-force gradient is only slightly greater for negative-thrust operation (about 18 lb per g). It would be expected that the use of negative thrust would result in higher stick-force gradients than with positive thrust because dC_m/dC_L is increased and $dC_m/d\delta_e$ is decreased with negative thrust. However, $dC_{h_e}/d\delta_e$ decreases faster than $dC_m/d\delta_e$ so that nearly identical stick-force gradients for positive and negative thrust are the net results. Similar results were found for the other model configurations. However, the model with the raised horizontal tail and inclined thrust axis gave considerably higher stick-force gradients (about 28 lb per g) for both dive pull-outs and steady turning flight.

The numerical values given for the stick-force gradients are higher than are desirable and could be reduced by redesigning the horizontal tail, but it is believed that design changes for the purpose of reducing the stick-force gradient with positive thrust will have a similar effect with negative thrust. Since the stick-force gradients are of the same magnitude for both positive-thrust and negative-thrust operation, the use of the propeller as a dive brake appears to be satisfactory from the standpoint of stick force in dive pull-outs.

Directional Characteristics

The directional-stability and directional control characteristics are discussed under the headings High speed and Low speed. High-speed characteristics were obtained at $\alpha_u = -2^\circ$ which, for positive-thrust operation, corresponds to high-speed level flight, and for negative-thrust operation corresponds to diving flight. Low-speed characteristics were obtained at $\alpha_u = 9^\circ$ which, for positive-thrust operation, corresponds to climbing flight, and for negative-thrust operation corresponds to decelerating level flight.

High speed.- Inspection of the C_n versus ψ curves for the model with tail removed $\alpha_u = -2^\circ$ (figs. 48 to 52) shows the model to be directionally unstable with the propeller removed and that the application of power $T_c = 0.03$ or -0.019 has little effect on the stability. As would be expected from consideration of the velocity effects of the propeller slipstream, the yawing moment supplied by the vertical tail is increased with positive-thrust and decreased with negative-thrust operation. The differences are small, however, and because of small differences in the stability of the model, tail off, the directional stability of the complete model is nearly the same for positive- and negative-thrust operation. Similar results were observed for the effectiveness of the rudder (fig. 70(a)).

Low speed.- The variation of C_n with ψ for the model with tail removed $\alpha_u = 9^\circ$ (figs. 53 to 59 indicates a marked reduction in stability for positive-thrust operation $T_c = 0.33$, particularly for moderate angles of yaw. Negative thrust with $T_c = -0.19$ has small effect on the stability, but with $T_c = -0.38$ the stability of the model with tail removed is positive for the range of angles of yaw between approximately $\pm 10^\circ$. For larger angles of yaw the stability becomes negative and approaches the value obtained with the propeller removed. The positive stability exhibited for moderate angles of yaw is greater with the single-rotation propeller than with the dual-rotation propeller (figs. 68 and 69).

These results may be explained by consideration of the effect of propeller normal force and the effect of the propeller wake on the wing-fuselage combination. Study of the sketch on page 14 will show the effect of propeller normal force with

positive thrust to be destabilizing, and computations show the effect to be small. For negative-thrust operation, the effect of propeller normal force is stabilizing, but of such small magnitude as to be inconsequential. Therefore, it is believed that the effect of the propeller wake on the wing-fuselage combination is the principal factor affecting the stability of the model with tail removed. Since the model is unstable with the propeller removed, it is logical that it should become more unstable when the fuselage is immersed in the high-velocity slipstream associated with positive thrust, and become less unstable when surrounded by the low-velocity wake associated with negative thrust. The reason for the S-shape of C_n versus ψ curves for $T_c = 0.38$ (figs. 68 and 69) is not understood, but it is believed to be primarily an effect caused by the emergence of the trailing portion of the fuselage from the propeller wake at large angles of yaw.

With the tail on, the directional stability of the model for negative-thrust operation is reduced to approximately half that obtained with the propeller removed. The stability for $T_c = -0.38$ is slightly greater than for $T_c = -0.19$. This apparently contradictory result is caused by the stability characteristics of the model with tail removed. The yawing moment supplied by the vertical tail is actually much less for $T_c = -0.38$ than for $T_c = -0.19$, but because of the positive stability exhibited by the model with tail removed ($T_c = -0.38$) the resultant stability is slightly greater.

The comparative effectiveness of the rudder (fig. 70(b)) is in the expected direction; that is, the effectiveness is increased with positive thrust and reduced with negative thrust. For negative-thrust operation $T_c = -0.38$ (approximately full power) the rudder effectiveness is so greatly reduced as to make the operation of the airplane exceedingly unsafe. It is estimated that about 5° of yaw can be produced by use of full rudder with the single-rotation propeller, and about 20° with the dual-rotation propeller. The reason for this difference in yaw is not greater rudder effectiveness with the dual-rotation propeller but lower directional stability which may be traced back to the directional characteristics with the tail removed. With T_c limited to -0.19 (approximately zero power) more than 20° of yaw can be produced by use of full rudder.

Rudder hinge-moment characteristics in general follow the same trends as the directional-stability and directional-control characteristics, but are not amenable to analysis because of secondary effects.

Some approximate rudder-pedal-force calculations were made neglecting the contribution of the lateral-control system to directional stability. For the high-speed attitude, $\alpha_u = -2^\circ$, and an indicated airspeed of 300 miles per hour, it was found that the average gradient of the rudder-pedal force was approximately the same for positive and negative thrust. Assuming an instantaneous change from positive to negative thrust (T_c = 0.03 to -0.19), the change in rudder angle required to hold zero sideslip is about $2\frac{1}{2}^\circ$ right rudder with the single-rotation propeller, and about $1\frac{1}{2}^\circ$ right rudder with the dual-rotation propeller. The corresponding average change in the untrimmed rudder-pedal force is about 40 pounds on the right rudder pedal.

For the low-speed altitude ($\alpha_u = 9^\circ$) and an indicated airspeed of 160 miles per hour, the change in rudder angle required to hold zero sideslip for the change from positive to negative thrust (T_c = 0.33 to -0.19) is about 23° right rudder with the single-rotation propeller, and about 3° right rudder with the dual-rotation propeller. The corresponding changes in rudder-pedal forces are about 120 pounds and 10 pounds on the right rudder pedal, respectively.

The effect of tilting the thrust axis is to reduce slightly both the pedal-force gradient and the change in pedal force for trim because of the slightly lower stability exhibited by the model with the tilted thrust axis. No rudder-deflected tests were made with the raised horizontal tail because of difficulties of deflecting the rudder. However, inspection of the C_n and C_{h_r} versus ψ curves for the tail-high configurations (figs. 60 to 69) shows a slight reduction of $dC_n/d\psi$ and $dC_{h_r}/d\psi$ for angles of yaw between ±16° and a considerable reduction for greater angles of yaw. This effect may be caused by interference between the horizontal and vertical tail, which in all probability would result in reduced rudder effectiveness.

From the standpoint of directional stability and control, it appears that the best model configuration is the normal

position of tail with the thrust axis tilted down. The use of a dual-rotation propeller will reduce the trim changes with use of power. For braking operation, the maximum amount of negative thrust which may be used with safety is that corresponding to a T_c of about -0.2 which can be produced with the use of little if any power (fig. 5).

It appears probable that the directional stability and control of a single-engine airplane would be improved for braking operation by the use of twin vertical tails. As one tail entered the low-velocity core of the propeller wake, the opposite tail would be emerging into the higher velocity of the free stream. Thus the combined effectiveness of the two tails would tend to remain more nearly uniform throughout the yaw range.

Dihedral Effect

The dihedral effect of the model progressively increases as power is applied to a propeller producing negative thrust (figs. 71, 72, and 73). Conversely, the dihedral effect is reduced with application of power to a propeller producing positive thrust. It has been proved that the effect with positive thrust results from the high slipstream velocity increasing the lift on the trailing wing, and that the effect is a function of wing lift coefficient, thrust coefficient, and distance from propeller to wing. It can be similarly reasoned that the effect with negative thrust results from the low slipstream velocity decreasing the lift on the trailing wing, and that it is a function of the same variables. The increment of dihedral effect can be computed within 20 percent by assuming that the propeller wake trails in the free-stream direction and that the loss in lift occurs where the wake crosses the wing.

The large dihedral effect is undesirable, particularly when coupled with the low directional stability associated with a braking propeller. The lateral-directional correspondence, as indicated by the ratio $dC_n/d\psi$ to $dC_l/d\psi$, varies over a wide range when power is changed from full-negative to full-positive thrust (fig. 74). As a result, if an airplane is designed for proper lateral-directional correspondence in the positive-thrust range (which in itself is a difficult compromise), it will become too sensitive in roll for high-negative-thrust operation. Since for the dive condition both lift and thrust coefficients are small, the

problem is not serious. If full-power braking is used for the torpedo launching run, a definite problem exists; however, other problems involved in the use of full-power braking at low speed probably will preclude its use. For zero-power braking, the lateral-directional characteristics would not be necessarily ideal but probably would be acceptable.

CONCLUDING REMARKS

The results of these tests indicate that the propeller may be used as a means of speed control for a single-engine tractor-type airplane to an extent which will be equally or more effective than conventional spoiler-type dive brakes, particularly at low speeds. The advantages in favor of using the propeller rather than conventional dive brakes, in addition to greater effectiveness at low speeds, are those of simplification of the aircraft structure and concomitant saving in weight. The disadvantages are the significant changes of the stability and control characteristics of the airplane produced by the braking propeller. These effects are largely caused by the low-velocity wake of the propeller flowing over wing, fuselage, and tail, rather than any direct forces acting on the propeller.

The results of the tests also show that the undesirable effects of a braking propeller may be minimized by proper design of the airplane. Tilting the propeller thrust axis and locating the tail as remote from the propeller wake as possible help to reduce the stability and control changes accompanying the use of negative thrust. The use of a dual-rotation propeller is of benefit in reducing the changes of rudder angle and rudder-pedal force required for trim with change of power.

By limiting the power output of the engine, thus restricting the amount of negative propeller thrust, the stability and control characteristics may be held within the limits required for safe operation and still produce adequate braking. The possibility of tail buffeting still remains to be investigated quantitatively, but visual observation of tufts indicated the absence of serious buffeting for the range of negative thrust corresponding to acceptable operation from the standpoint of stability and control.

Ames Aeronautical Laboratory,
National Advisory Committee for Aeronautics,
Moffett Field, Calif., Jan. 20, 1945.

REFERENCES

1. Hedrick, William S., and Douglass, William M.: An Experimental Investigation of the Thrust and Torque Produced by Propellers Used as Aerodynamic Brakes. NACA ARR No. 4H26, 1944.

2. Silverstein, Abe, Katzoff, S., and Bullivant, W. Kenneth: Downwash and Wake Behind Plain and Flapped Airfoils. NACA Rep. No. 651, 1939.

APPENDIX

CONFIGURATION KEY FOR THE STABILITY MODEL

S basic configuration, model in normal flying condition but without propeller (i.e., wing, fuselage, vertical tail, horizontal tail in normal position, flaps and gear retracted)

P propeller

subscript S denotes single rotation

subscript D denotes dual rotation

superscript denotes blade angle β in degrees at 0.75 radius station

H horizontal tail

V vertical tail

COEFFICIENTS AND SYMBOLS

All coefficients are given in NACA standard form referred to the stability axes, and are defined as follows:

C_L lift coefficient (L/qS)

C_D drag coefficient (D/qS)

C_Y lateral-force coefficient (Y/qS)

C_m pitching-moment coefficient (M/qSc)

C_n yawing-moment coefficient (N/qSb)

C_l rolling-moment coefficient (L'/qSb)

C_{h_e} elevator hinge-moment coefficient (H_e/qS_ec_e)

C_{h_r} rudder hinge-moment coefficient (H_r/qS_rc_r)

T_c thrust coefficient $(T/\rho V^2 D^2)$

where

L lift, lb

D drag, lb (also propeller diameter = 2.52 ft)

Y cross-wind force, lb

M pitching moment, ft-lb

N yawing moment, ft-lb

L' rolling moment, ft-lb

H_e elevator hinge-moment, ft-lb

H_r rudder hinge-moment, ft-lb

T effective thrust, lb

q dynamic pressure $\left(\frac{1}{2}\rho V^2\right)$ lb/sq ft

S wing area (13.18 sq ft)

c mean aerodynamic chord (1.627 ft)

b wing span (8.48 ft)

S_e elevator area aft of hinge line (0.819 sq ft)

c_e elevator chord aft of hinge line (0.274 ft)

S_r rudder area aft of hinge line (0.369 sq ft)

c_r rudder chord aft of hinge line (0.321 ft)

ρ mass density of air, slugs/cu ft

V airspeed, ft/sec

n revolutions per second

In presentation and analysis of the results, the following symbols are used in addition to the coefficients:

α_u uncorrected angle of attack of the fuselage reference line, degrees

α angle of attack of the fuselage reference line corrected for flow inclination and tunnel-wall effects, degrees

α_t effective angle of attack of the horizontal tail, degrees

ψ angle of yaw of line of symmetry, degrees

C_{m_t} pitching-moment coefficient produced by the tail

i_p angle of incidence of propeller thrust axis with respect to fuselage reference line, degrees

i_t angle of incidence of horizontal tail with respect to fuselage reference line, degrees

δ control-surface deflection, degrees

subscripts

e elevator

r rudder

t horizontal tail

CORRECTIONS

The following tunnel-wall corrections were applied and are all additive:

$$\Delta C_D = \delta_1 \frac{S}{C} C_{L_u}{}^2$$

$$\Delta\alpha = \delta_2 \frac{S}{C} C_{L_u} \times 57.3$$

$$\Delta C_m{}^* = -\delta_3 \frac{S}{C} C_{L_u} \times 57.3 \times \frac{dC_m}{di_t}$$

---

*Applied to tail-on data only.

where

$\delta_1 = 0.122$

$\delta_2 = 0.135$

$\delta_3 = 0.0966$

C = 70 sq ft

C_{L_u} = uncorrected lift coefficient with tail removed

$\frac{dC_m}{di_t} = -0.031$

TABLE I.- DIMENSIONS OF STABILITY MODEL

	Wing	Horizontal tail	Vertical tail
Area, total, sq ft	13.181	3.007	1.160
Span, ft	8.479	3.667	1.250
Mean aerodynamic chord, ft	1.627	----------	----------
Aspect ratio	5.4	4.52	1.345
Taper ratio	.500	.513	.592
Root chord, ft	2.093	1.093	1.188
Tip chord, ft	1.047	.561	.703
Root section	NACA 2418 constant to station 1.766 feet outboard of center line	NACA 0012-64 modified to 10.71 percent thick	NACA 0012-64 modified to 8.9 percent thick
Tip section	NACA 2415	NACA 0012-64 modified to 10.71 percent thick	NACA 0012-64 modified to 8.9 percent thick
Dihedral	8°	7°	----------
Incidence with respect to fuselage reference line	2°	0°	0° with center line. 2° to left with raised horizontal tail
Area of movable surface aft of hinge line, sq ft	----------	0.819	0.369
Hinge line, percent chord	----------	66.89	66.46
Aerodynamic balance, percent of area aft of hinge line	----------	29.9	28.2
Tail length, 25 percent mean aerodynamic chord to center line hinge, feet	----------	4.315	4.320
Assumed mechanical advantage of control for computing control forces, force/C_h q	----------	20	20

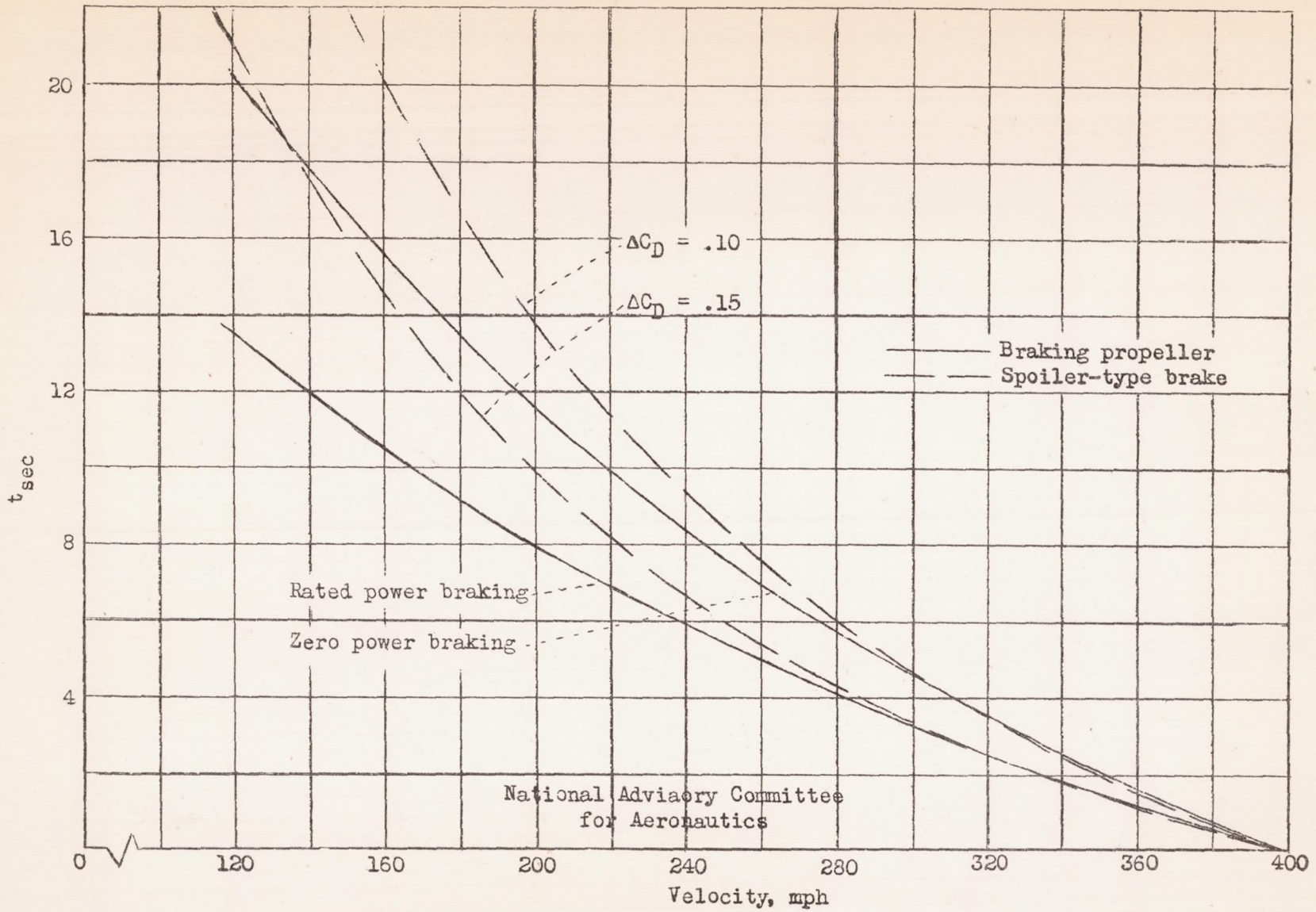

Figure 1.- The variation of speed with time for the stability model equipped with spoiler-type brake or braking propeller.

A-19

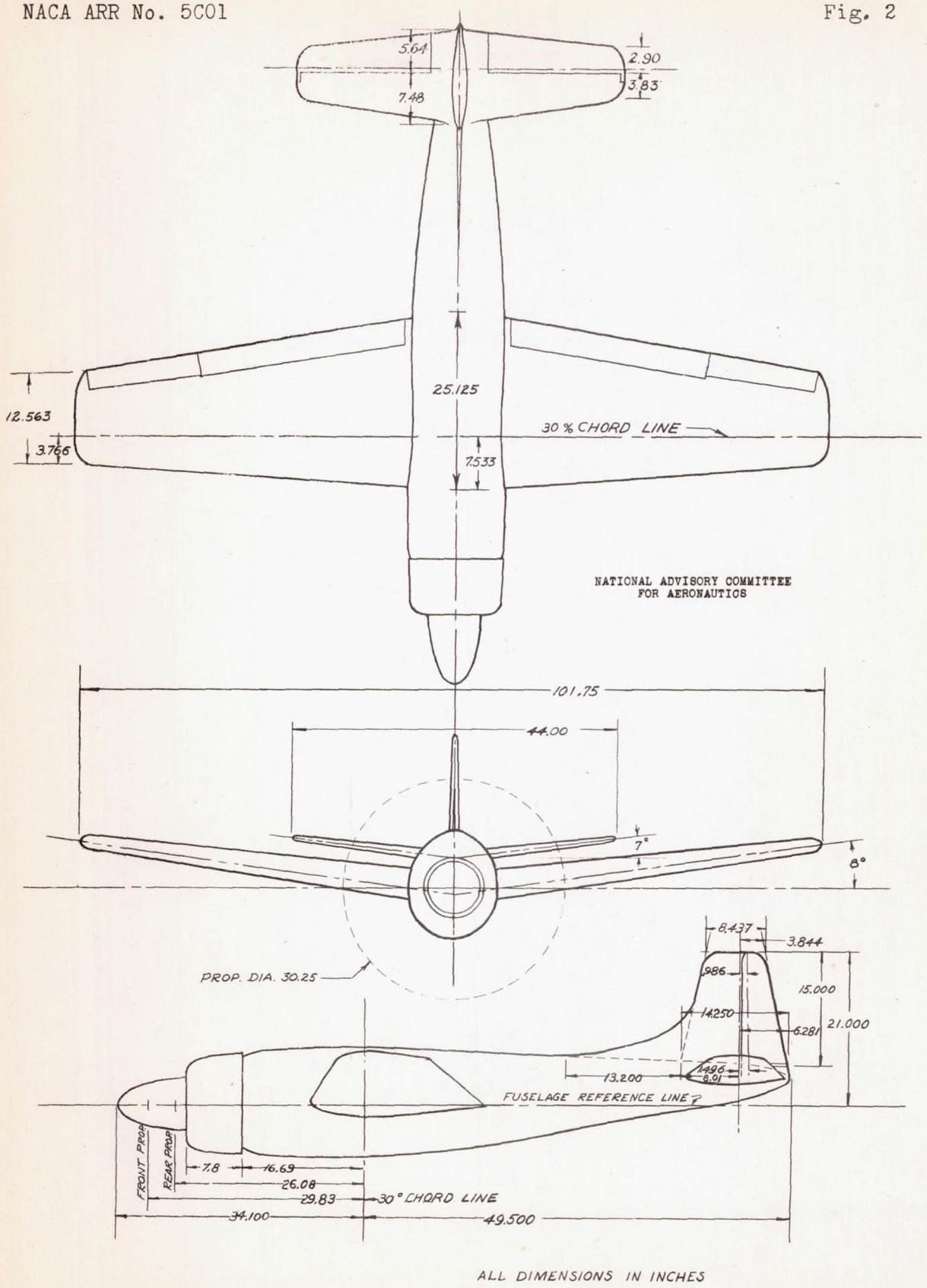

FIGURE 2.- THREE-VIEW DRAWING OF THE STABILITY MODEL.

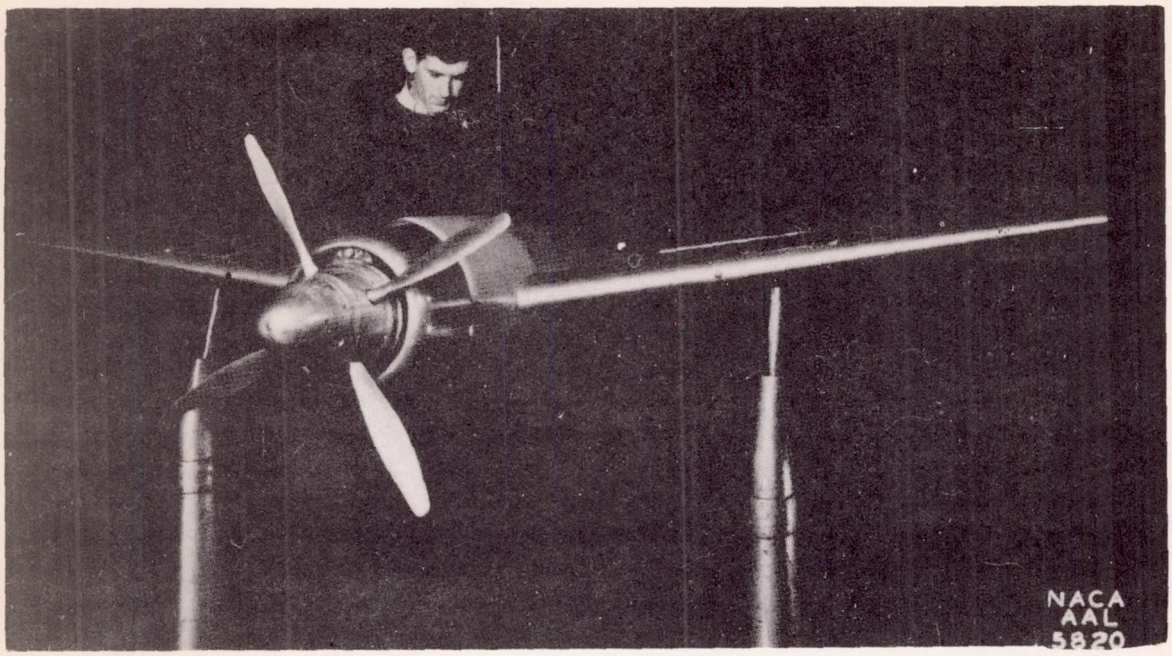

(a) Normal tail position and thrust axis.

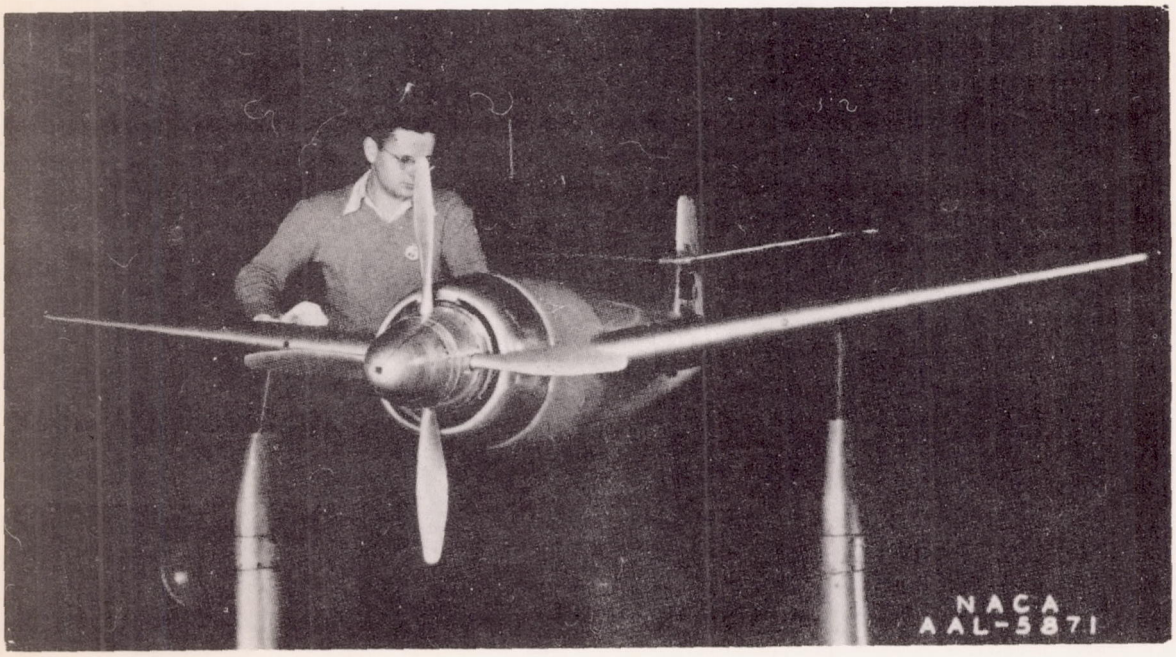

(b) Raised horizontal tail and thrust axis tilted down 5°.

Figure 3.- Photographs of the stability model mounted in the Ames 7- by 10-foot tunnel.

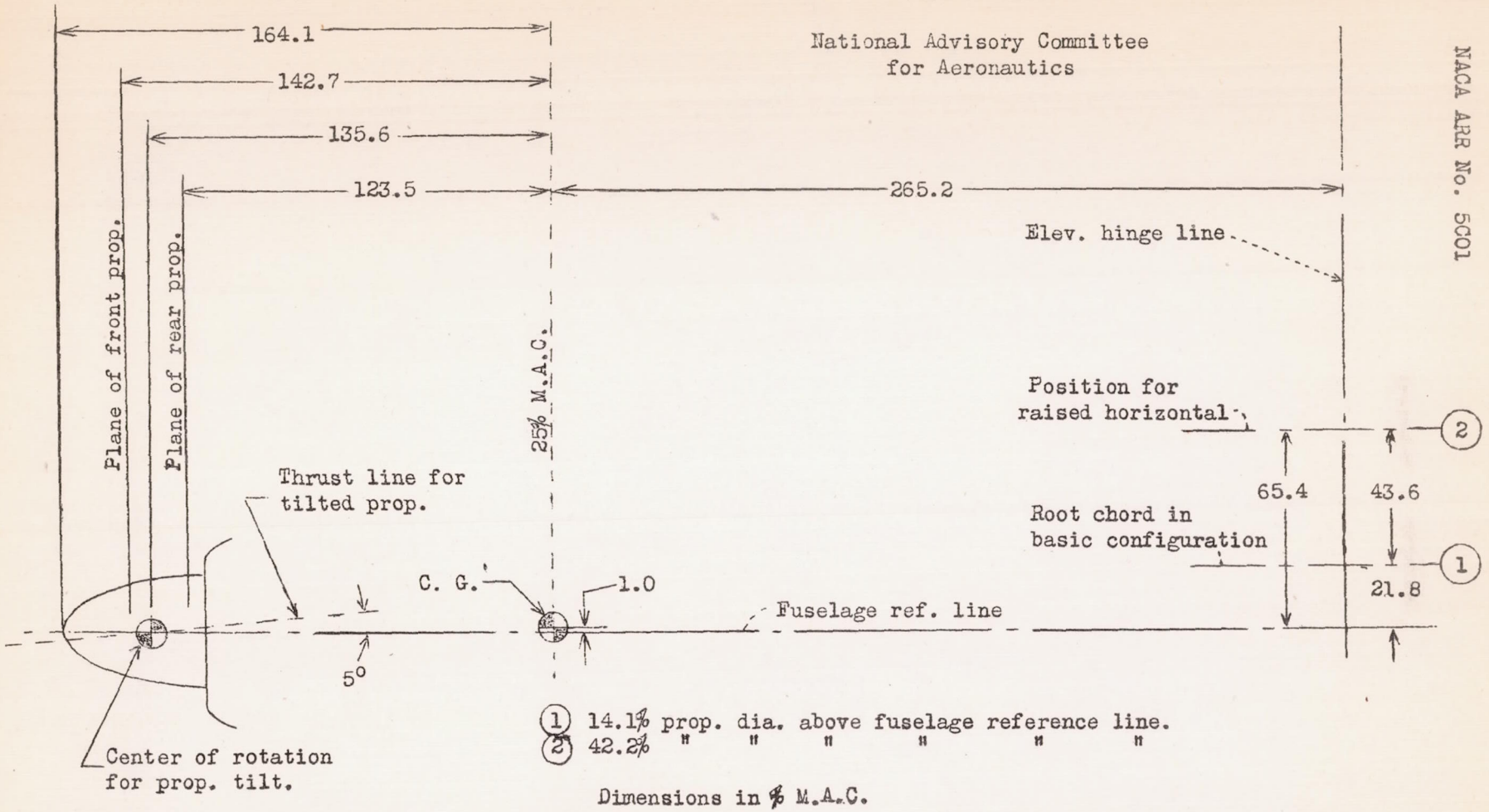

Figure 4.- Sketch of relative location of propeller, horizontal tail, and center of gravity. Stability model.

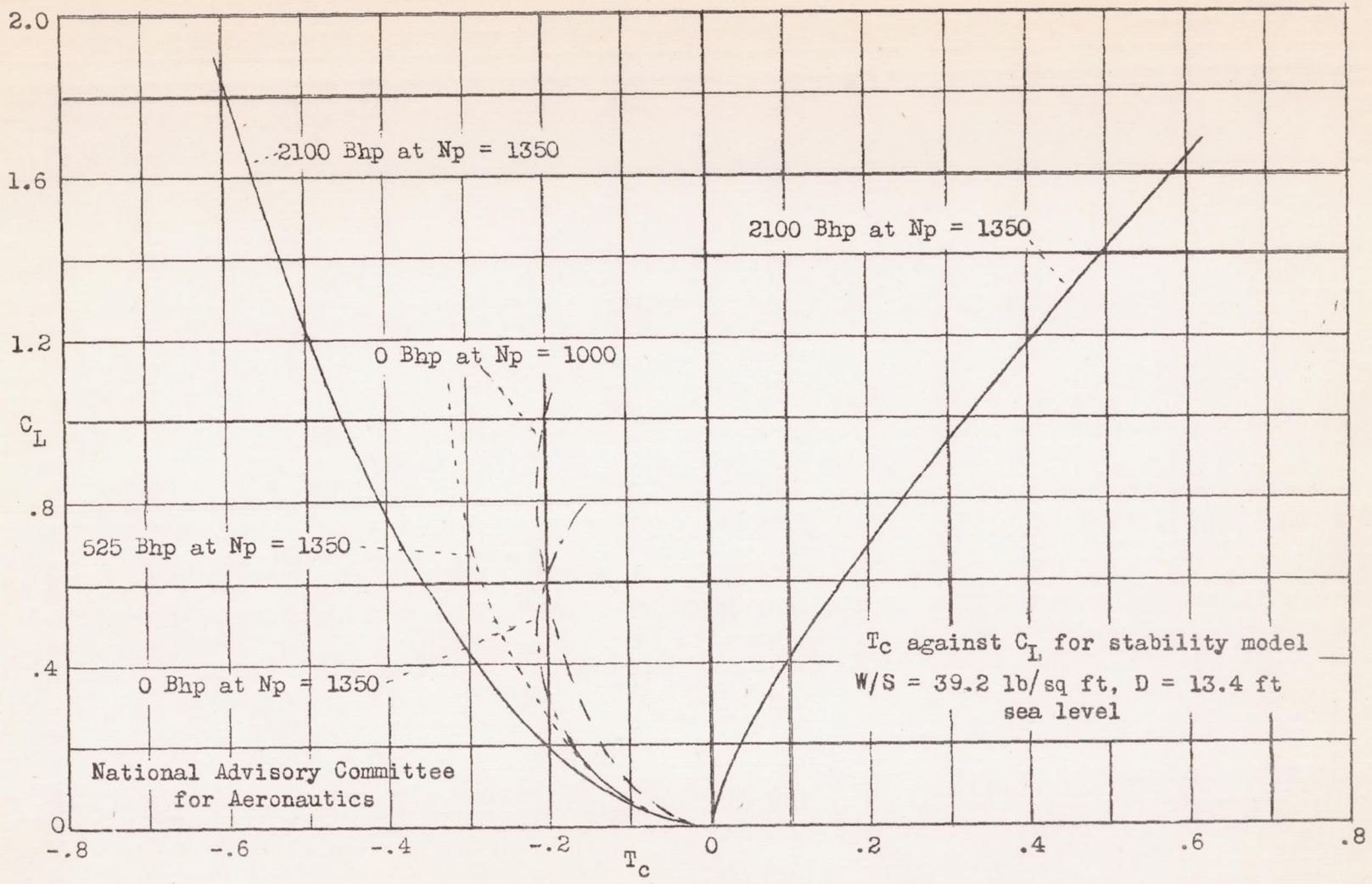

Figure 5.- Variation of thrust coefficient with lift coefficient for several power conditions. Stability model.

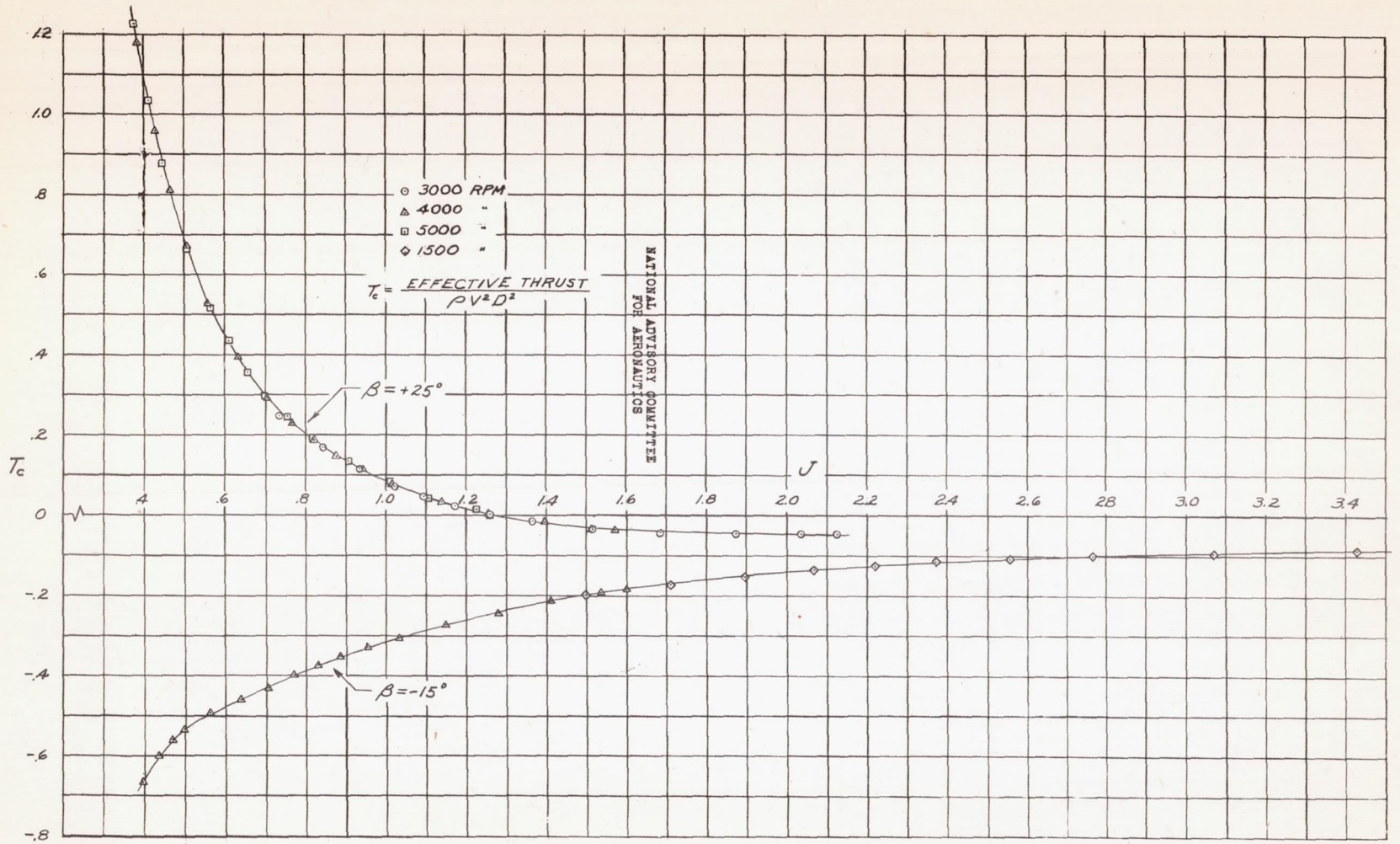

FIGURE 6.--VARIATION OF THRUST COEFFICIENT WITH ADVANCE RATIO FOR POSITIVE AND NEGATIVE THRUST, SINGLE ROTATION, β= 25° AND -15°. STABILITY MODEL.

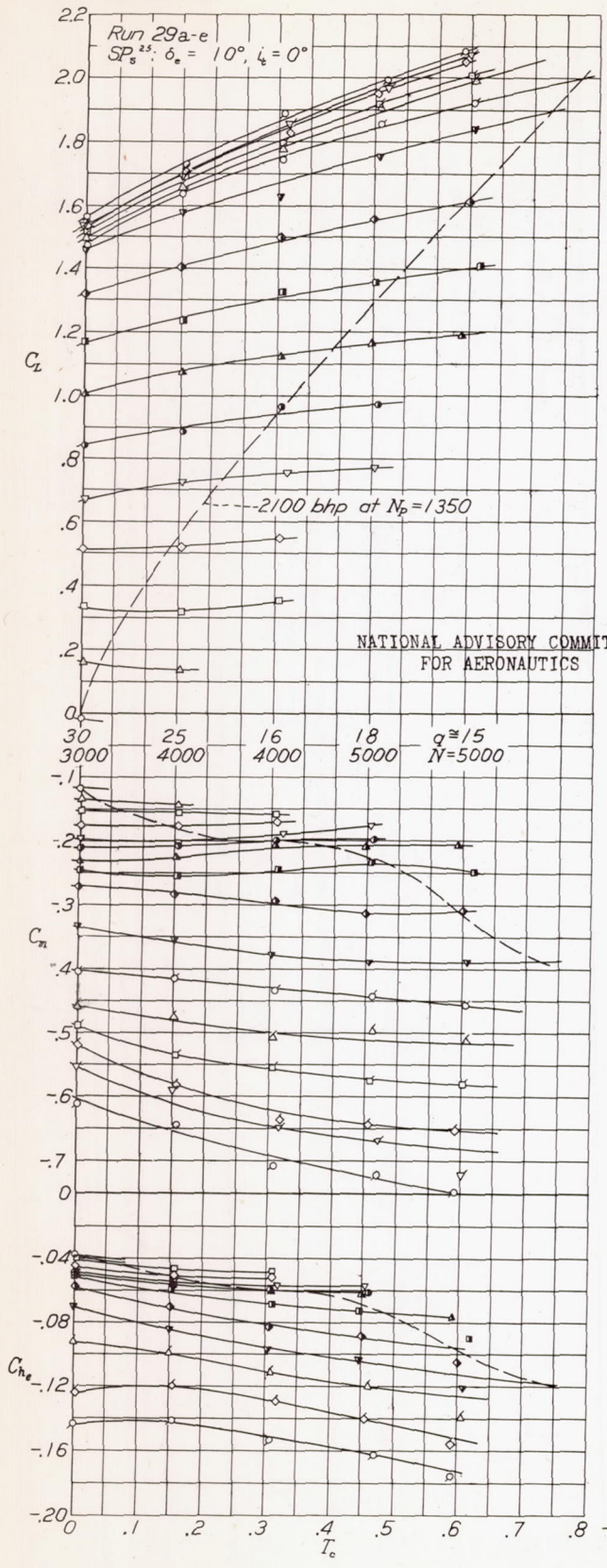

Figure 7.- Effect of thrust coefficient on characteristics of stability model in pitch. Basic configuration, elevator deflected 10°, single rotation, β = 25°.

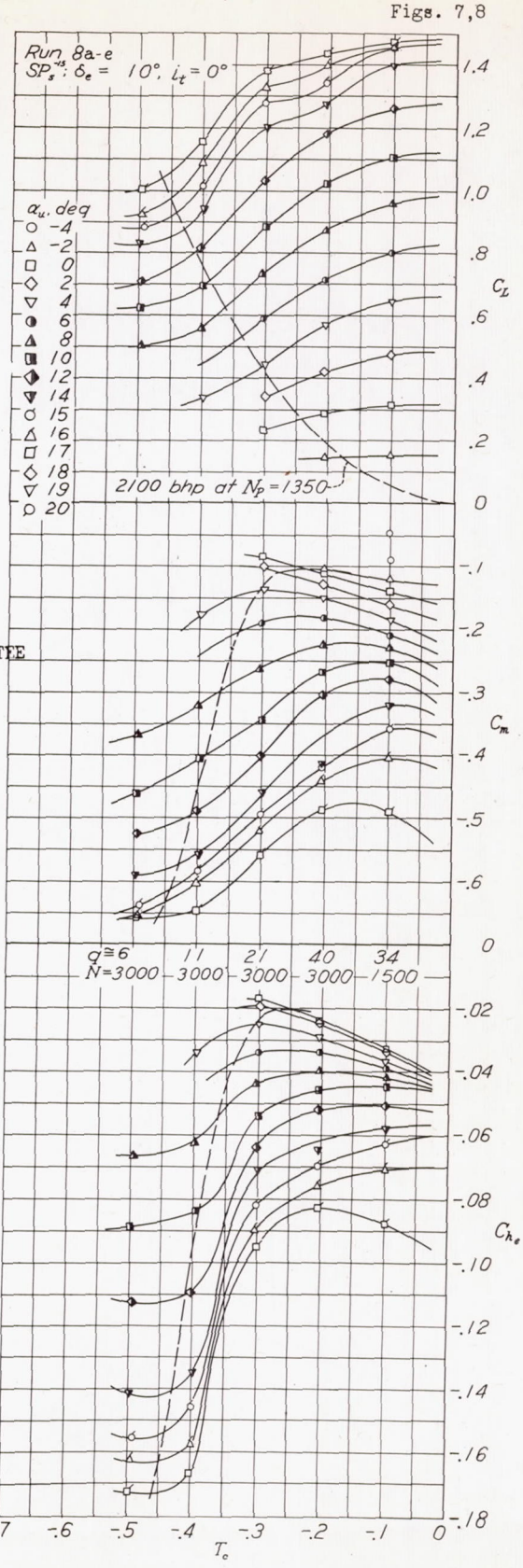

Figure 8.- Effect of thrust coefficient on characteristics of stability model in pitch. Basic configuration, elevator deflected 10°, single rotation, β = -15°.

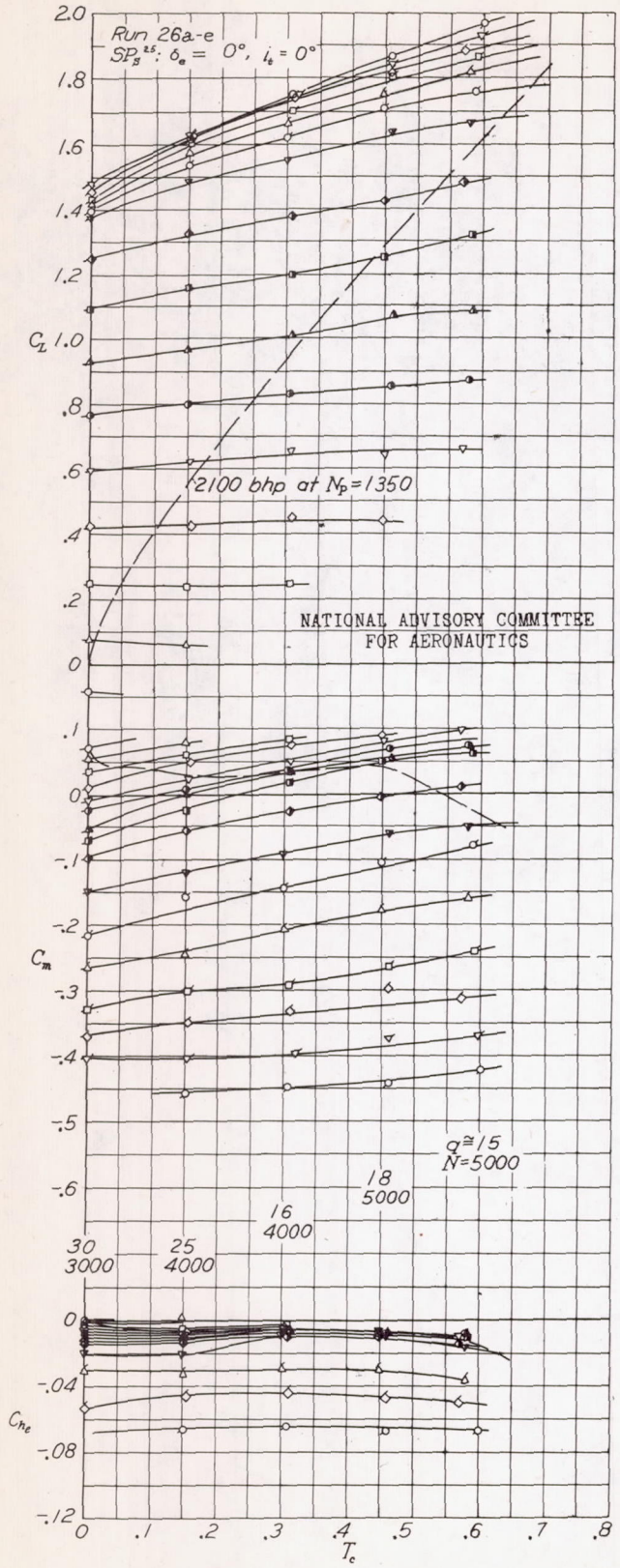

Figure 9.- Effect of thrust coefficient on characteristics of stability model in pitch. Basic configuration, elevator undeflected, single rotation, β = 25°.

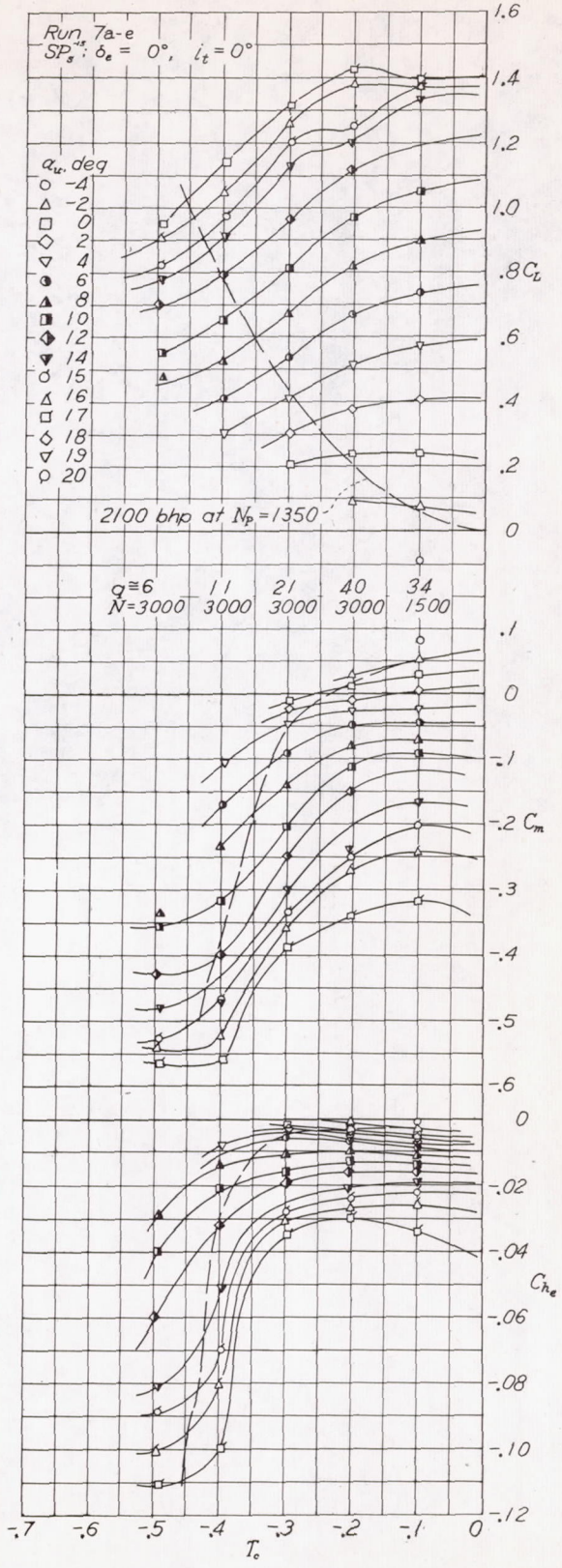

Figure 10.- Effect of thrust coefficient on characteristics of stability model in pitch. Basic configuration, elevator undeflected, single rotation, β = -15°.

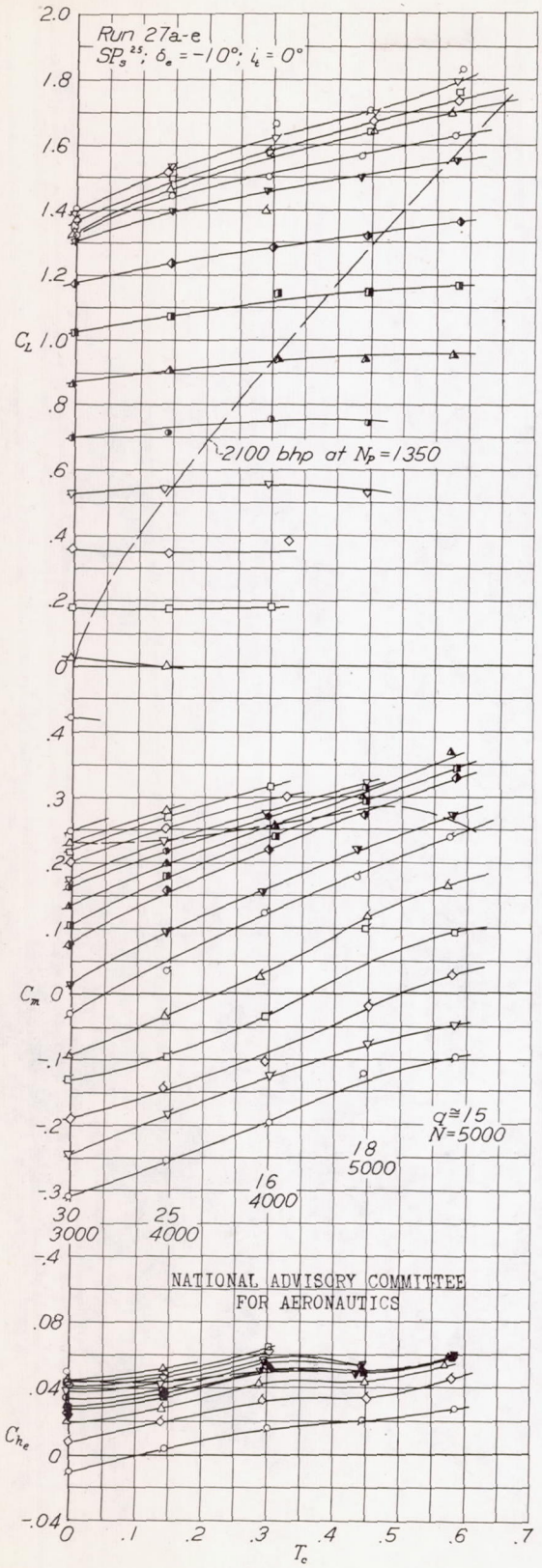

Figure 11.- Effect of thrust coefficient on characteristics of stability model in pitch. Basic configuration, elevator deflected -10°, single rotation, β = 25°.

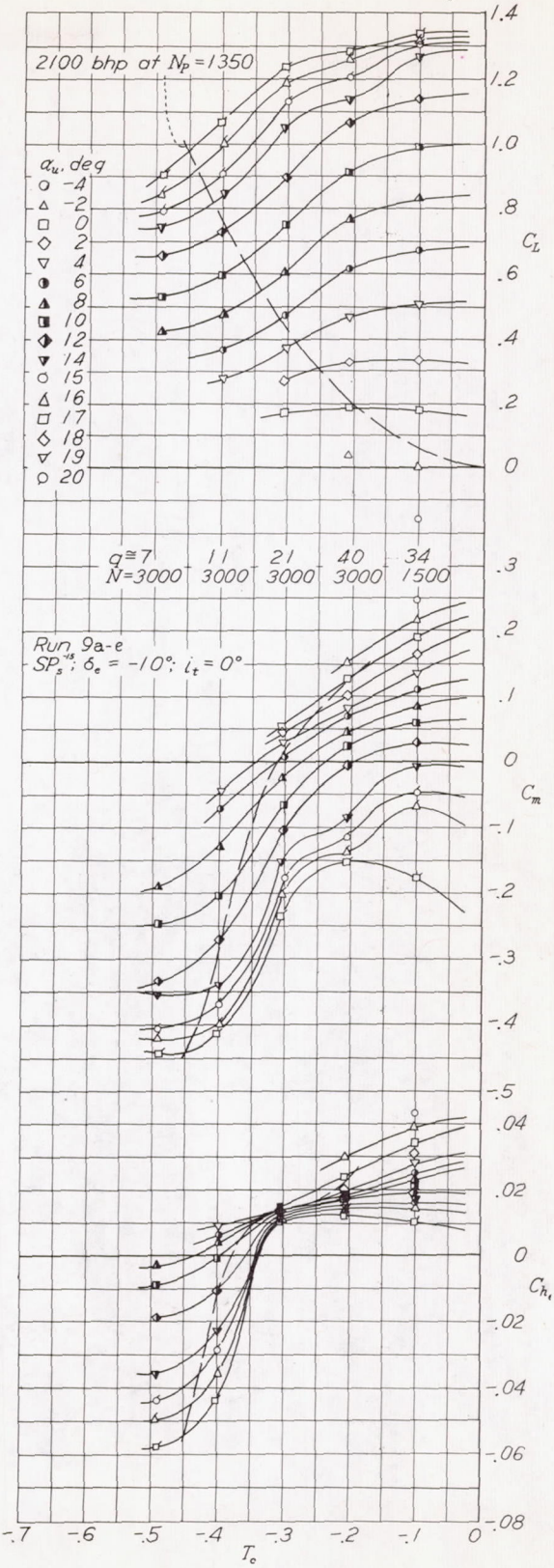

Figure 12.- Effect of thrust coefficient on characteristics of stability model in pitch. Basic configuration, elevator deflected -10°, single rotation, β = -15°.

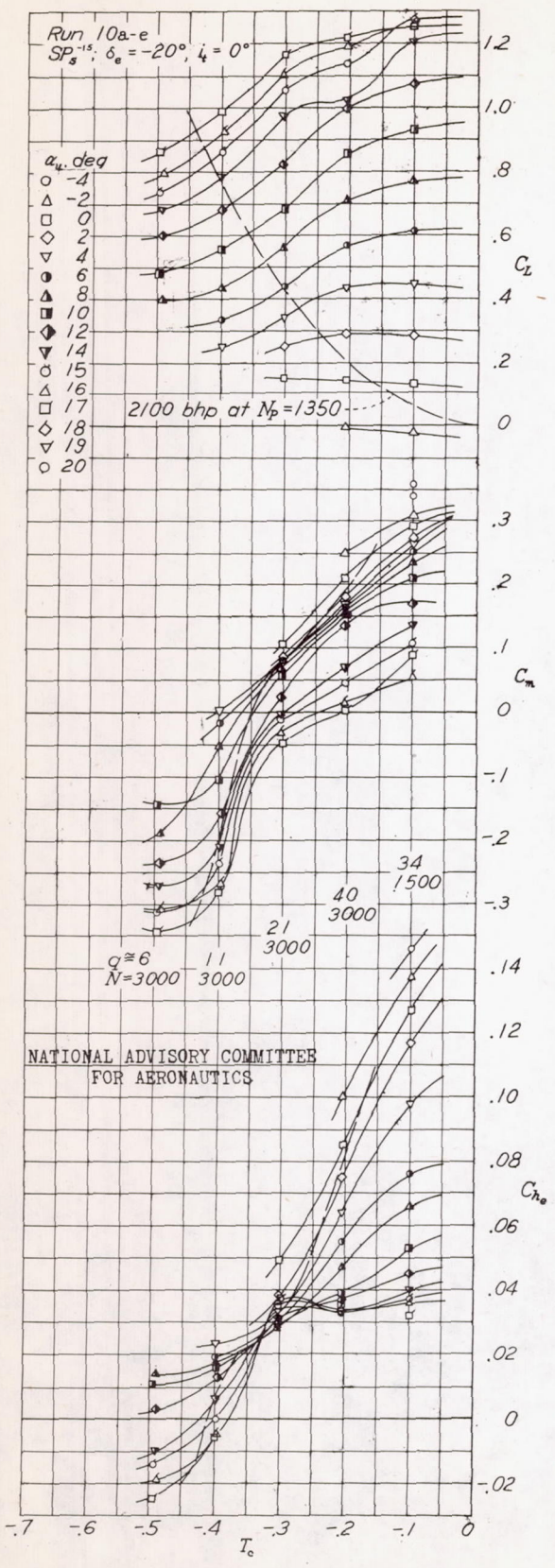

Figure 13.- Effect of thrust coefficient on characteristics of stability model in pitch. Basic configuration, elevator deflected -20°, single rotation, β = -15°.

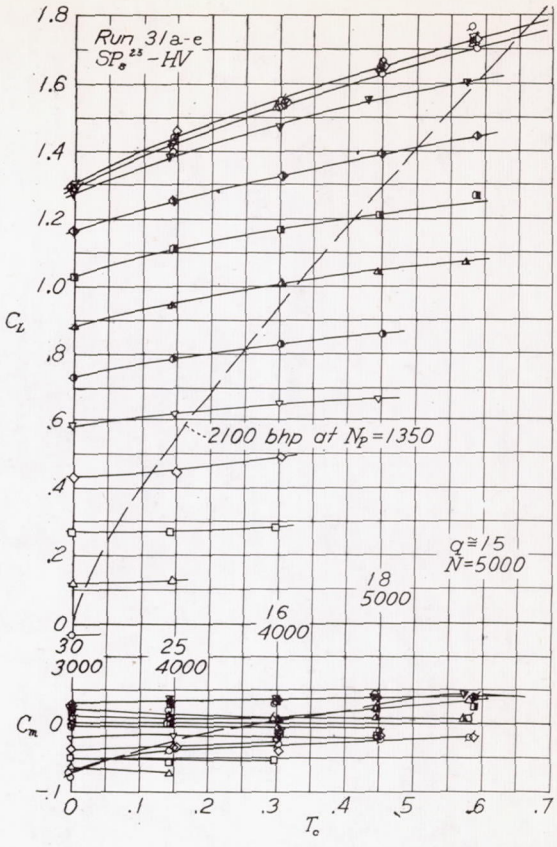

Figure 14.- β = 25°.

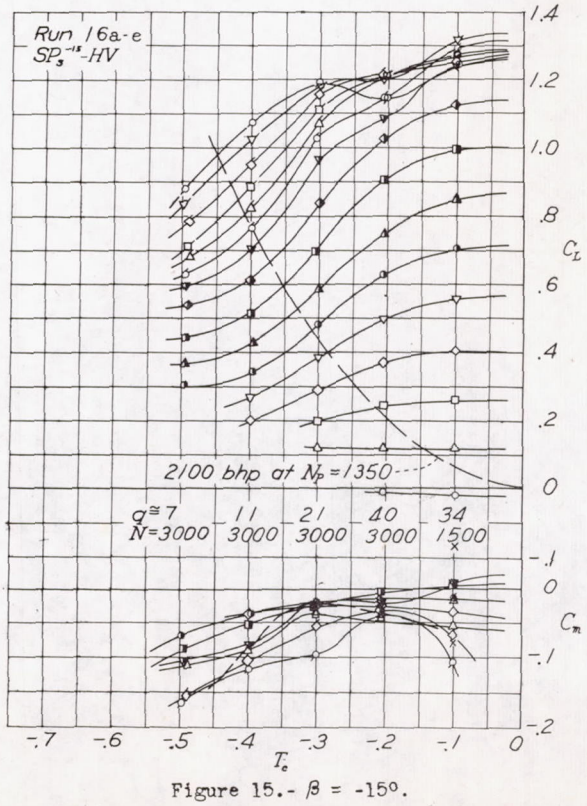

Figure 15.- β = -15°.

Figures 14 and 15.- Effect of thrust coefficient on characteristics of stability model. Basic configuration with tail removed, single rotation.

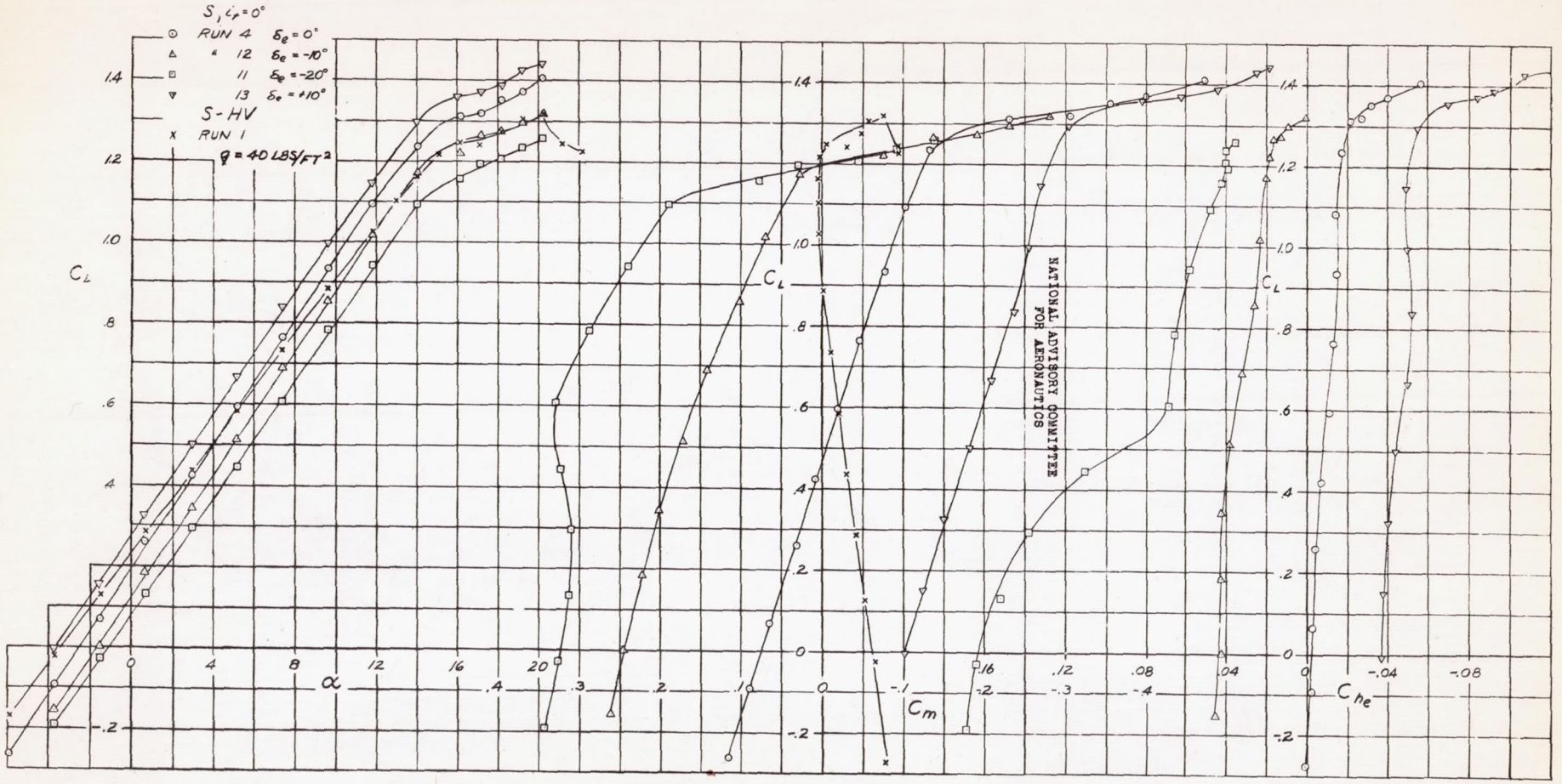

FIGURE 16.- EFFECT OF ELEVATOR DEFLECTION ON CHARARACTERISTICS OF STABILITY MODEL IN PITCH. BASIC CONFIGURATION WITH PROPELLERS REMOVED.

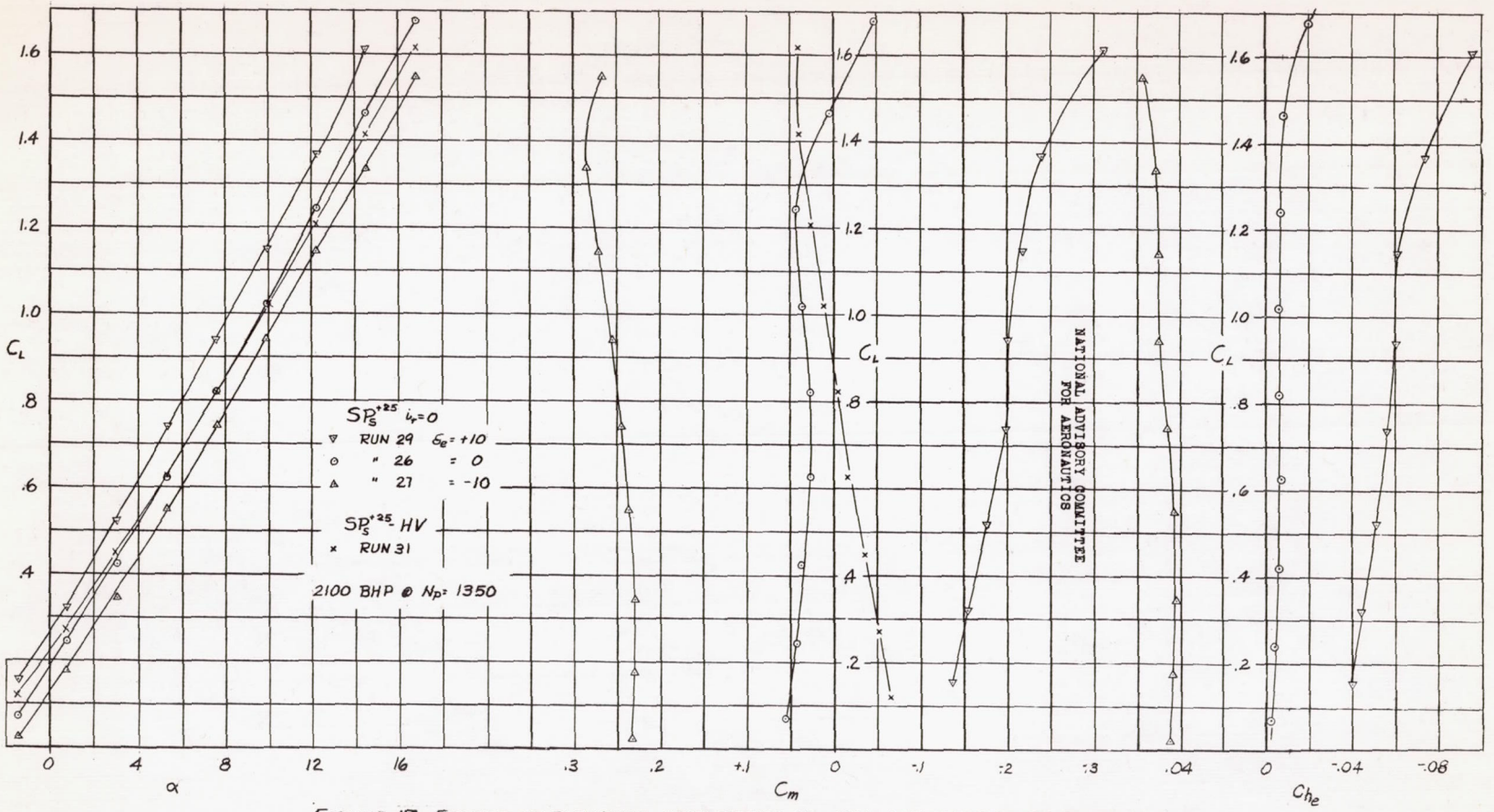

FIGURE 17.- EFFECT OF ELEVATOR DEFLECTION ON CHARACTERISTICS OF STABILITY MODEL IN PITCH. BASIC CONFIGURATION, SINGLE ROTATION, β = 25° RATED POWER.

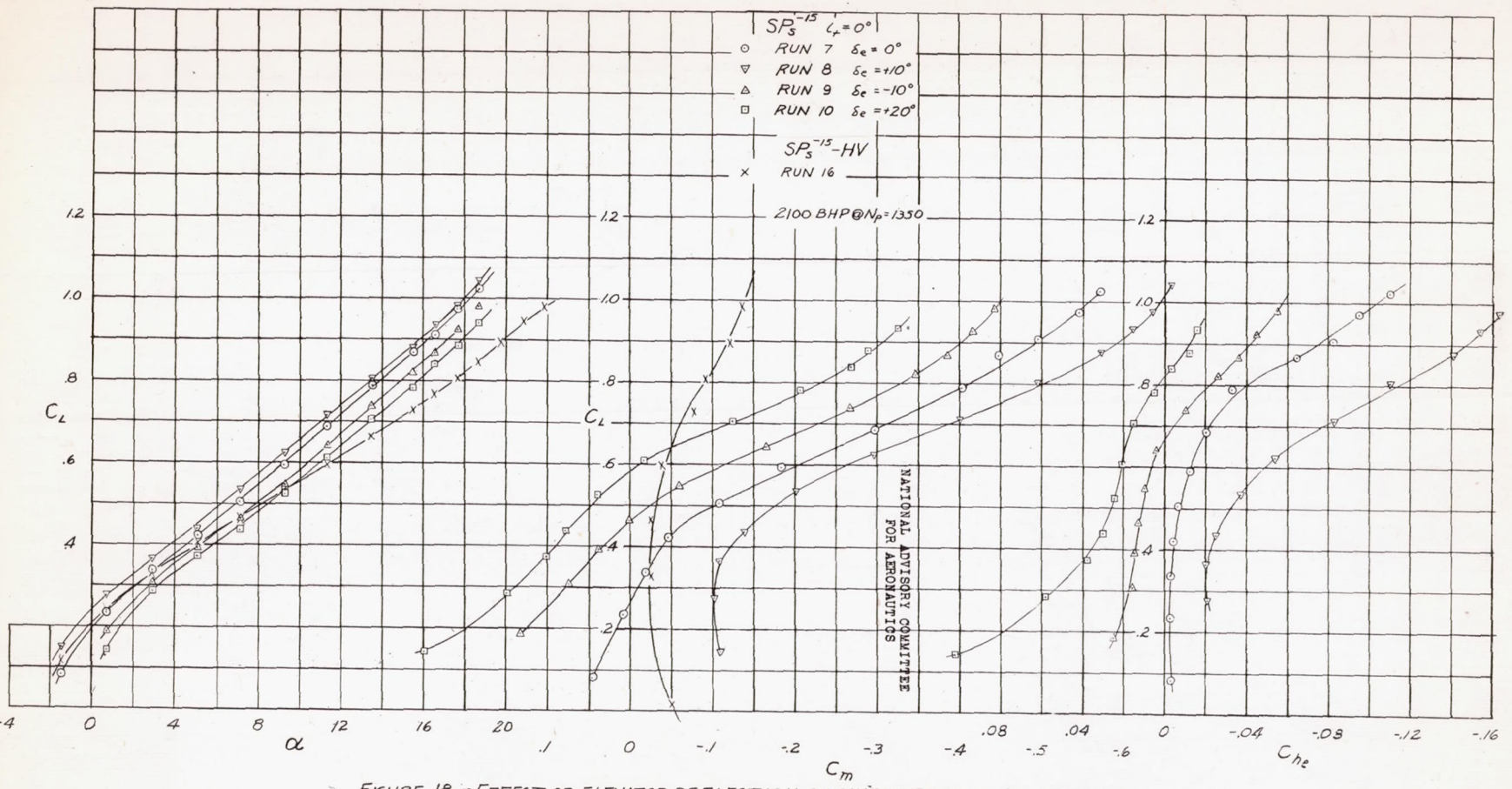

FIGURE 18.- EFFECT OF ELEVATOR DEFLECTION ON CHARACTERISTICS OF STABILITY. MODEL IN PITCH. BASIC CONFIGURATION, SINGLE ROTATION, β=-15°, RATED POWER.

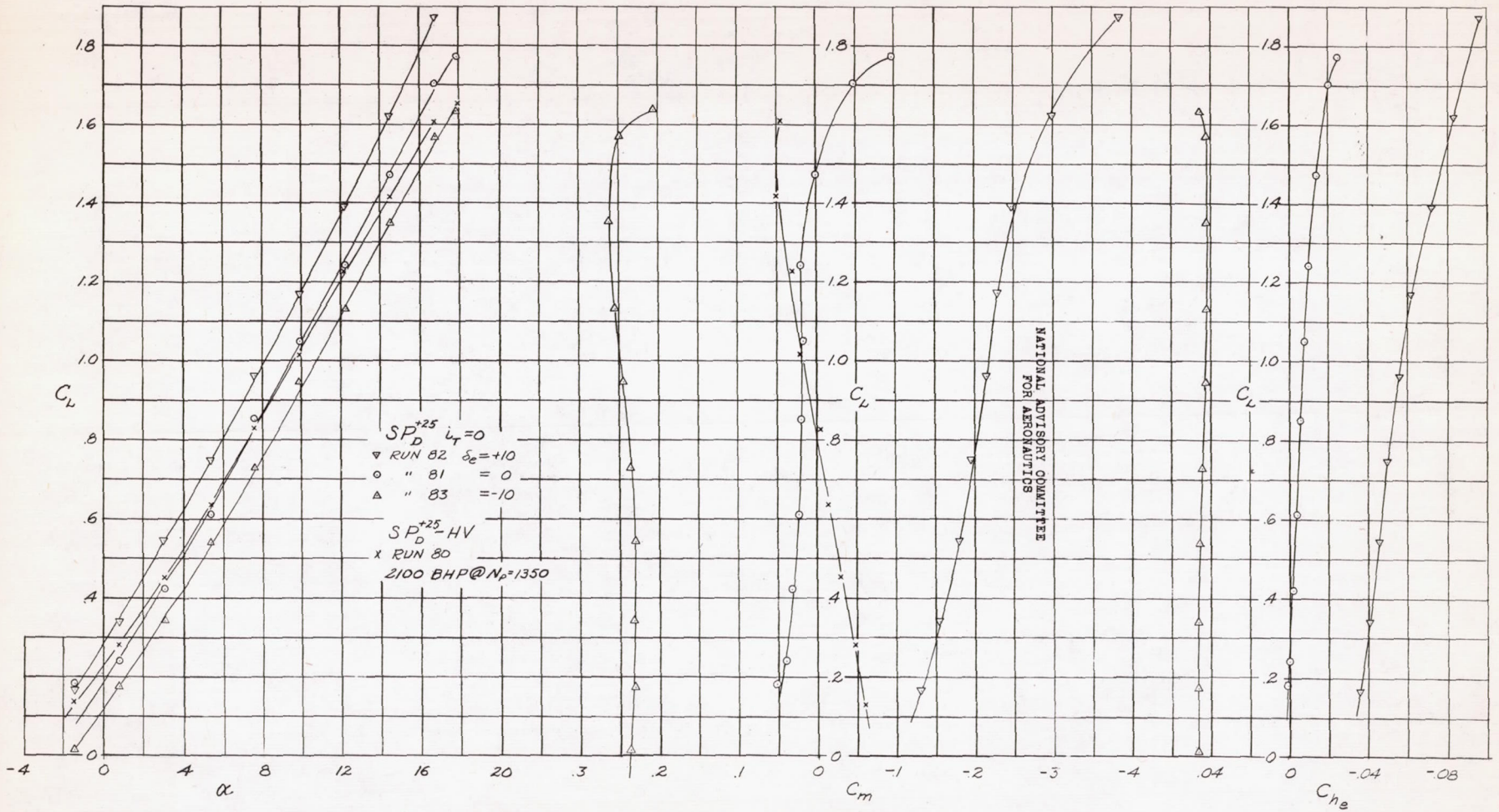

FIGURE 19.-EFFECT OF ELEVATOR DEFLECTION ON CHARACTERISTICS OF STABILITY MODEL IN PITCH. BASIC CONFIGURATION, DUAL ROTATION, β= 25°, RATED POWER.

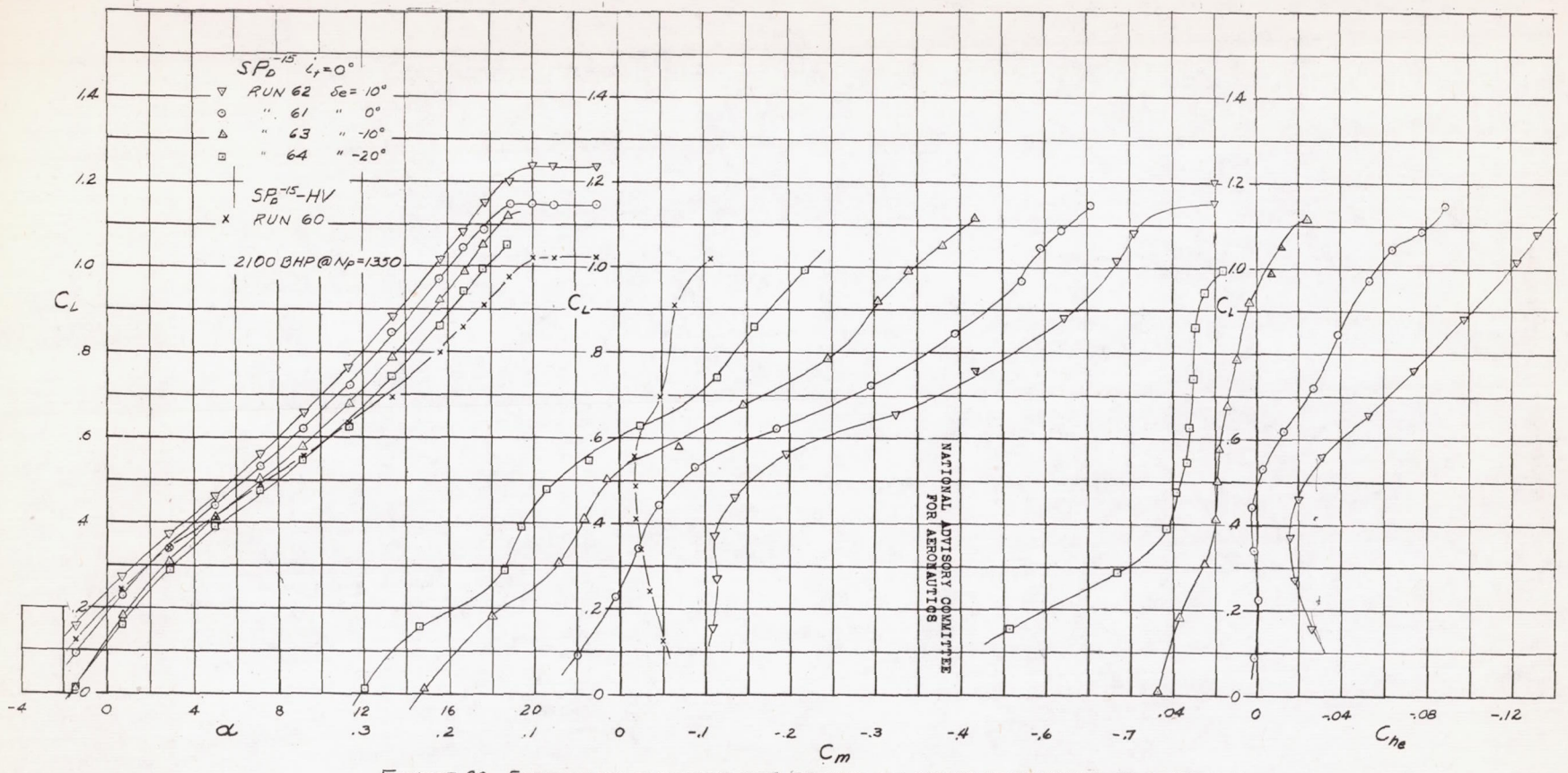

FIGURE 20.- EFFECT OF ELEVATOR DEFLECTION ON CHARACTERISTICS OF STABILITY MODEL IN PITCH. BASIC CONFIGURATION, DUAL ROTATION, $\beta=-15°$, RATED POWER.

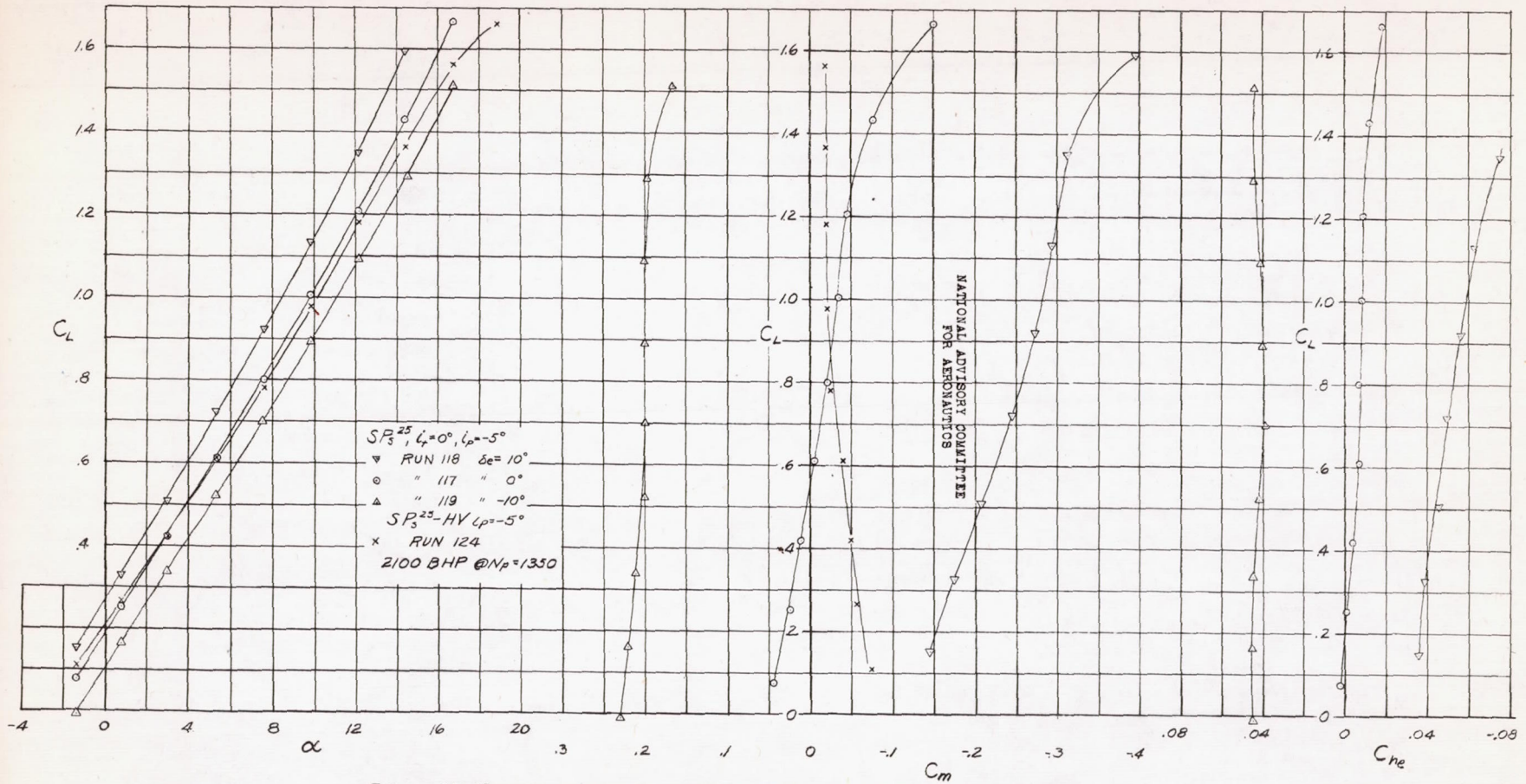

FIGURE 21.- EFFECT OF ELEVATOR DEFLECTION ON CHARACTERISTICS OF STABILITY MODEL IN PITCH. THRUST AXIS TILTED 5°, SINGLE ROTATION, β= 25°, RATED POWER.

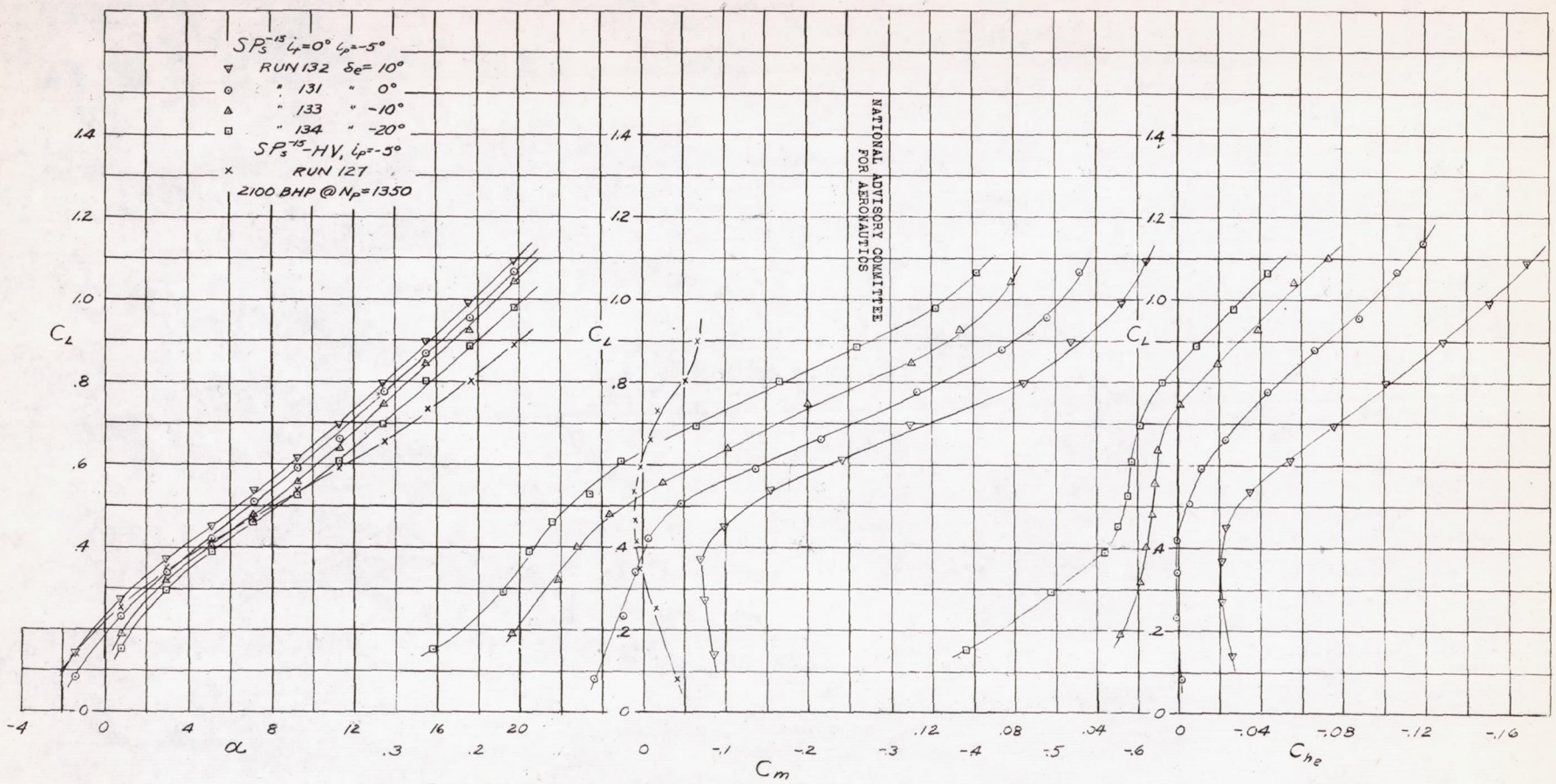

FIGURE 22 - EFFECT OF ELEVATOR DEFLECTION ON CHARACTERISTICS OF STABILITY MODEL IN PITCH. THRUST AXIS TILTED 5°, SINGLE ROTATION, β=-15°, RATED POWER.

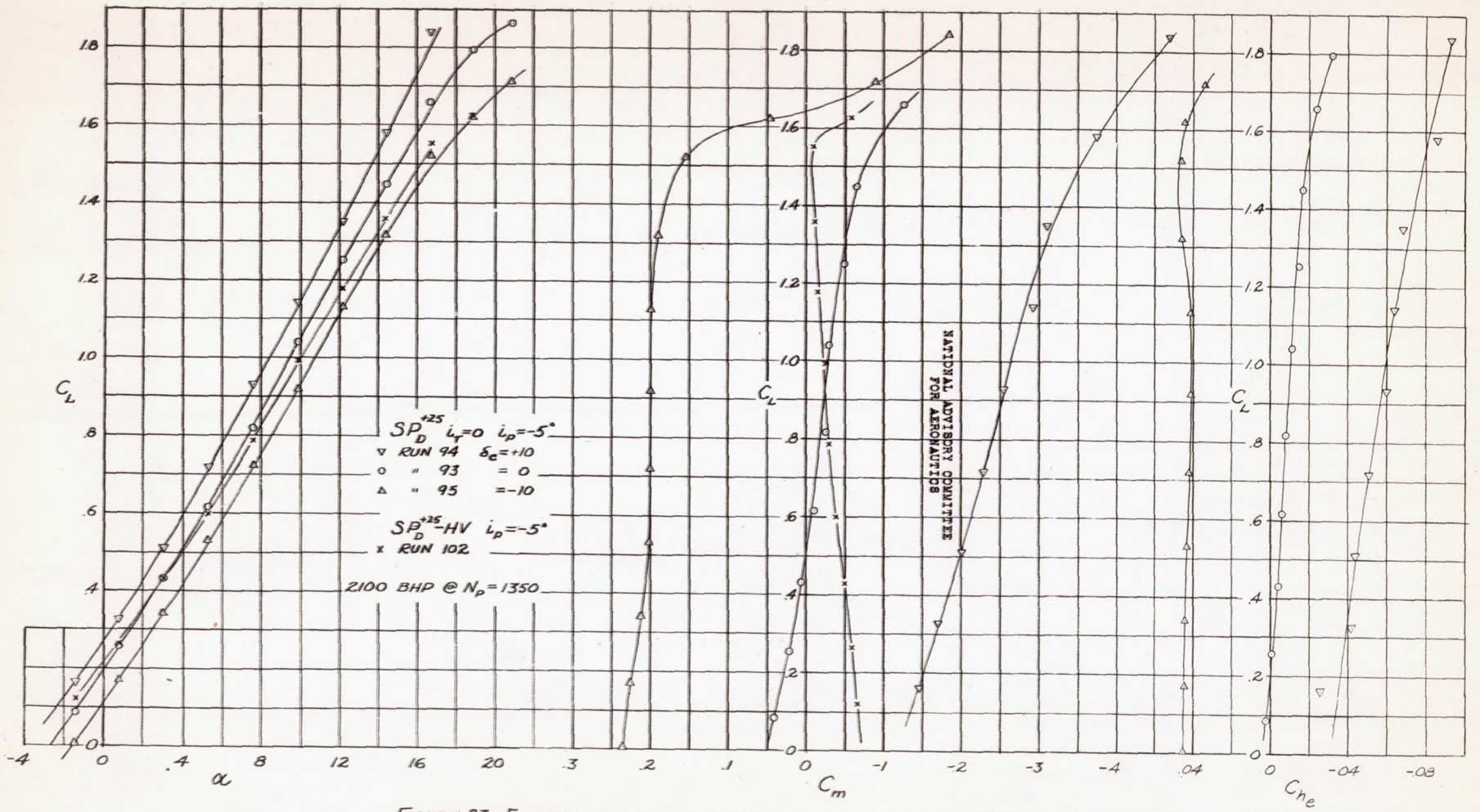

FIGURE 23.-EFFECT OF ELEVATOR DEFLECTION ON CHARACTERISTICS OF STABILITY MODEL IN PITCH. THRUST AXIS TILTED 5°, DUAL ROTATION, β = 25° RATED POWER.

Fig. 23

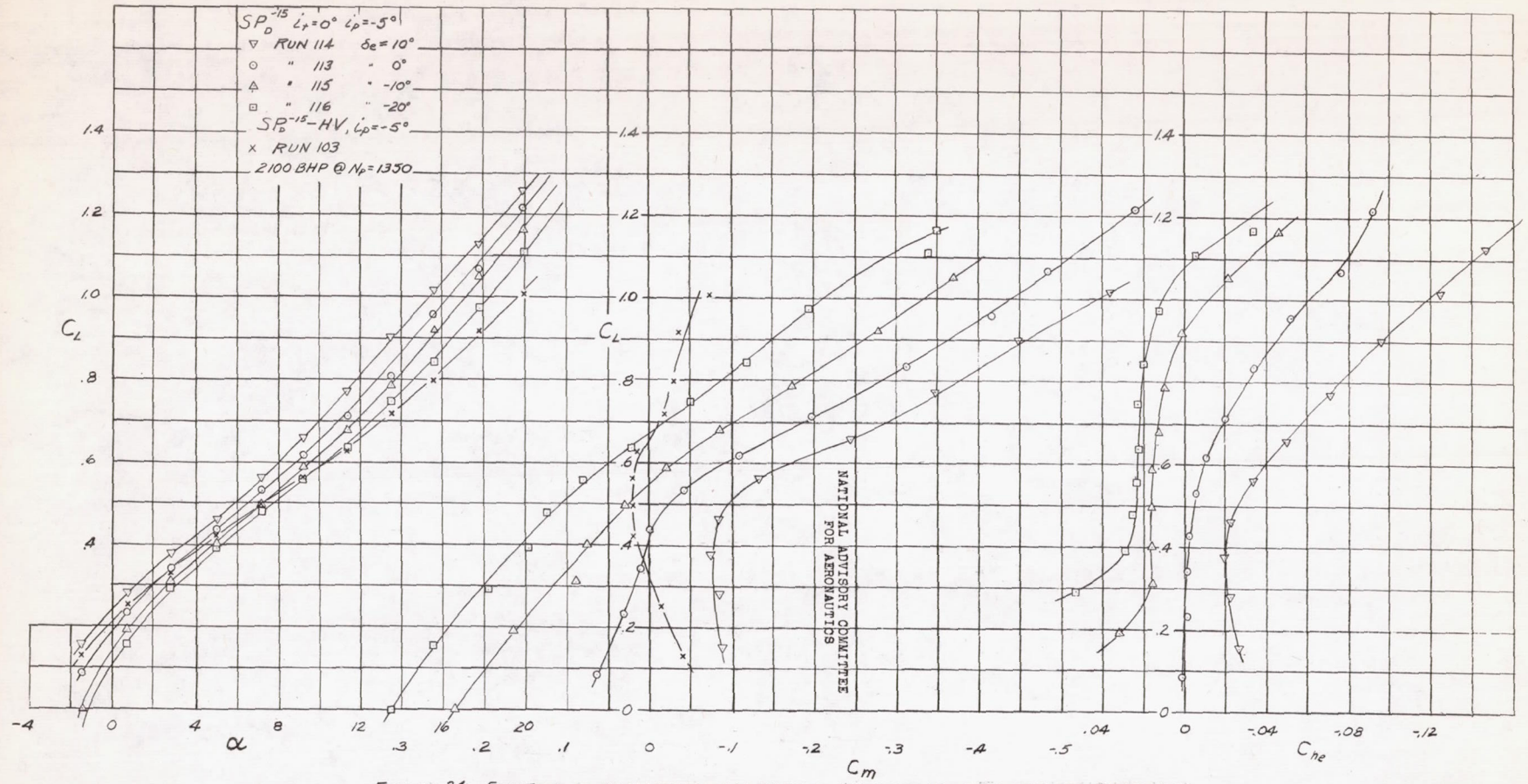

FIGURE 24.-EFFECT OF ELEVATOR DEFLECTION ON CHARACTERISTICS OF STABILITY MODEL IN PITCH. THRUST AXIS TILTED 5°, DUAL ROTATION, β=-15°, RATED POWER.

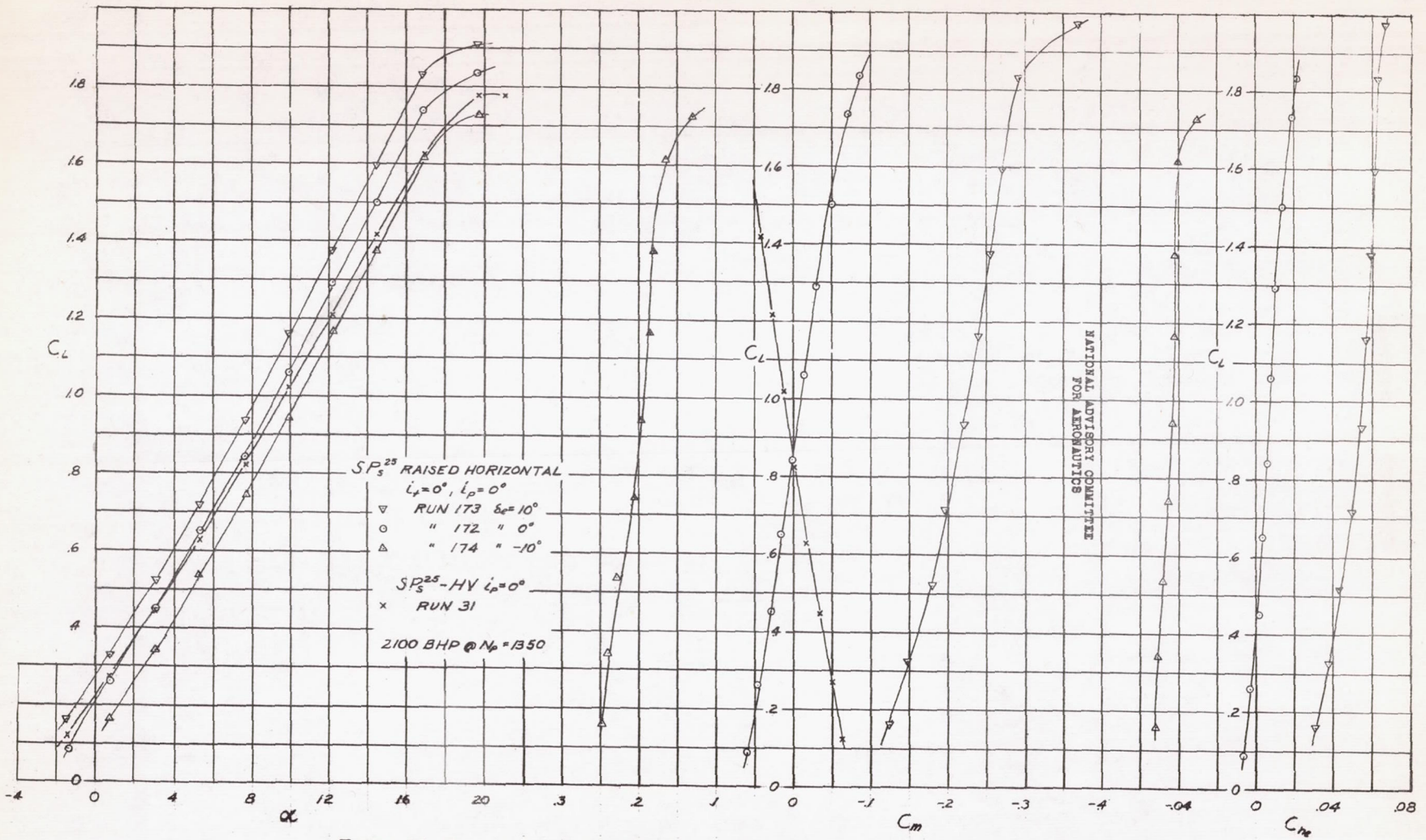

FIGURE 25.- EFFECT OF ELEVATOR DEFLECTION ON CHARACTERISTICS OF STABILITY MODEL IN PITCH. RAISED HORIZONTAL TAIL, SINGLE ROTATION β= 25°, RATED POWER.

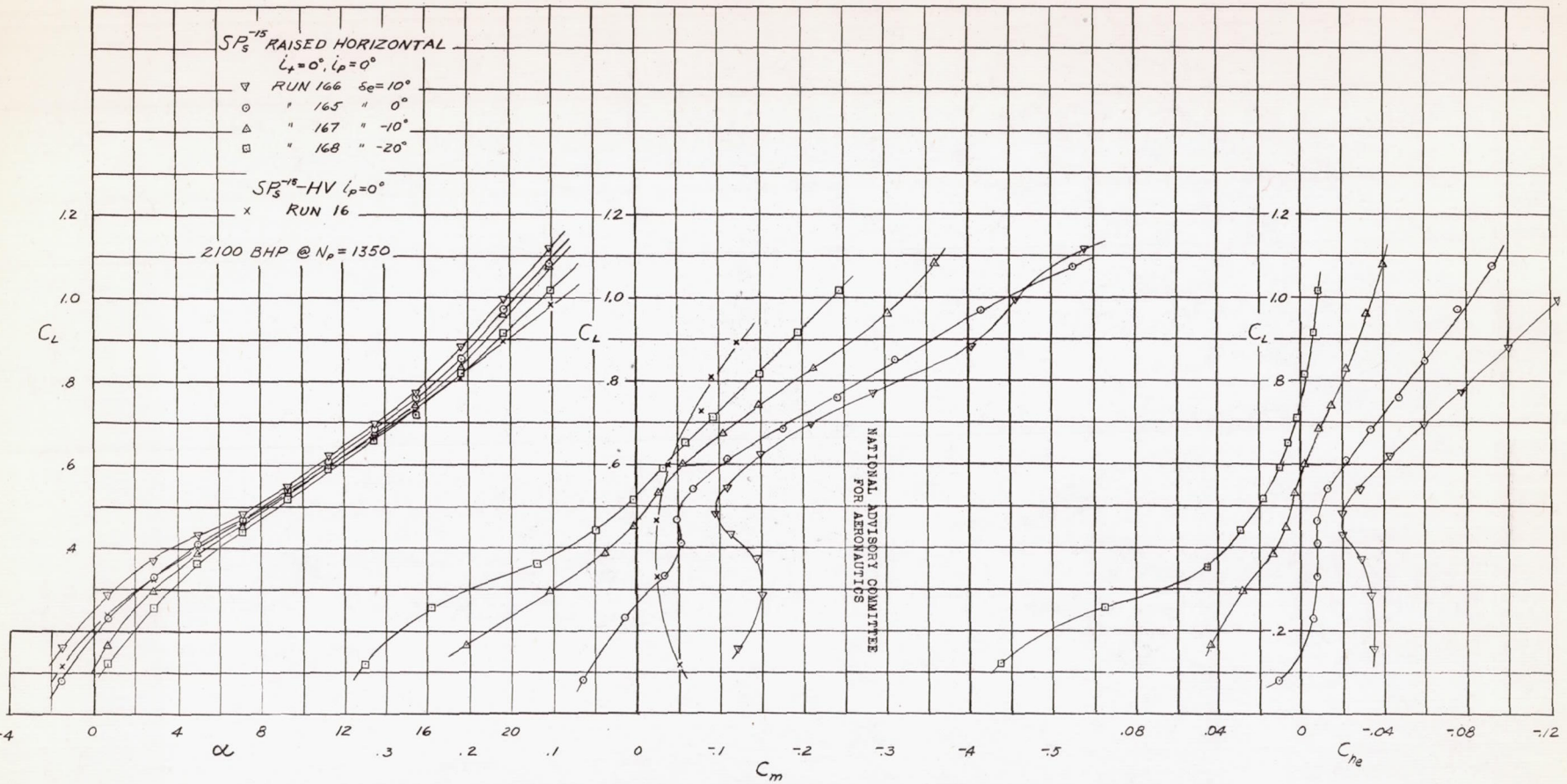

FIGURE 26.-EFFECT OF ELEVATOR DEFLECTION ON CHARACTERISTICS OF STABILITY MODEL IN PITCH. RAISED HORIZONTAL TAIL, SINGLE ROTATION, $\beta = -15°$, RATED POWER.

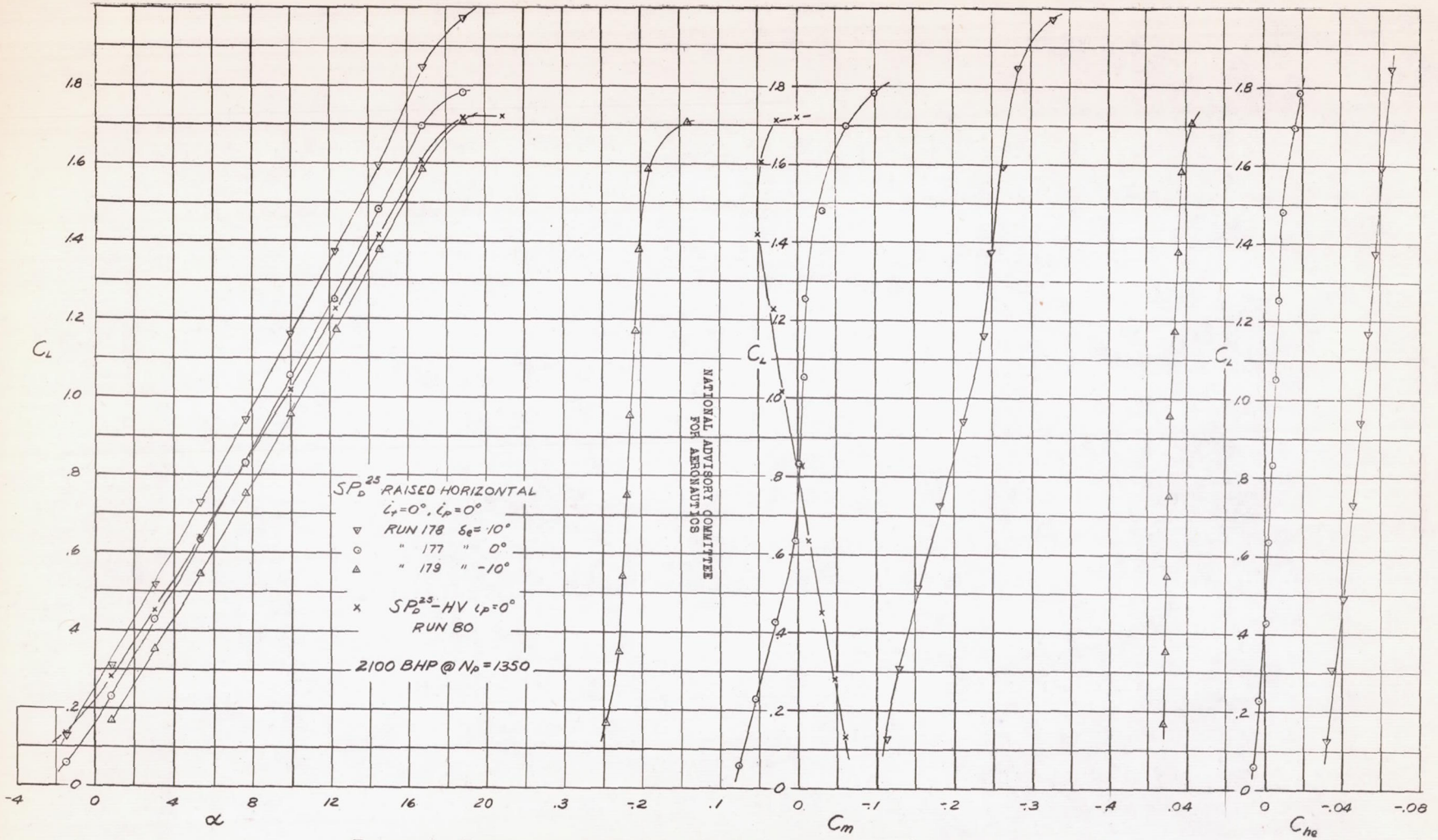

FIGURE 27-EFFECT OF ELEVATOR DEFLECTION ON CHARACTERISTICS OF STABILITY MODEL IN PITCH. RAISED HORIZONTAL TAIL, DUAL ROTATION, β= 25°, RATED POWER.

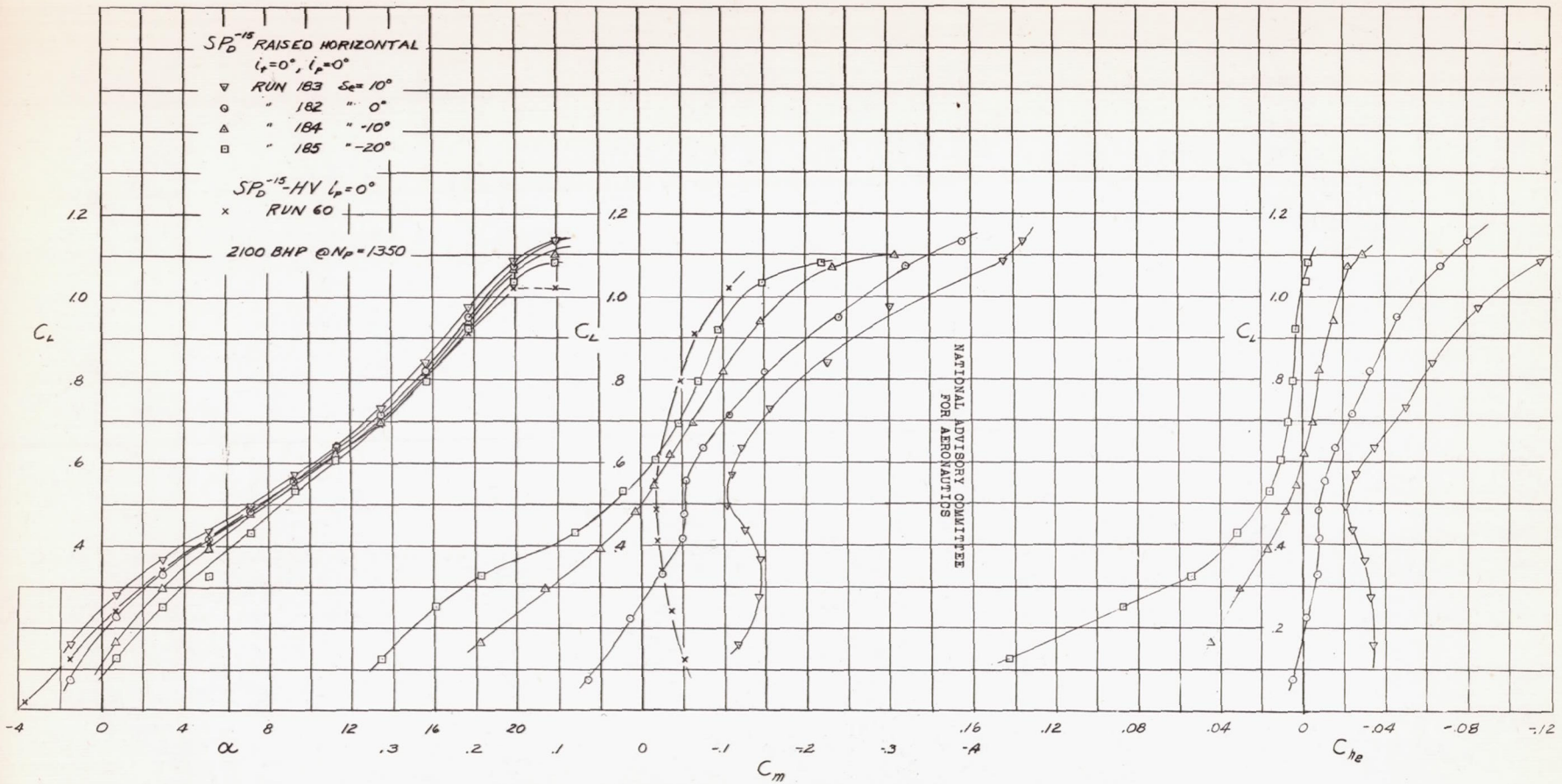

FIGURE 28.-EFFECT OF ELEVATOR DEFLECTION ON CHARACTERISTICS OF STABILITY MODEL IN PITCH. RAISED HORIZONTAL TAIL, DUAL ROTATION, β=-15°, RATED POWER.

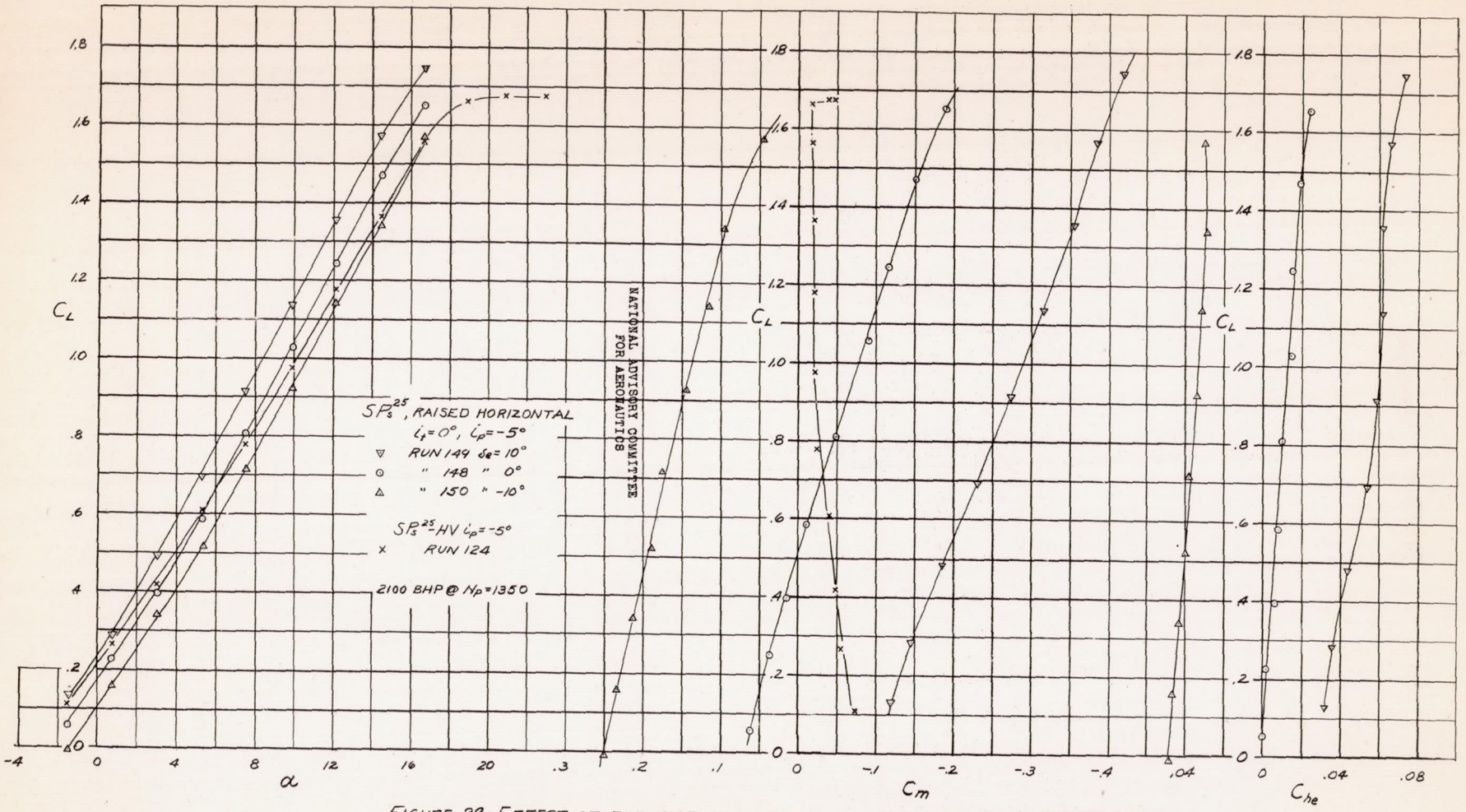

FIGURE 29-EFFECT OF ELEVATOR DEFLECTION ON CHARACTERISTICS OF STABILITY MODEL IN PITCH. RAISED HORIZONTAL TAIL, THRUST AXIS TILTED 5°, SINGLE ROTATION, β = 25°, RATED POWER.

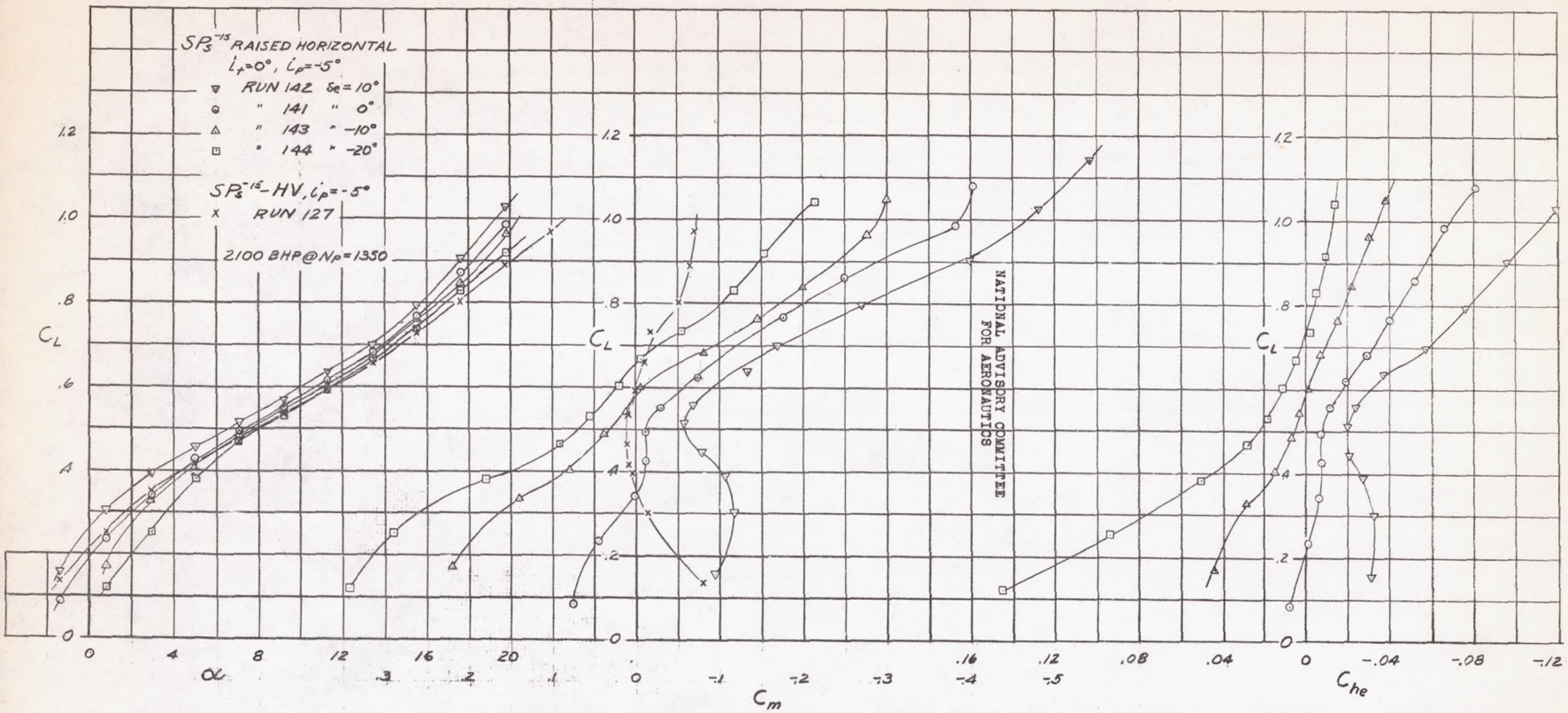

FIGURE 30.-EFFECT OF ELEVATOR DEFLECTION ON CHARACTERISTICS OF STABILITY MODEL IN PITCH. RAISED HORIZONTAL TAIL, THRUST AXIS TILTED 5°, SINGLE ROTATION, $\beta = -15°$, RATED POWER.

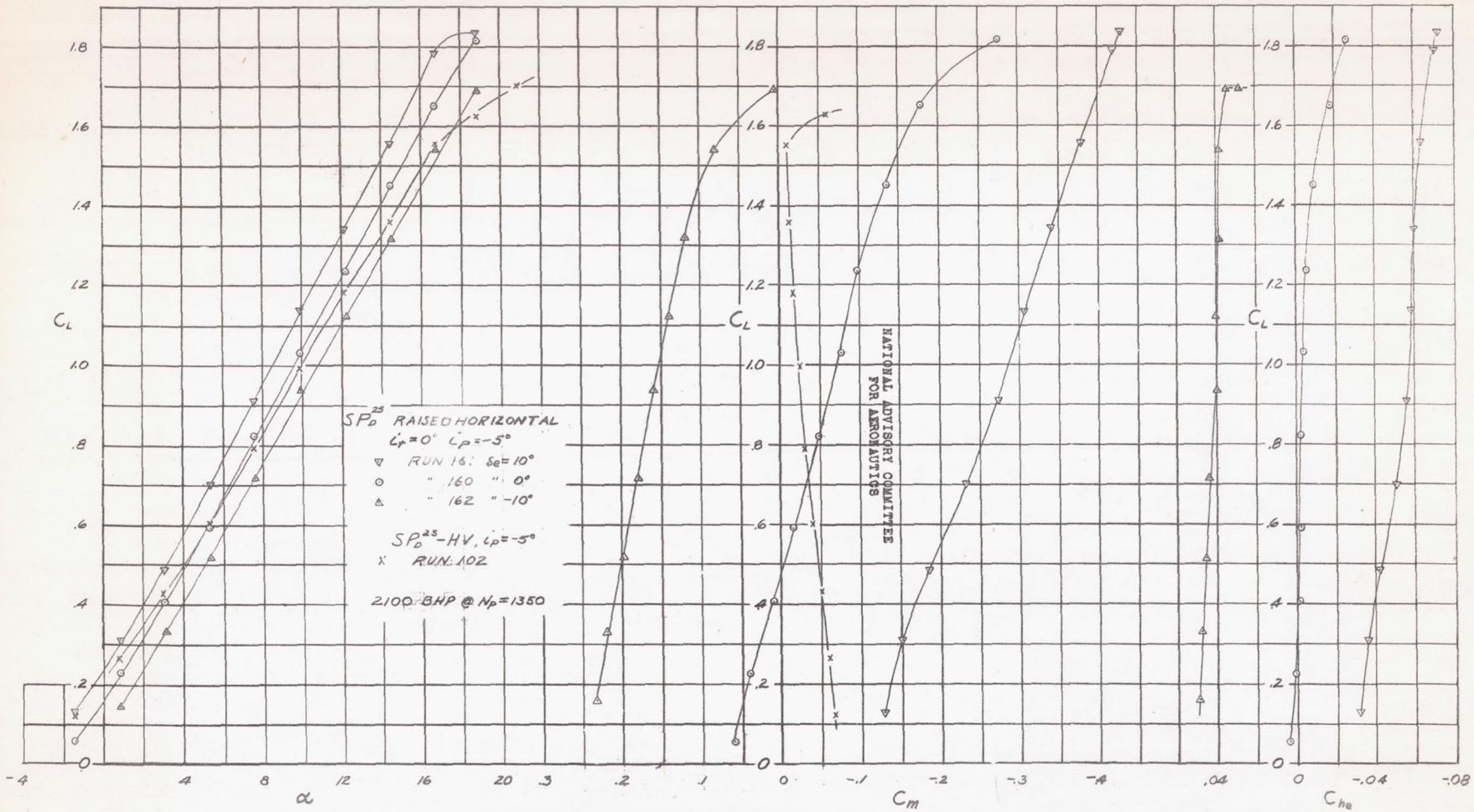

FIGURE 31.- EFFECT OF ELEVATOR DEFLECTION ON CHARACTERISTICS OF STABILITY MODEL IN PITCH. RAISED HORIZONTAL, THRUST AXIS TILTED 5°, DUAL ROTATION, β = 25°, RATED POWER.

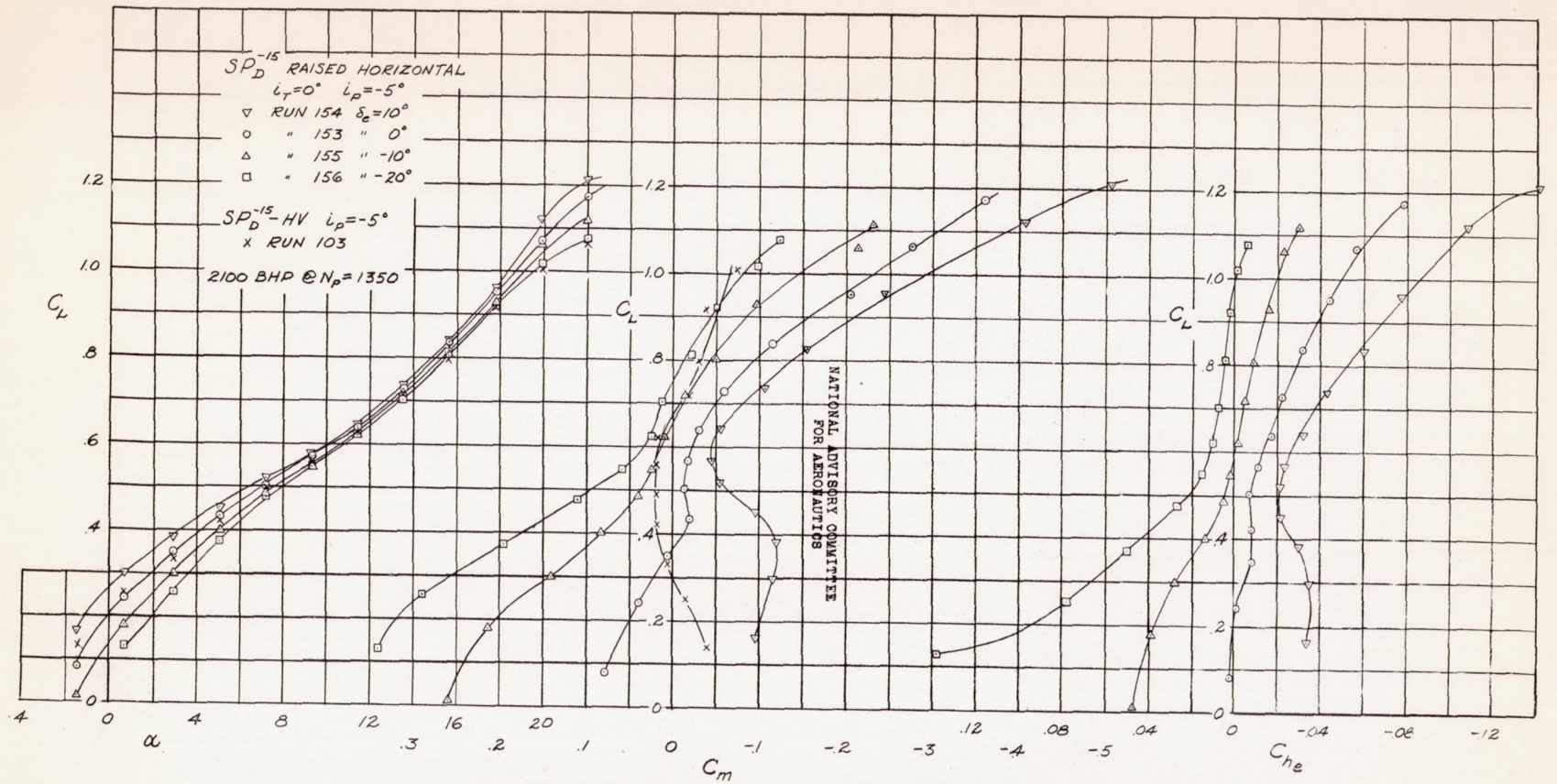

FIGURE 32-EFFECT OF ELEVATOR DEFLECTION ON CHARACTERISTICS OF STABILTY MODEL IN PITCH. RAISED HORIZONTAL, THRUST AXIS TILTED 5°, DUAL ROTATION, β=-15°, RATED POWER.

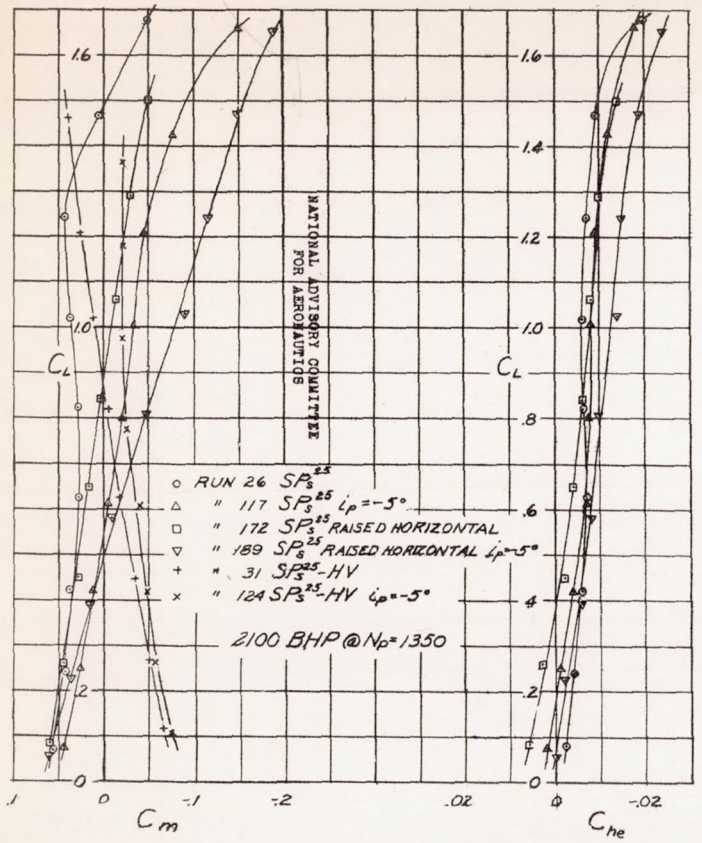

FIGURE 33.- EFFECT OF CONFIGURATION CHANGES ON CHARACTERISTICS OF STABILITY MODEL IN PITCH. SINGLE ROTATION, $\beta = 25°$, RATED POWER, ELEVATOR UNDEFLECTED.

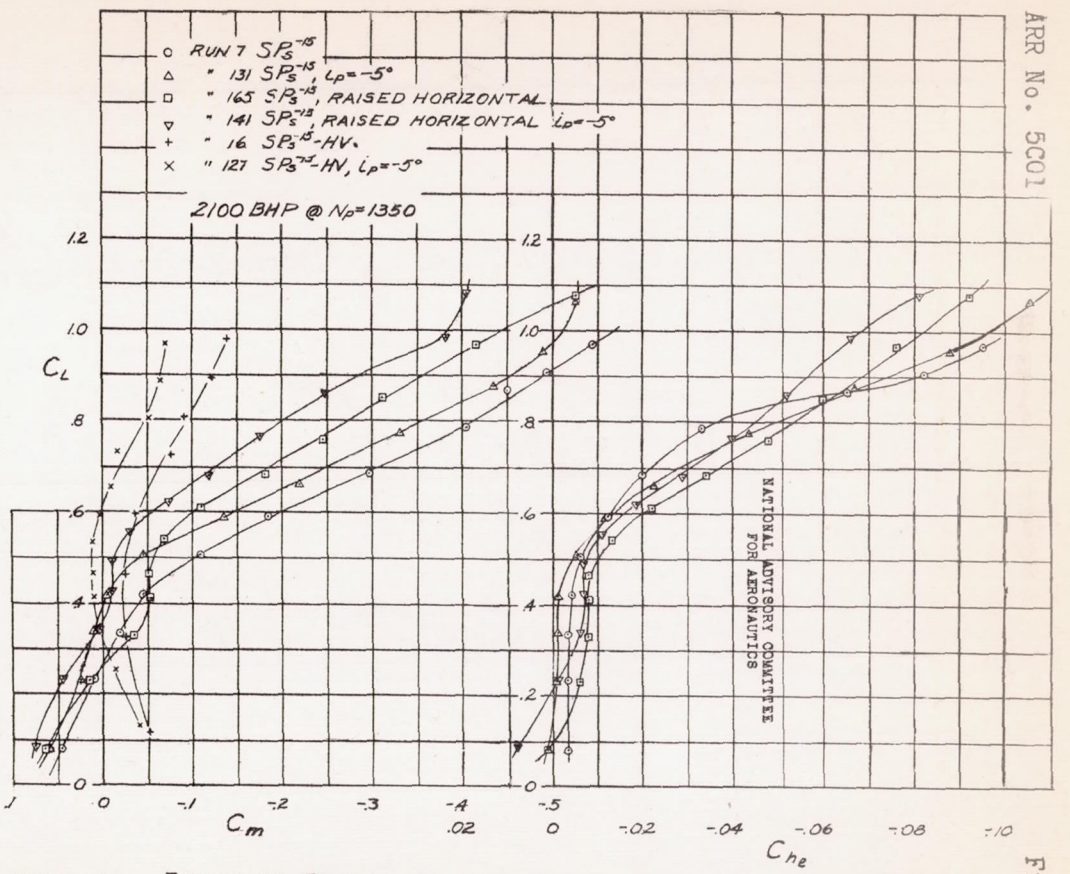

FIGURE 34.- EFFECT OF CONFIGURATION CHANGES ON CHARACTERISTICS OF STABILITY MODEL IN PITCH. SINGLE ROTATION, $\beta = -15°$, RATED POWER, ELEVATOR UNDEFLECTED.

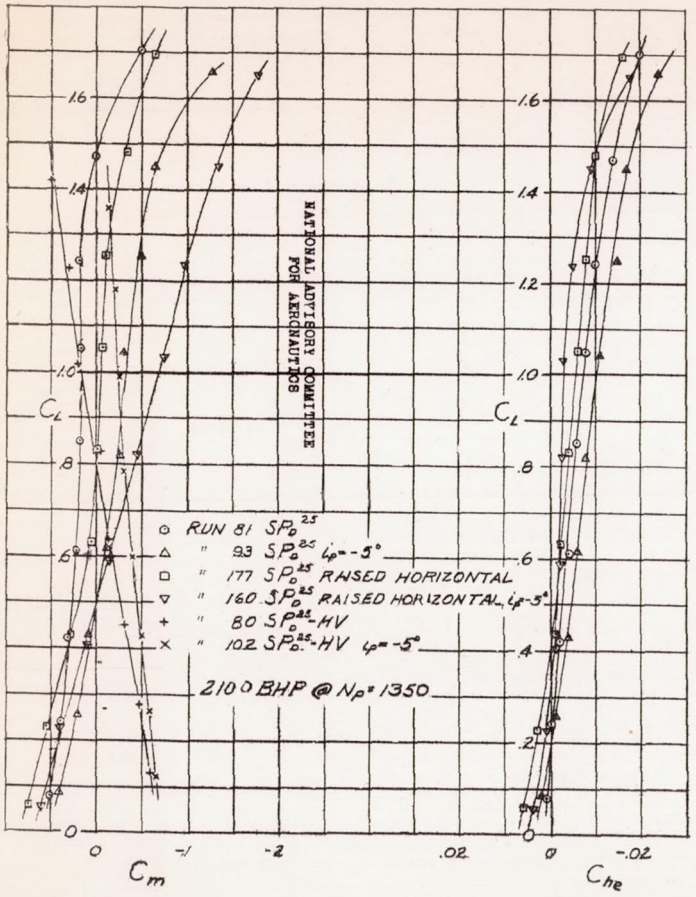

FIGURE 35.- EFFECT OF CONFIGURATION CHANGES ON CHARACTERISTICS OF STABILITY MODEL IN PITCH. DUAL ROTATION, β = 25° RATED POWER, ELEVATOR UNDEFLECTED

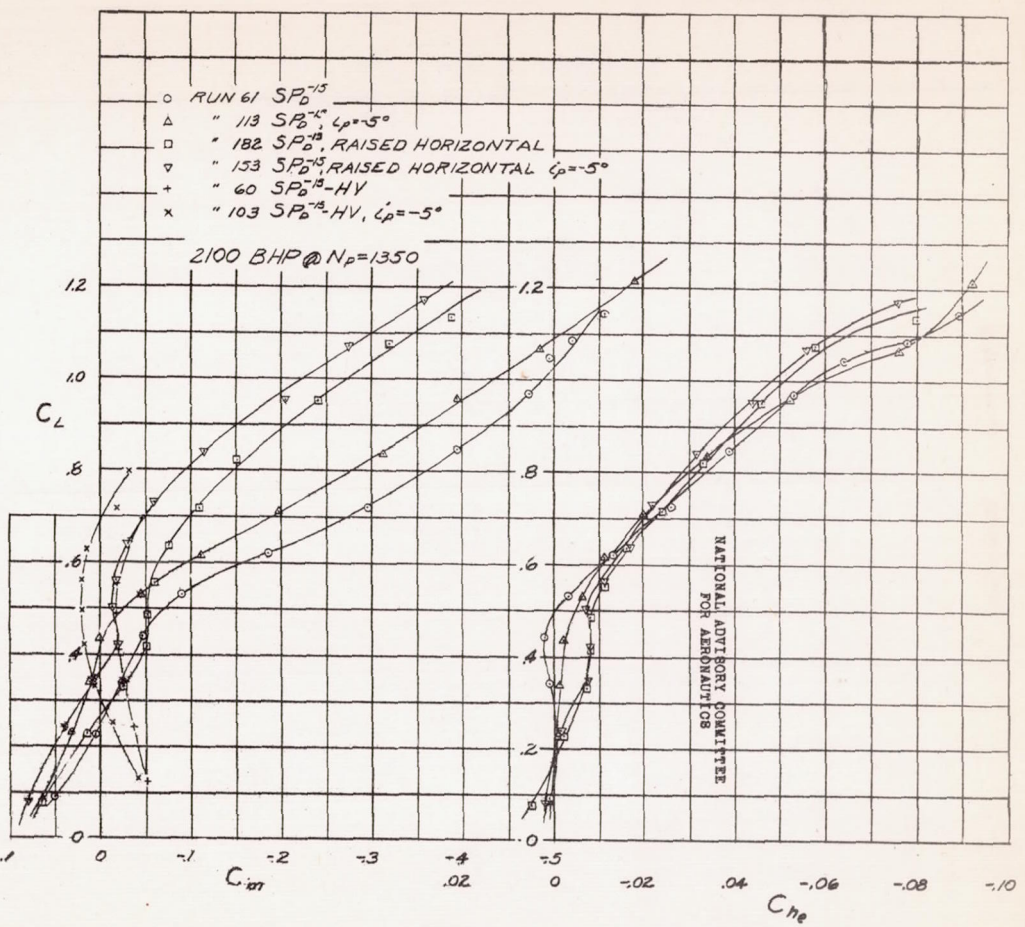

FIGURE 36.-EFFECT OF CONFIGURATION CHANGES ON CHARACTERISTICS OF STABILITY MODEL IN PITCH. DUAL ROTATION, β = -15°, RATED POWER, ELEVATOR UNDEFLECTED.

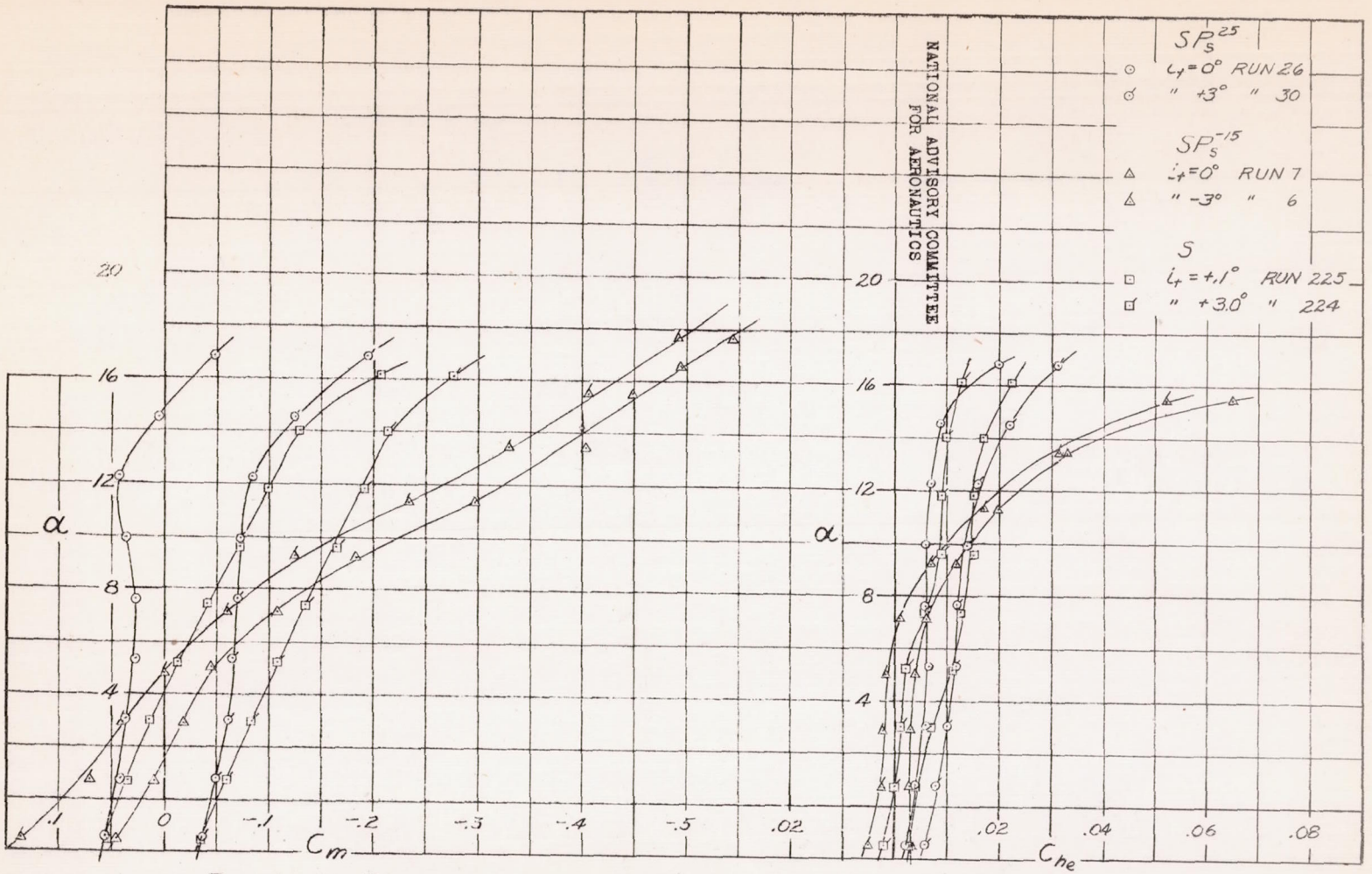

FIGURE 37-EFFECT OF TAIL INCIDENCE ON CHARACTERISTICS OF STABILITY MODEL IN PITCH. BASIC CONFIGURATION, SINGLE ROTATION, β= 25° AND -15°, RATED POWER, AND PROPELLER REMOVED, ELEVATOR UNDEFLECTED.

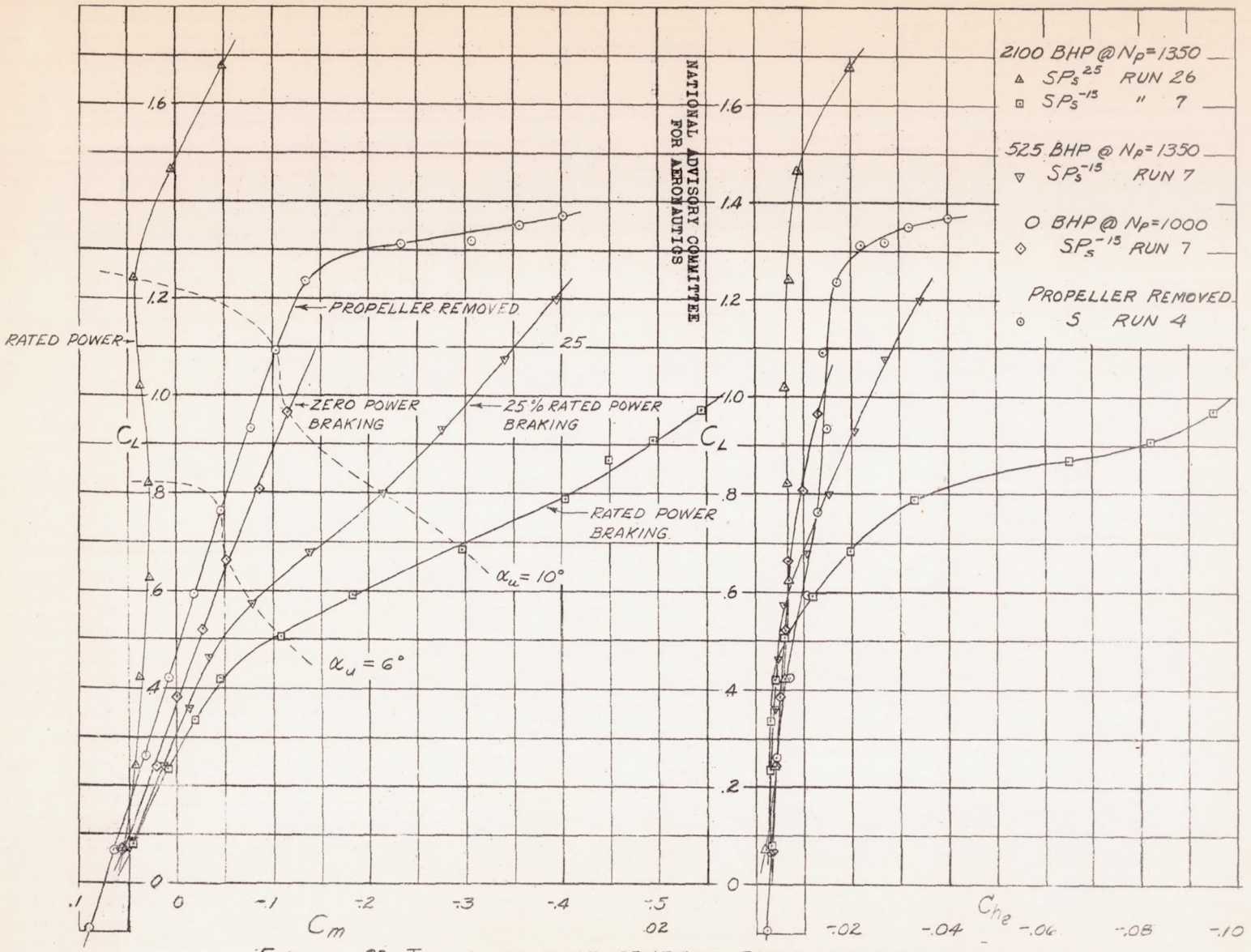

FIGURE 38.- THE EFFECTS OF SEVERAL POWER CONDITIONS, POSITIVE AND NEGATIVE THRUST, ON THE CHARACTERISTICS OF THE STABILITY MODEL IN PITCH. BASIC CONFIGURATION, ELEVATOR UNDEFLECTED.

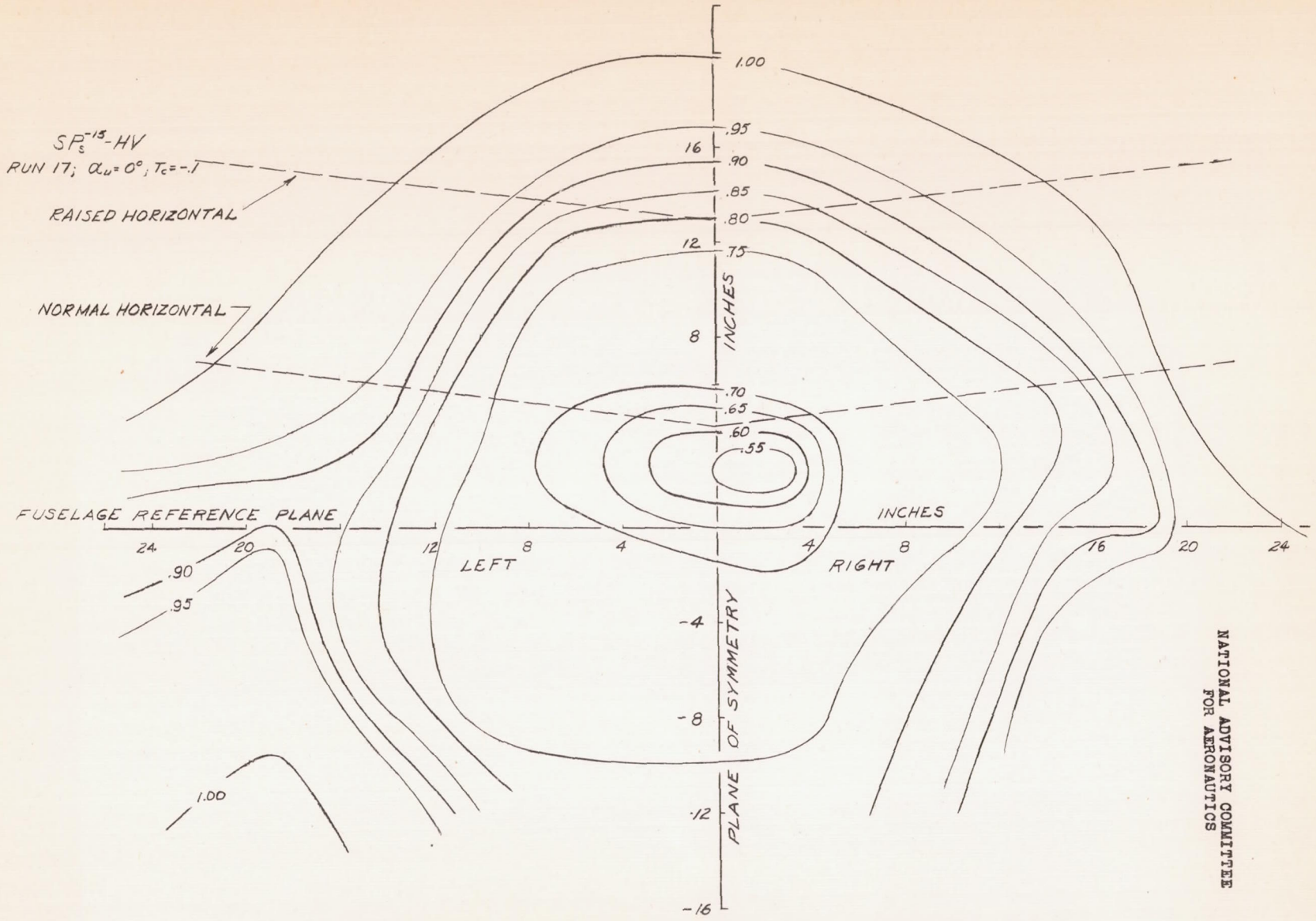

(a) $T_c = -0.1$

FIGURE 39.- VELOCITY CONTOURS IN THE VICINITY OF THE HORIZONTAL TAIL OF THE STABILITY MODEL. SINGLE ROTATION, $\beta = -15°$, $\alpha_u = 0°$, $T_c = -0.1$.

NATIONAL ADVISORY COMMITTEE FOR AERONAUTICS

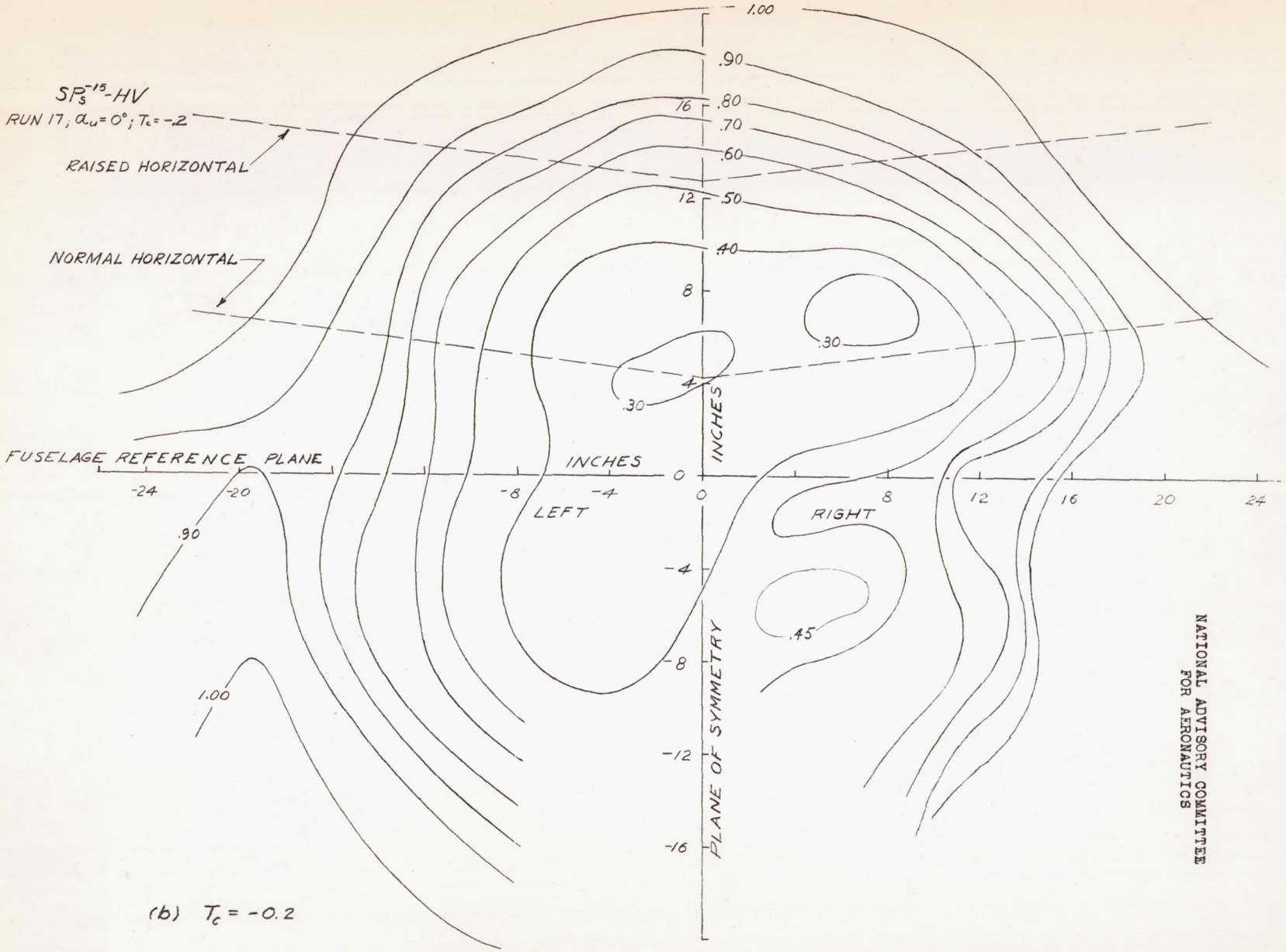

(b) $T_c = -0.2$

FIGURE 39.- CONCLUDED. STABILITY MODEL.

NATIONAL ADVISORY COMMITTEE FOR AERONAUTICS

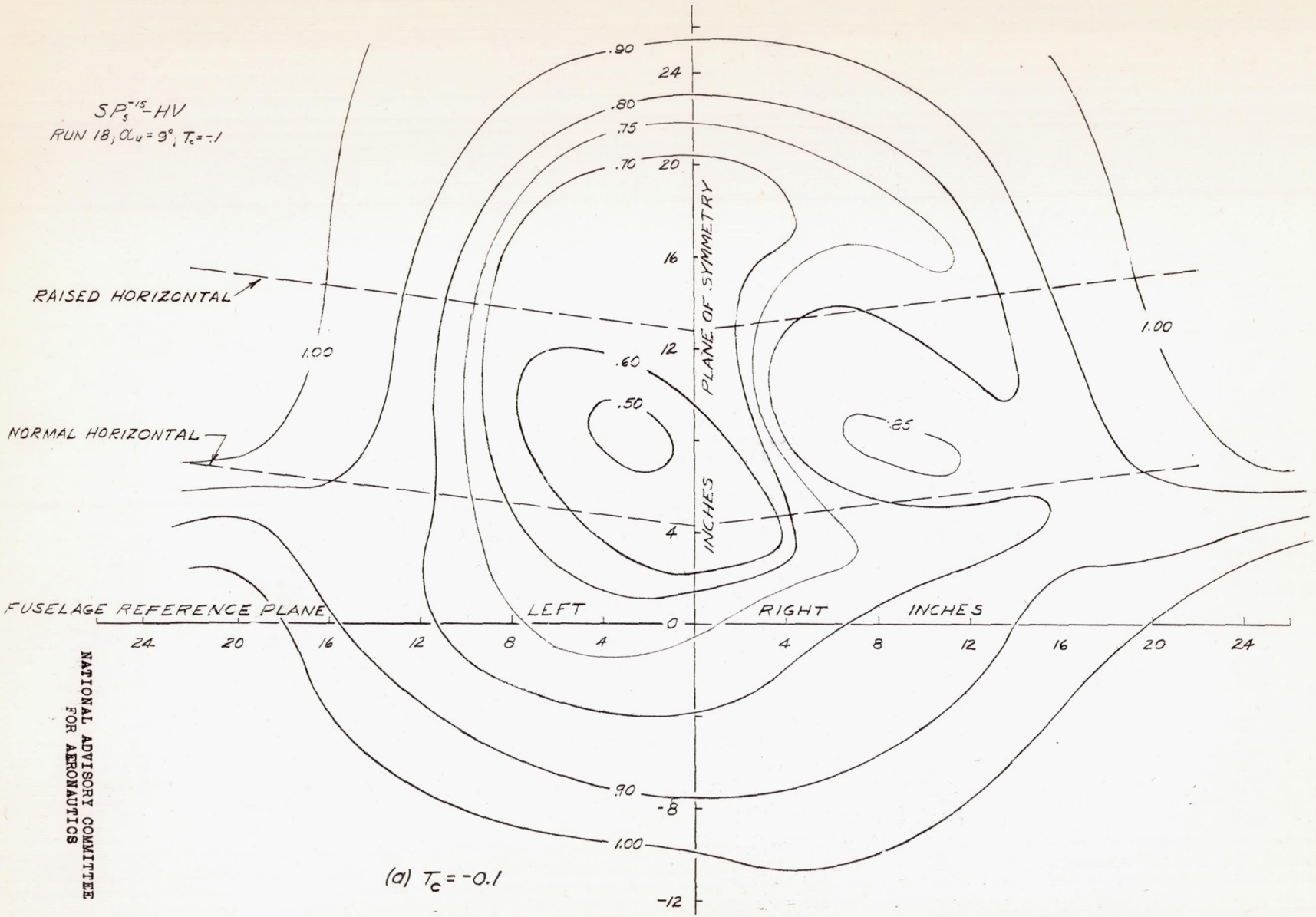

(a) $T_c = -0.1$

FIGURE 40 - VELOCITY CONTOURS IN THE VICINITY OF THE HORIZONTAL TAIL OF THE STABILITY MODEL. SINGLE ROTATION, $\beta = -15°$, $\alpha_u = 9°$, $T_c = -0.1$.

NATIONAL ADVISORY COMMITTEE FOR AERONAUTICS

NACA ARR NO. 5C01

Fig. 40a

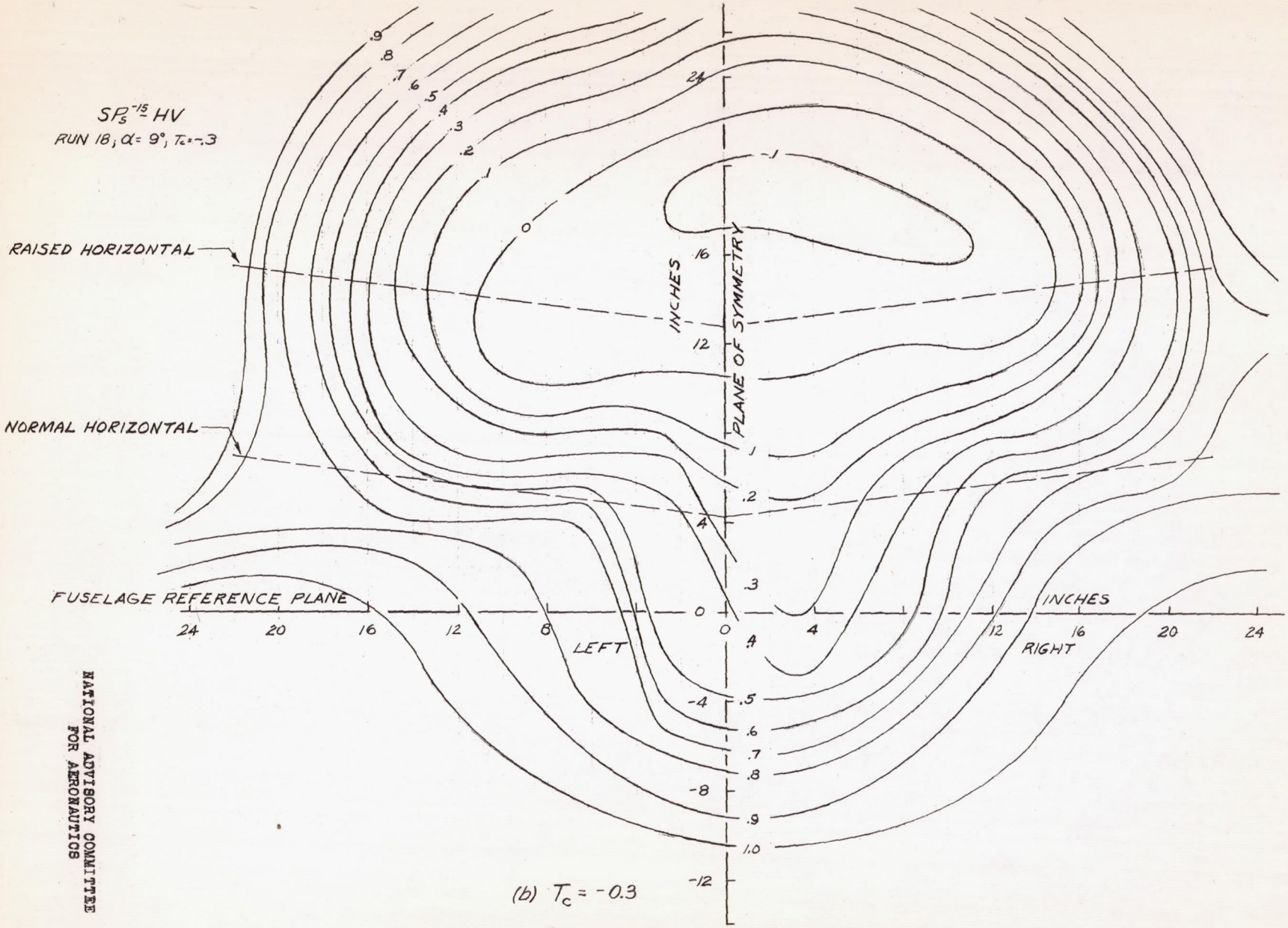

(b) $T_c = -0.3$

FIGURE 40.- CONTINUED. STABILITY MODEL.

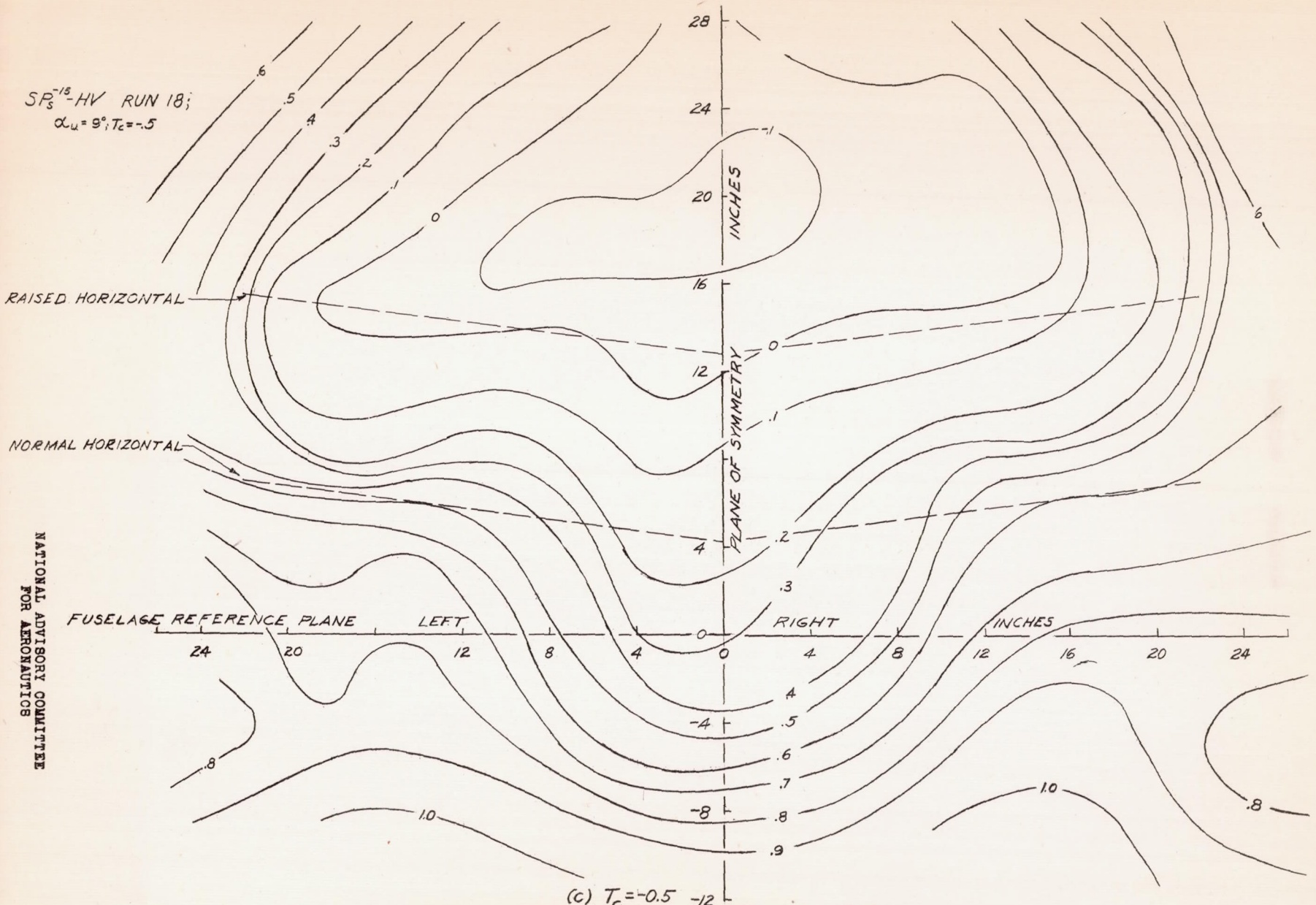

(c) $T_c = -0.5$

FIGURE 40.- CONCLUDED. STABILITY MODEL.

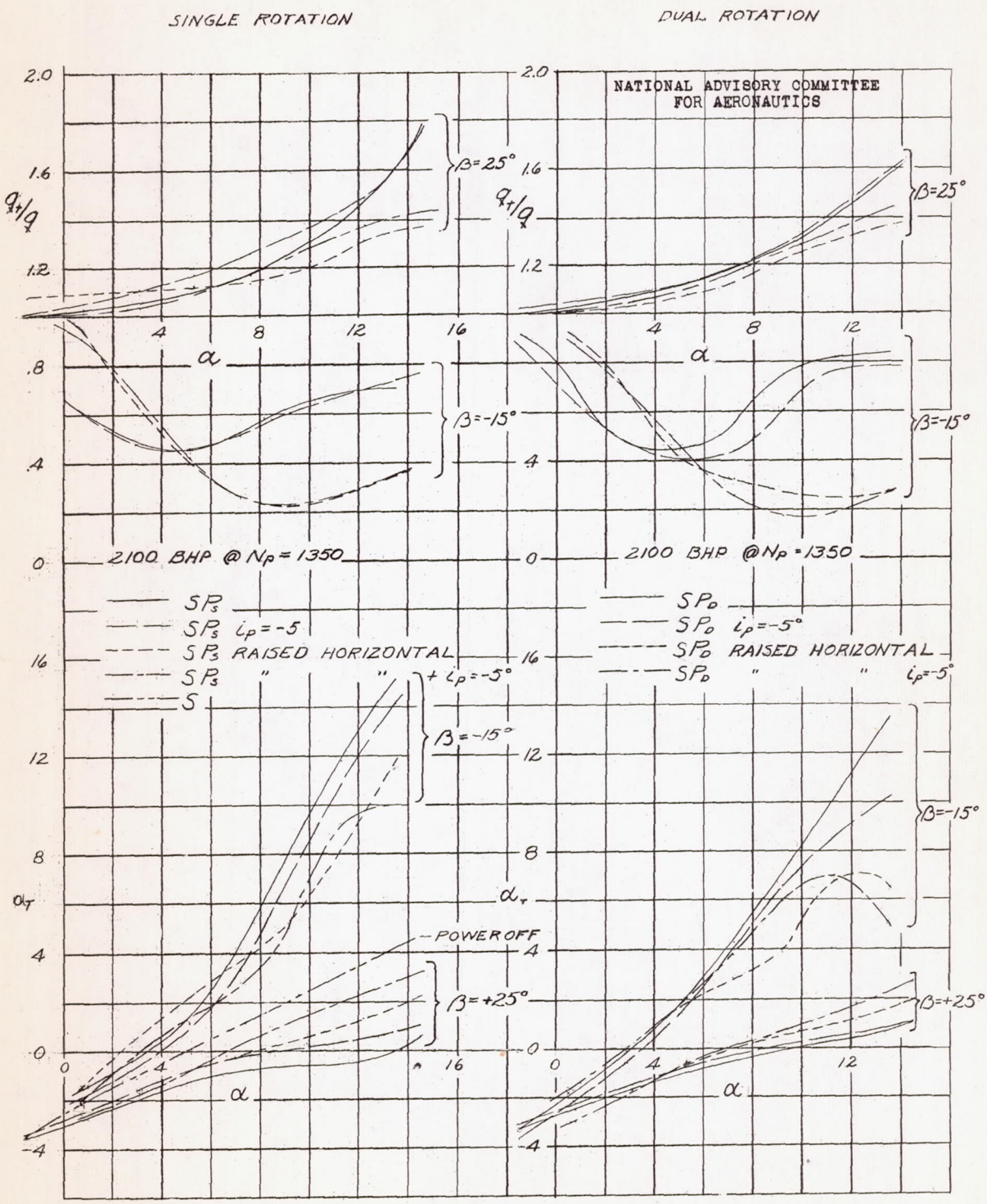

FIGURE 41.- THE VARIATION OF DYNAMIC PRESSURE AND ANGLE OF ATTACK AT THE TAIL WITH ANGLE OF ATTACK FOR STABILITY MODEL IN VARIOUS CONFIGURATIONS. SINGLE AND DUAL ROTATION, β = 25° AND -15°, RATED POWER.

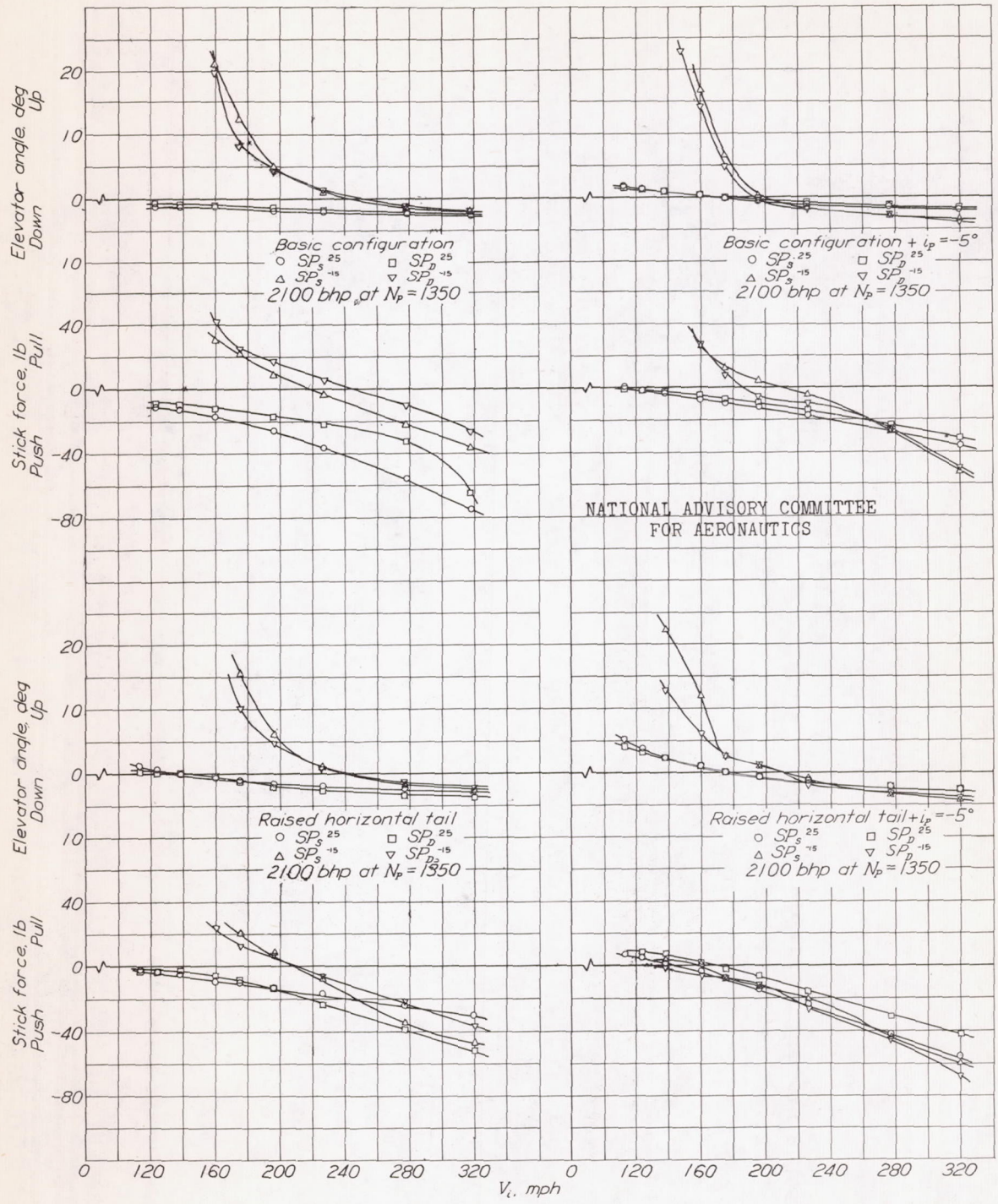

Figure 42.- The variation of elevator angle and stick force with speed in steady flight for the stability model. Rated power, positive and negative thrust, single and dual rotation.

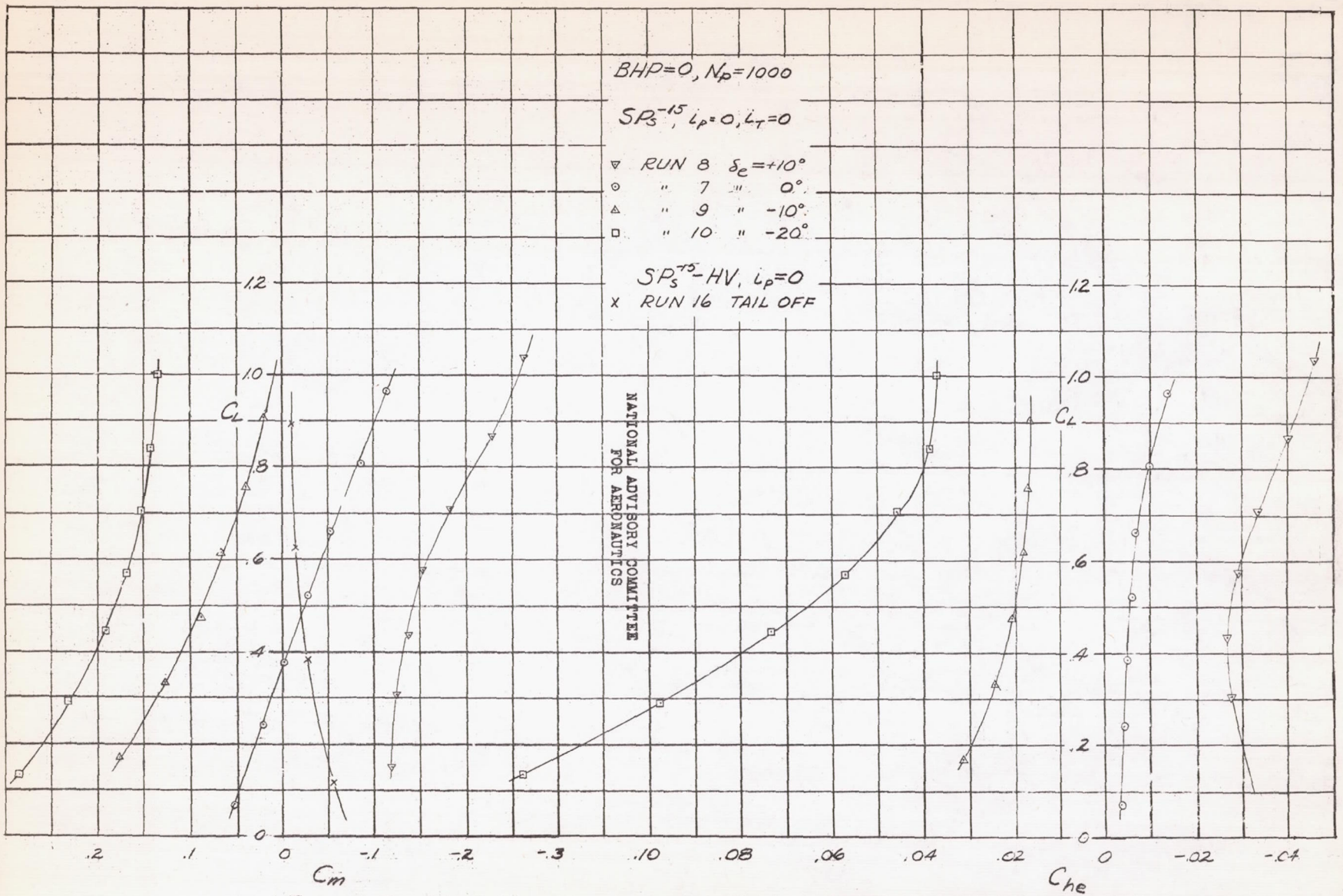

FIGURE 43- EFFECT OF ELEVATOR DEFLECTION ON CHARACTERISTICS OF STABILITY MODEL IN PITCH. BASIC CONFIGURATION, SINGLE ROTATION, β=-15° ZERO POWER, PROPELLER RPM 1000.

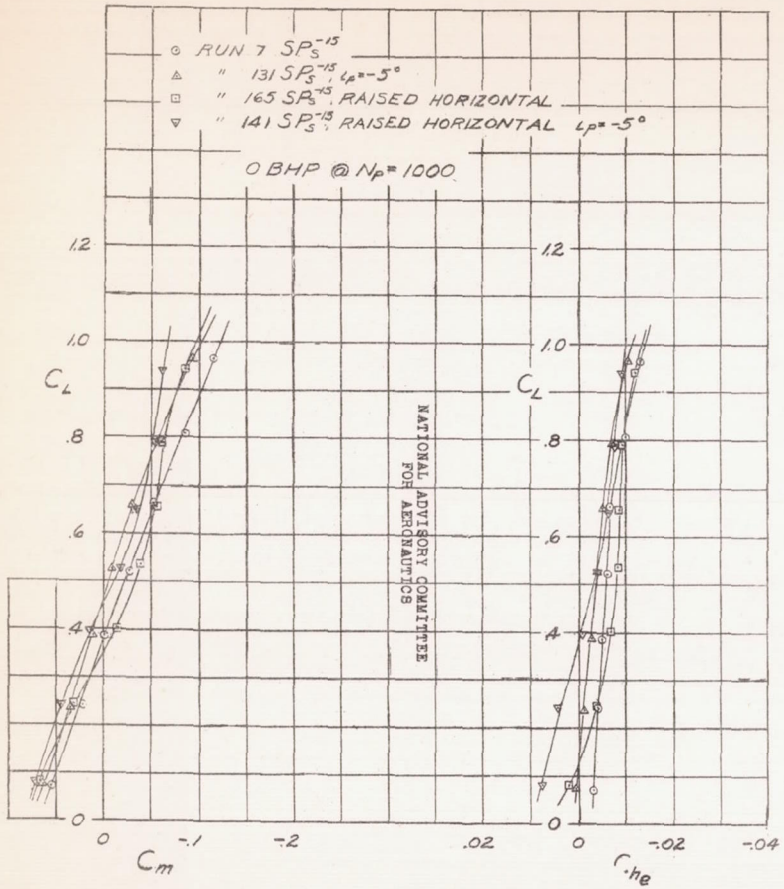

FIGURE 44-EFFECT OF CONFIGURATION CHANGES ON CHARACTERISTICS OF STABILITY MODEL IN PITCH. SINGLE ROTATION, β=-15° ZERO POWER AT 1000 RPM, ELEVATOR UNDEFLECTED.

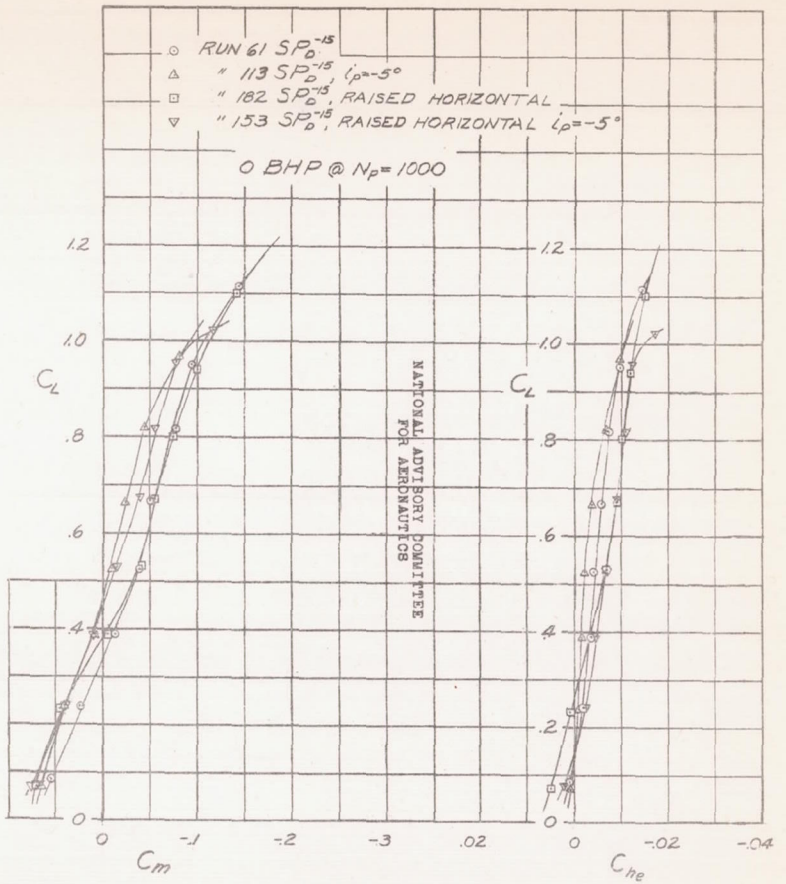

FIGURE 45-EFFECT OF CONFIGURATION CHANGES ON CHARACTERISTICS OF STABILITY MODEL IN PITCH. DUAL ROTATION, β=-15°, ZERO POWER AT 1000 RPM, ELEVATOR UNDEFLECTED.

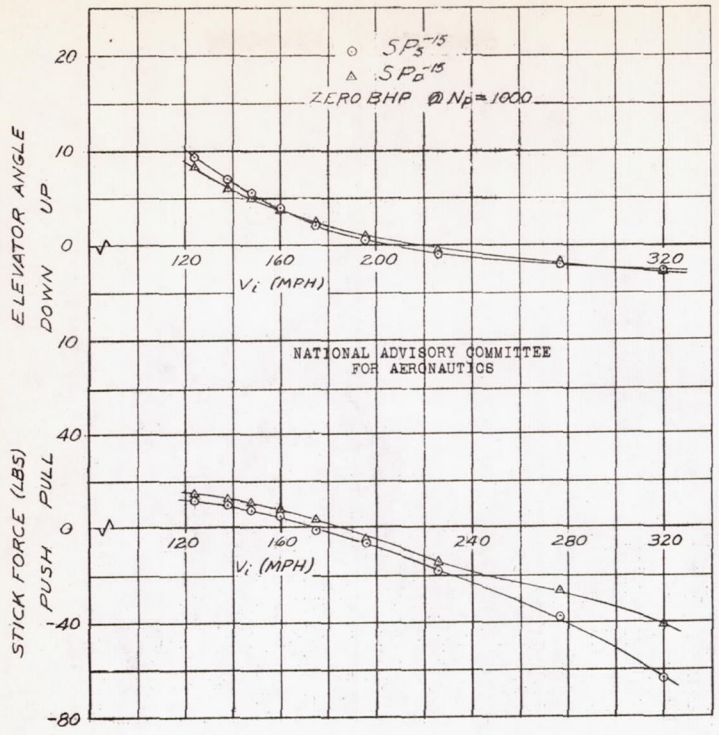

FIGURE 46.-THE VARIATION OF ELEVATOR ANGLE AND STICK FORCE WITH SPEED IN STEADY FLIGHT FOR THE STABILITY MODEL. ZERO POWER, NEGATIVE THRUST, SINGLE AND DUAL ROTATION.

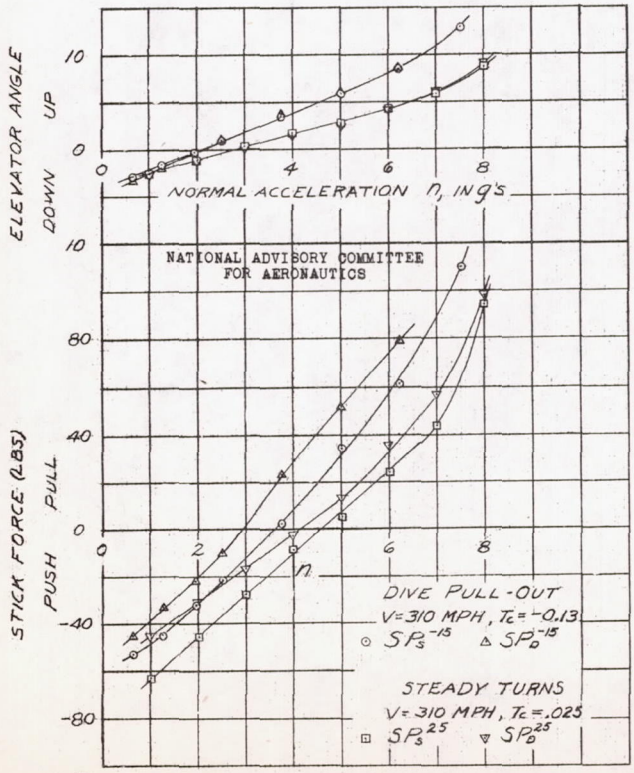

FIGURE 47.-THE VARIATION OF ELEVATOR ANGLE AND STICK FORCE WITH NORMAL ACCELERATION IN DIVE PULL-OUTS AND STEADY TURNING FLIGHT FOR THE STABILITY MODEL, SINGLE AND DUAL ROTATION.

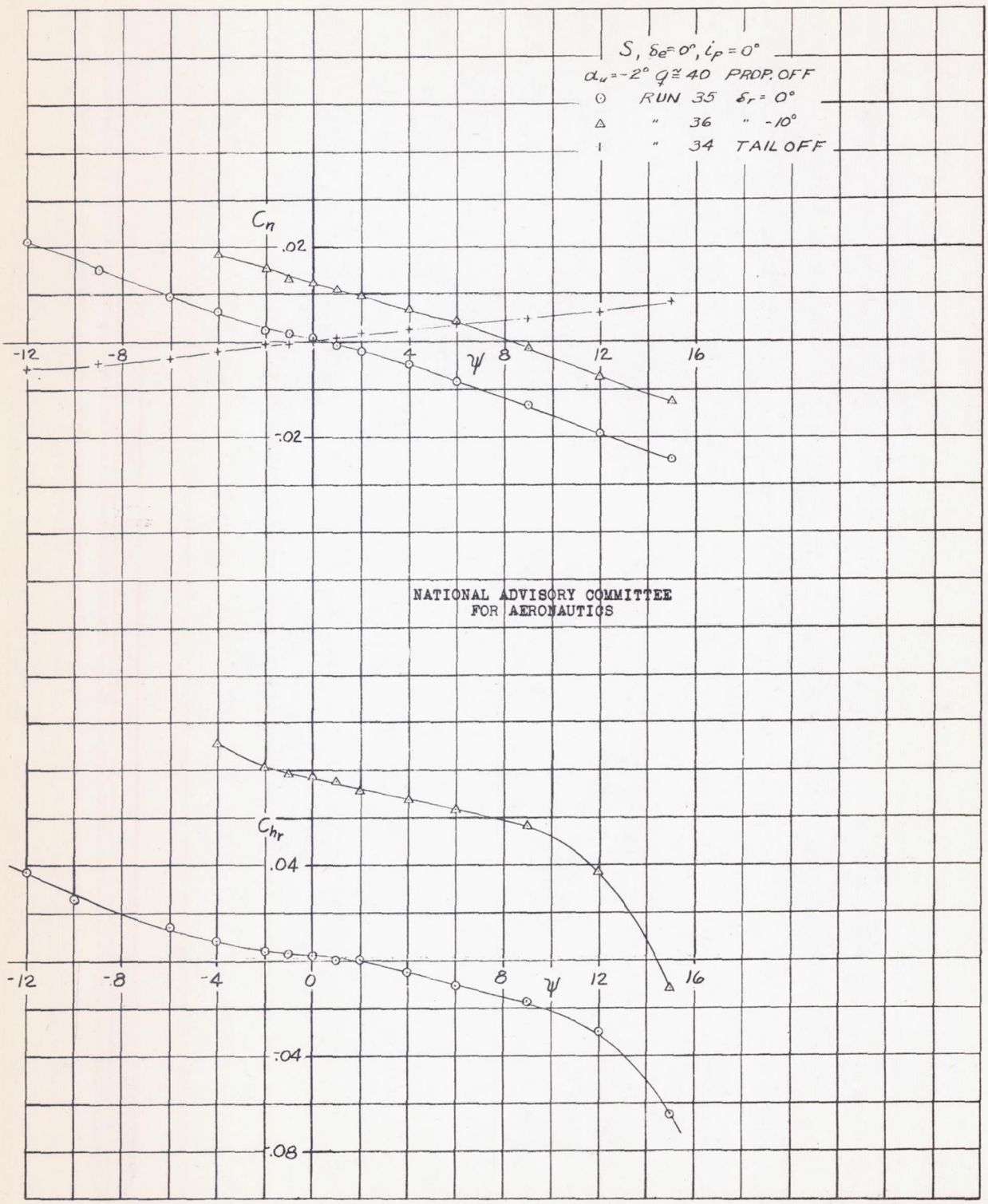

FIGURE 48.-EFFECT OF RUDDER DEFLECTION ON CHARACTERISTICS OF STABILITY MODEL IN YAW, PROPELLER REMOVED, $\alpha_u = -2°$.

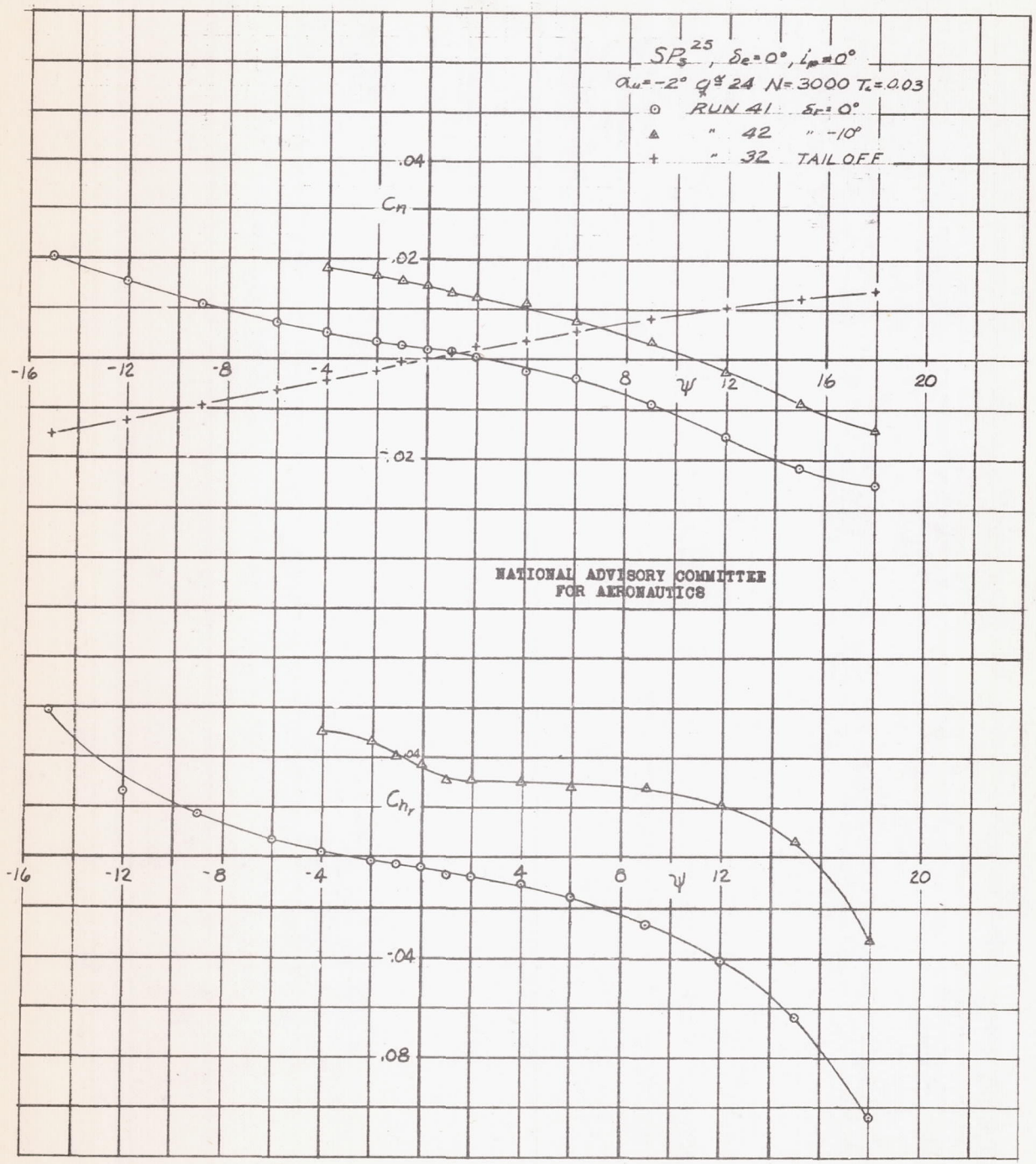

FIGURE 49.- EFFECT OF RUDDER DEFLECTION ON CHARACTERISTICS OF STABILITY MODEL IN YAW. $\alpha_u = -2°$, $T_c = 0.03$, SINGLE ROTATION, $\beta = 25°$.

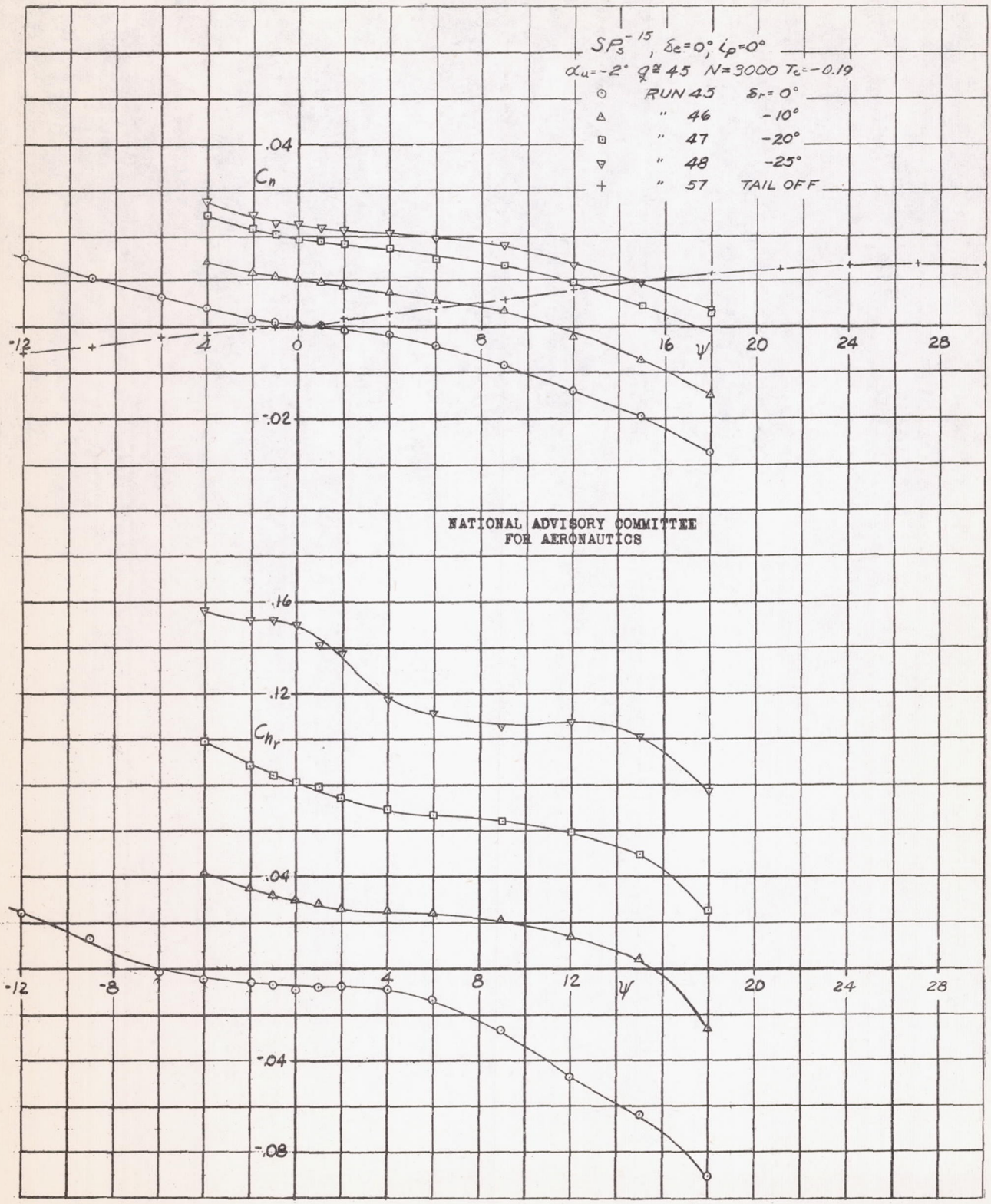

FIGURE 50-EFFECT OF RUDDER DEFLECTION ON CHARACTERISTICS OF STABILITY MODEL IN YAW. $\alpha_u=-2°$, $T_c=-0.19$, SINGLE ROTATION, $\beta=-15°$.

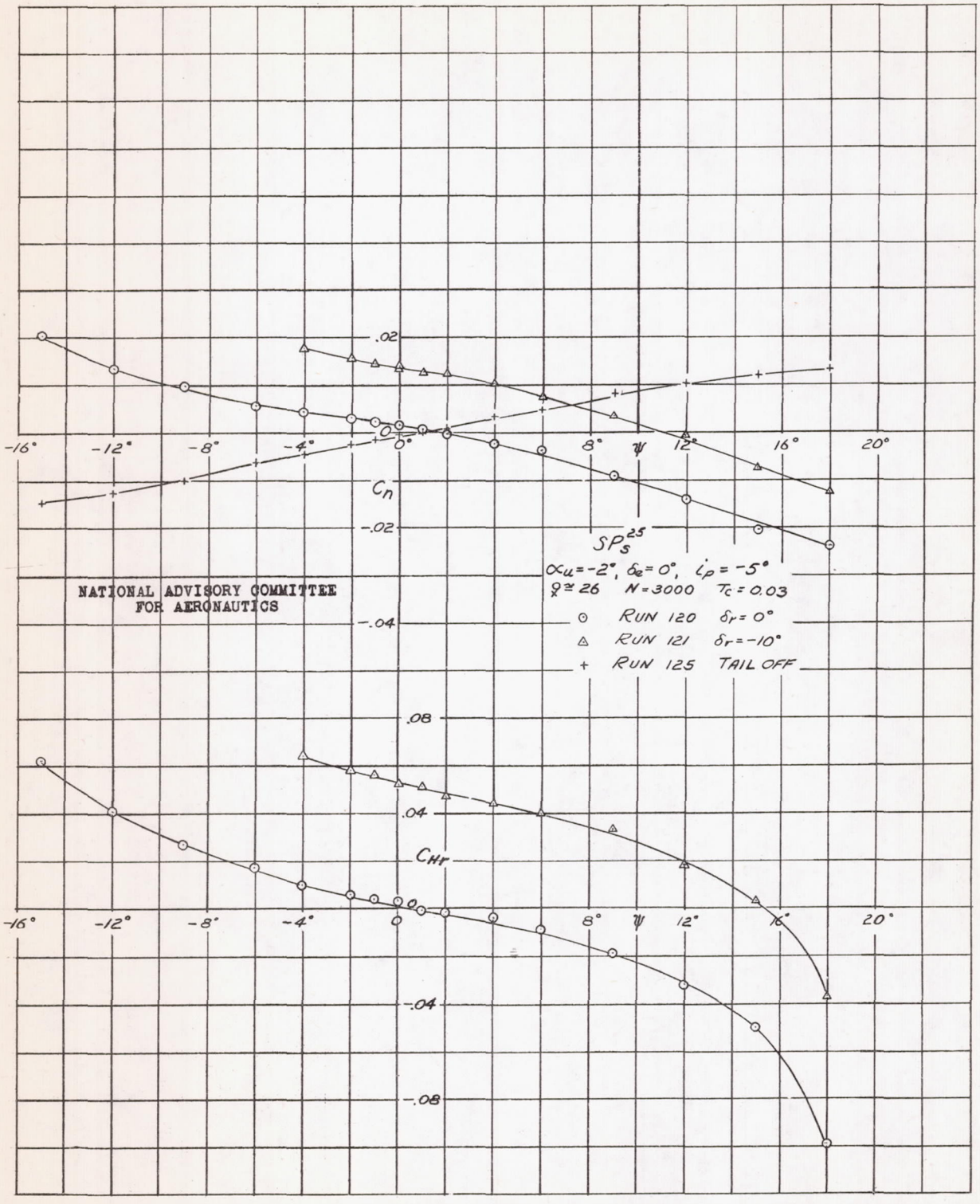

FIGURE 51.-EFFECT OF RUDDER DEFLECTION ON CHARACTERISTICS OF STABILITY MODEL IN YAW. $\alpha_u = -2°$, $i_p = -5°$, $T_c = 0.03$, SINGLE ROTATION, $\beta = 25°$.

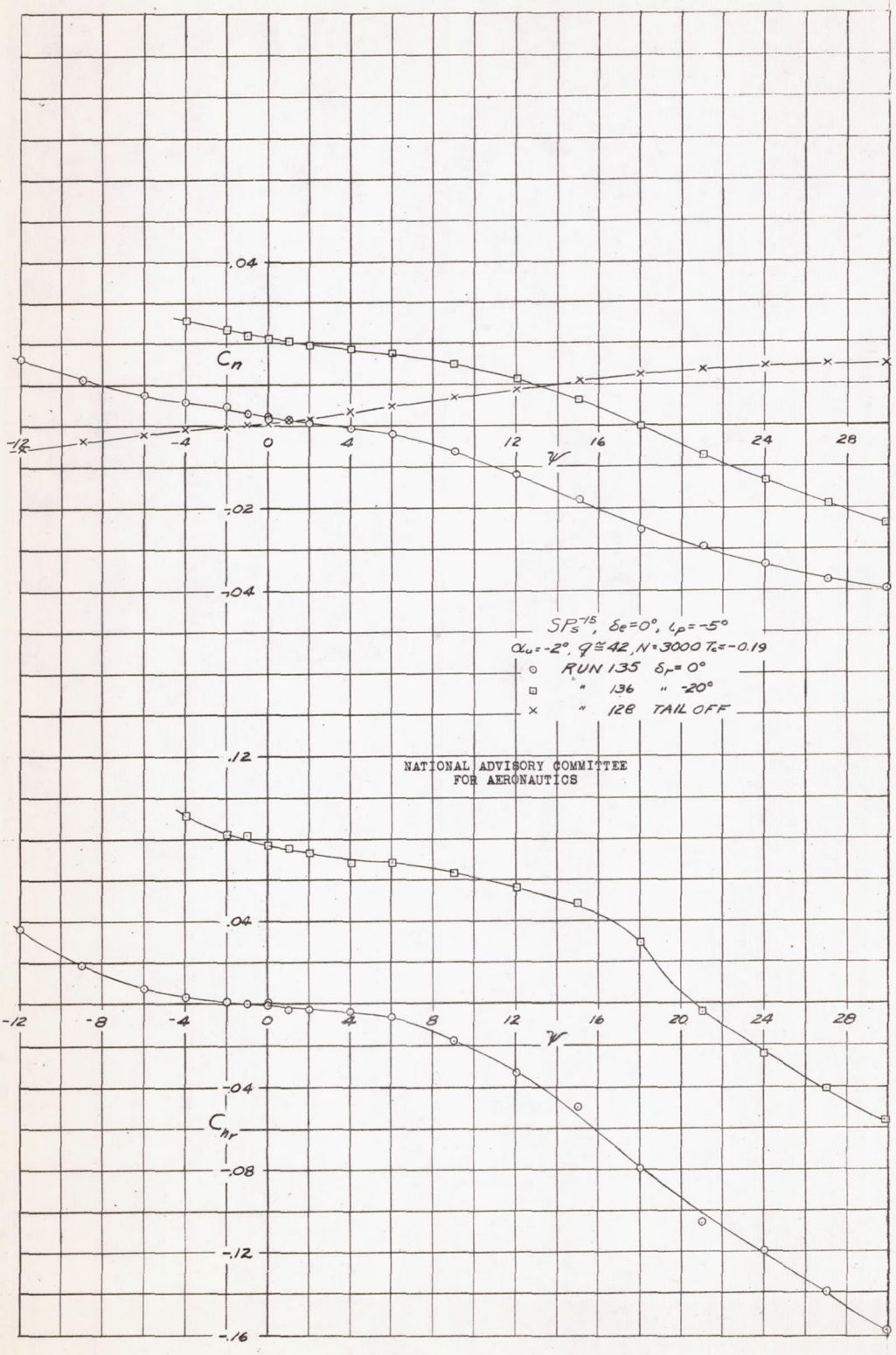

FIGURE 52-EFFECT OF RUDDER DEFLECTION ON CHARACTERISTICS OF STABILITY MODEL IN YAW. α_u=-2°, i_p=-5°, T_c=-0.19, SINGLE ROTATION, β=-15°.

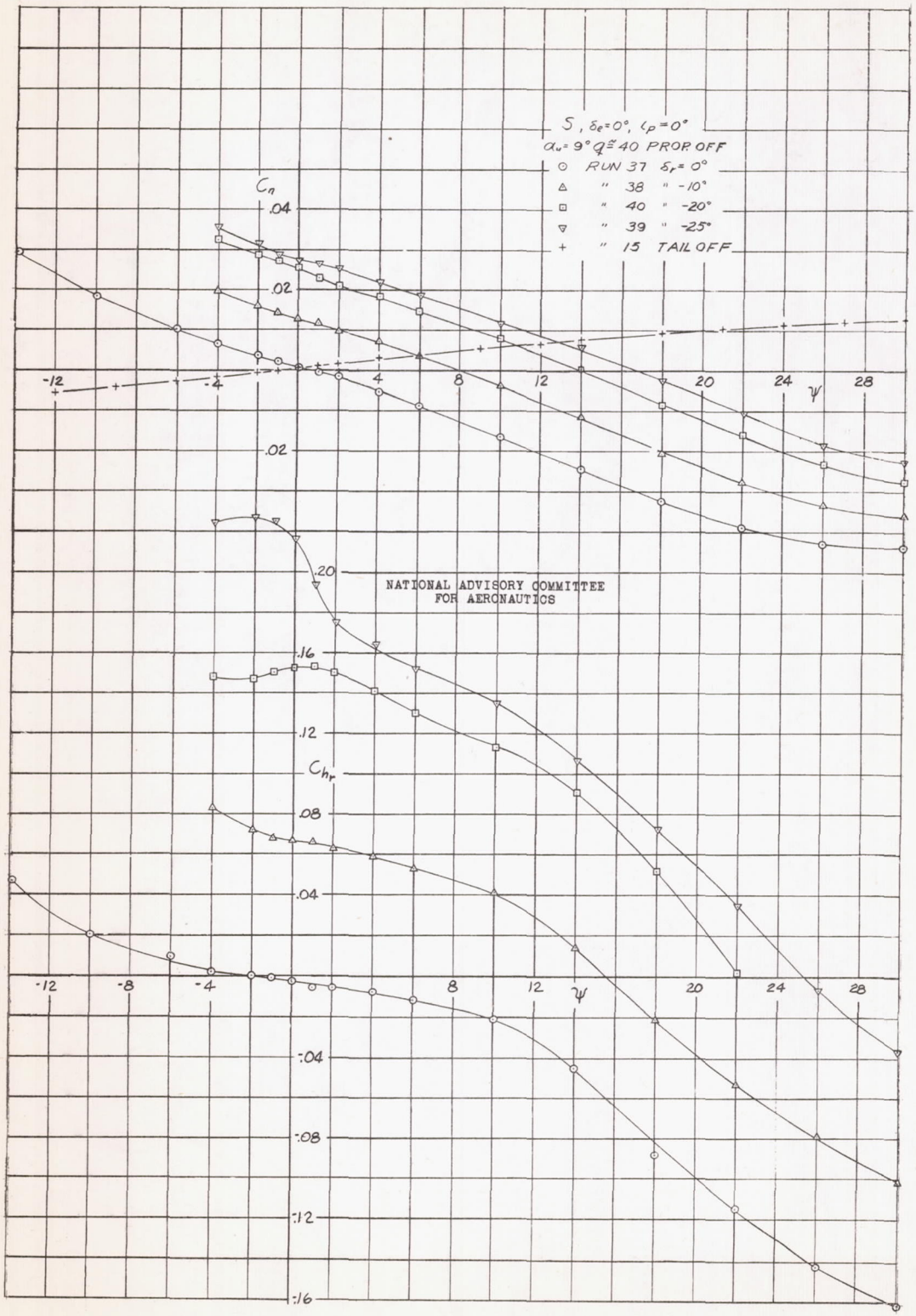

FIGURE 53.- EFFECT OF RUDDER DEFLECTION ON CHARACTERISTICS OF STABILITY MODEL IN YAW, PROPELLER REMOVED, $\alpha_u = 9°$.

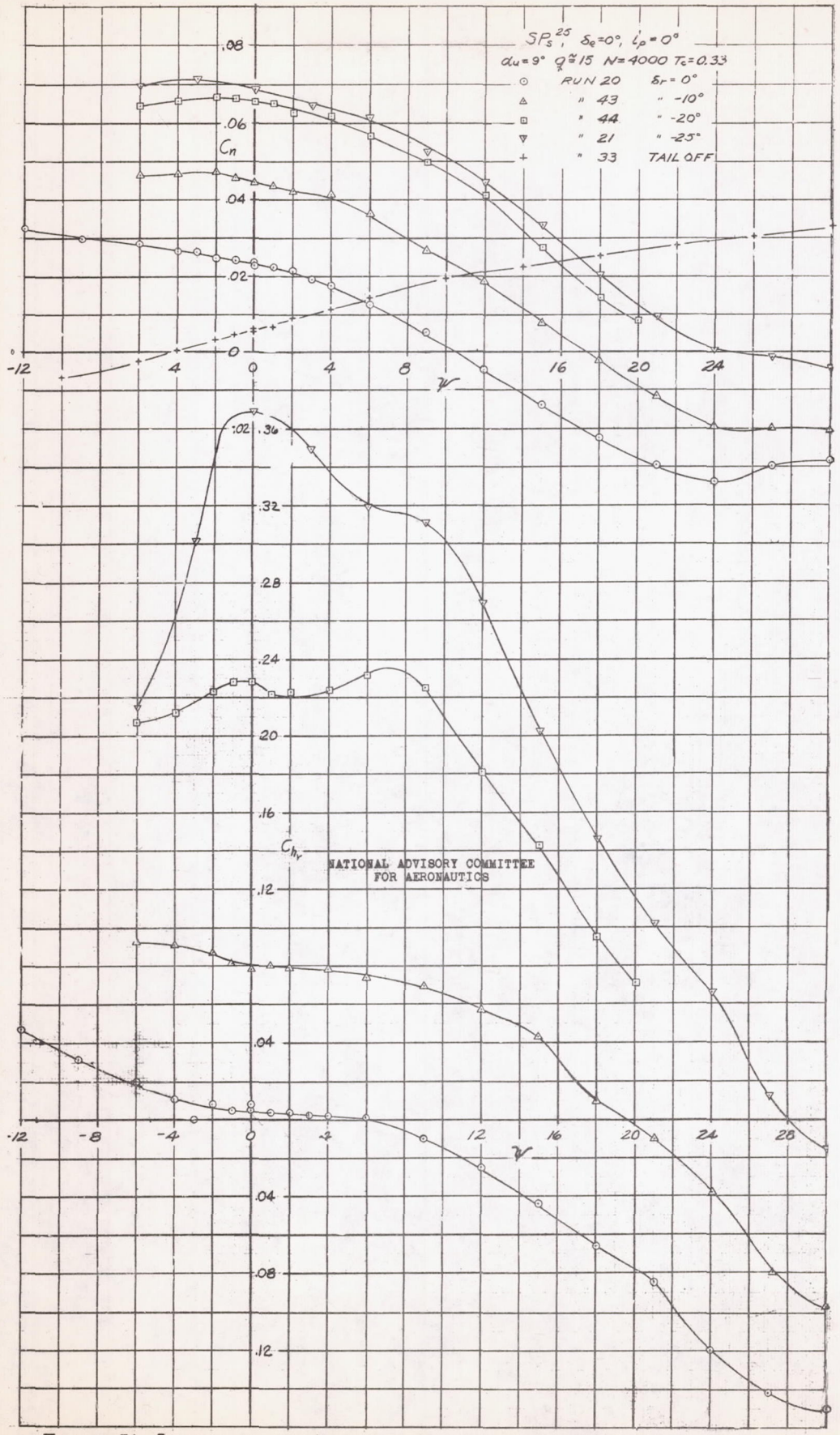

FIGURE 54.- EFFECT OF RUDDER DEFLECTION ON CHARACTERISTICS OF STABILITY MODEL IN YAW. α_u = 9°, T_c=0.33, SINGLE ROTATION, β = 25°.

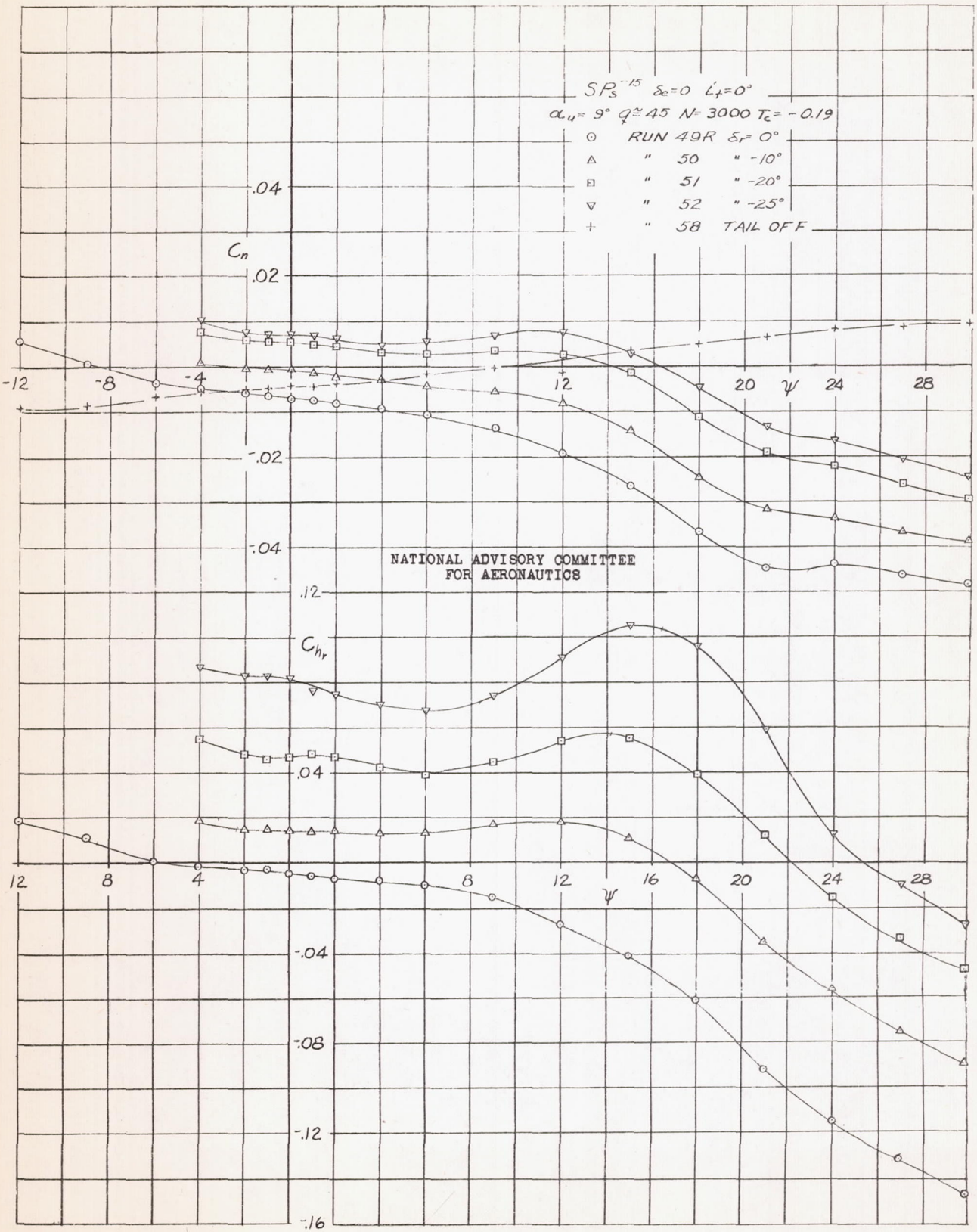

FIGURE 55.- EFFECT OF RUDDER DEFLECTION ON CHARACTERISTICS OF STABILITY MODEL IN YAW. $\alpha_u = 9°$, $T_c = -0.19$, SINGLE ROTATION, $\beta = -15°$.

A-19

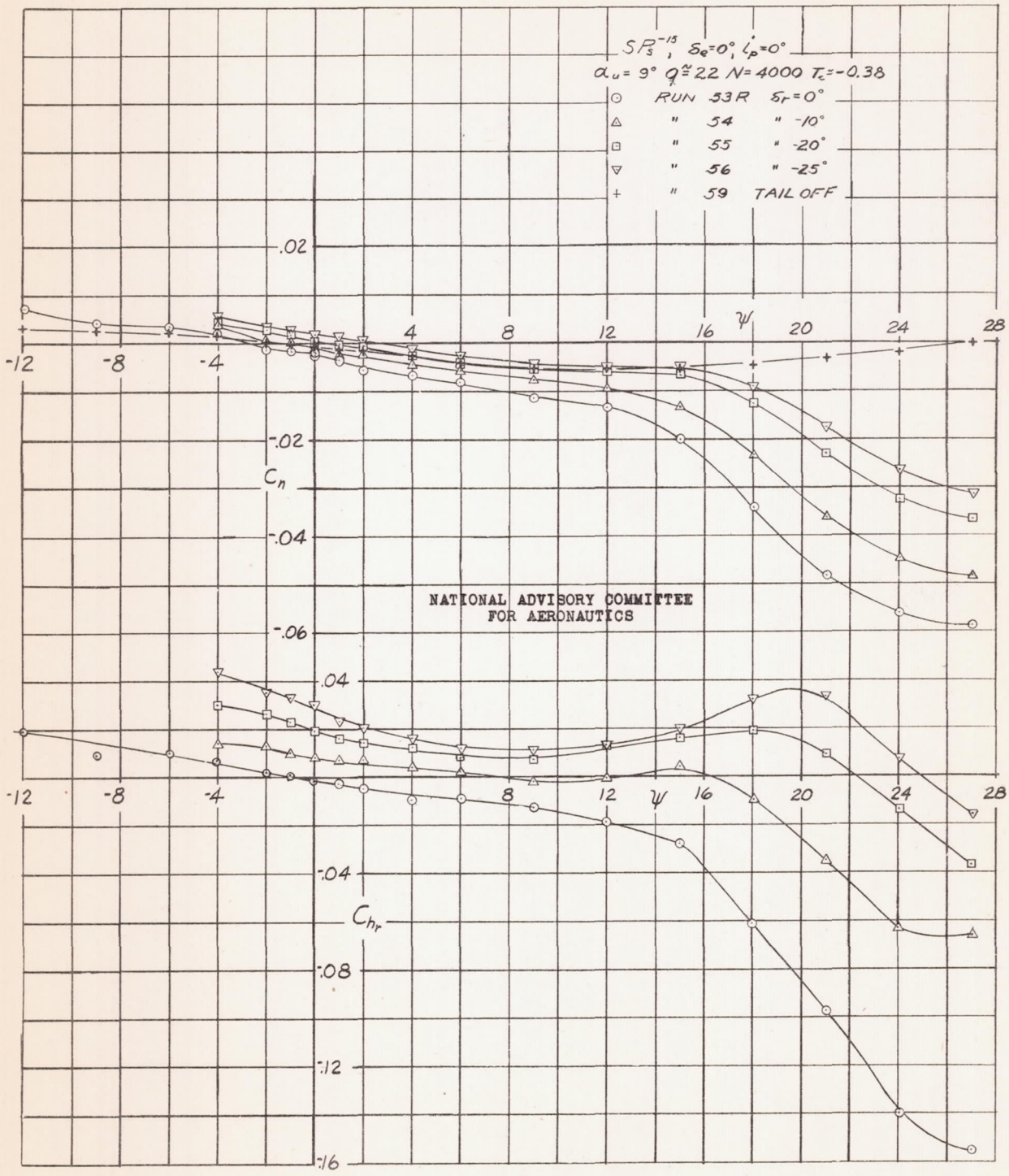

FIGURE 56.-EFFECT OF RUDDER DEFLECTION ON CHARACTERISTICS OF STABILITY MODEL IN YAW. $\alpha_u = 9°$, $T_c = -0.38$, SINGLE ROTATION, $\beta = -15°$.

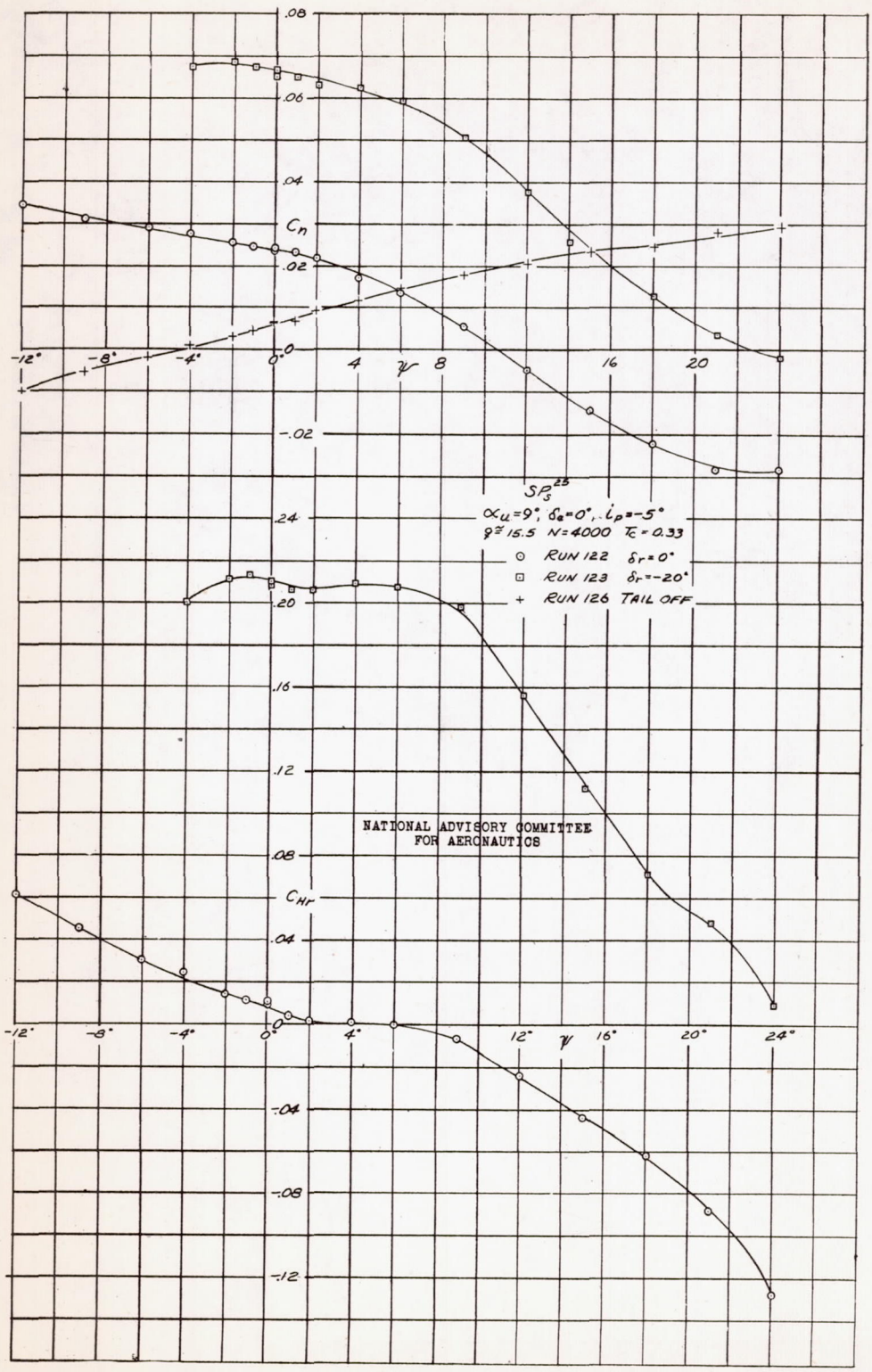

FIGURE 57.--EFFECT OF RUDDER DEFLECTION ON CHARACTERISTICS OF STABILITY MODEL IN YAW. α_u = 9°, i_p = -5°, T_c = 0.33, SINGLE ROTATION, β = +25°.

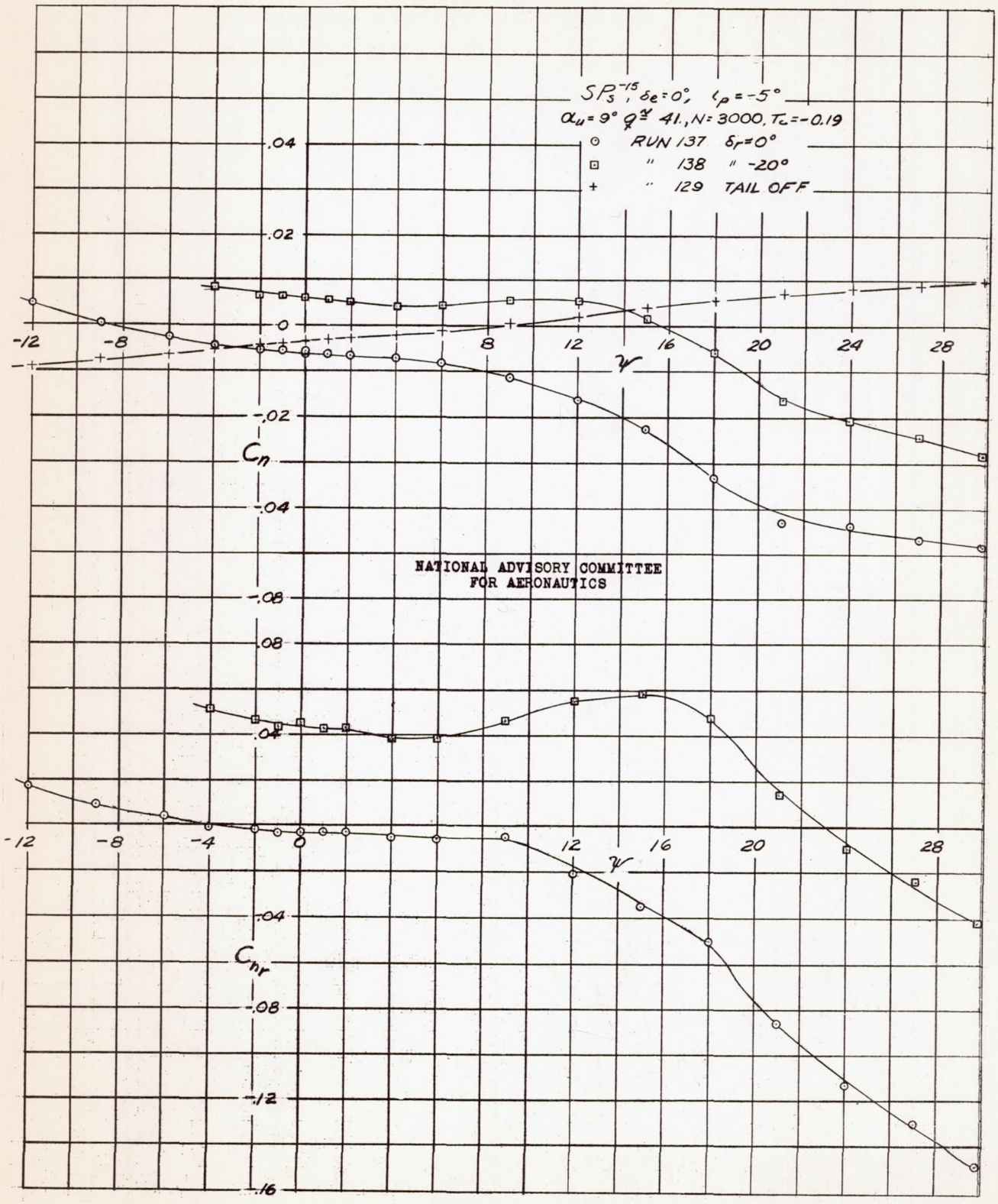

FIGURE 58.- EFFECT OF RUDDER DEFLECTION ON CHARACTERISTICS OF STABILITY MODEL IN YAW. $\alpha_u = 9°$, $i_p = -5°$, $T_c = -0.19$, SINGLE ROTATION, $\beta = -15°$.

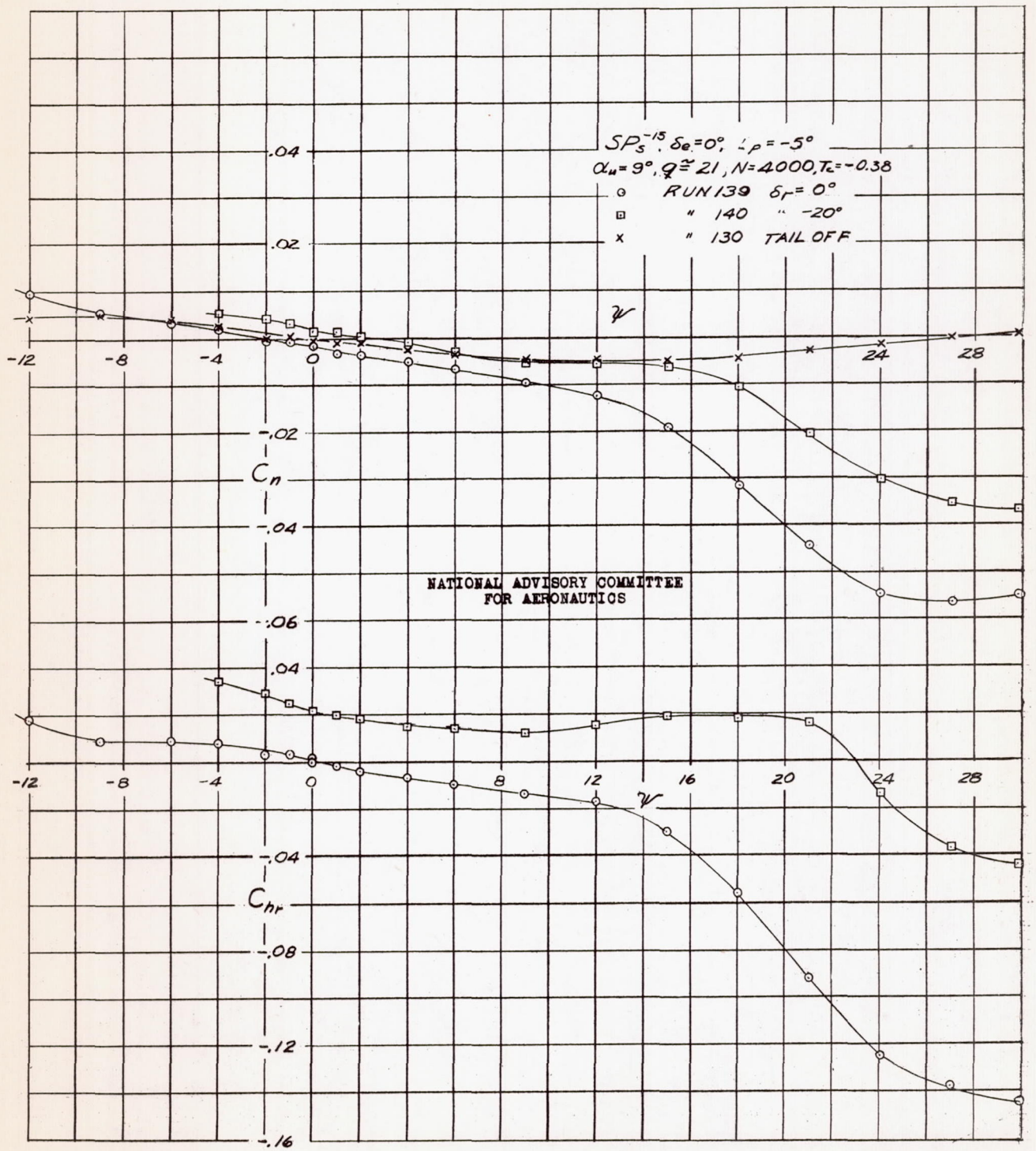

FIGURE 59 - EFFECT OF RUDDER DEFLECTION ON CHARACTERISTICS OF STABILITY MODEL IN YAW. α_w = 9°, i_p = -5°, T_c = -0.38, SINGLE ROTATION, β = -15°.

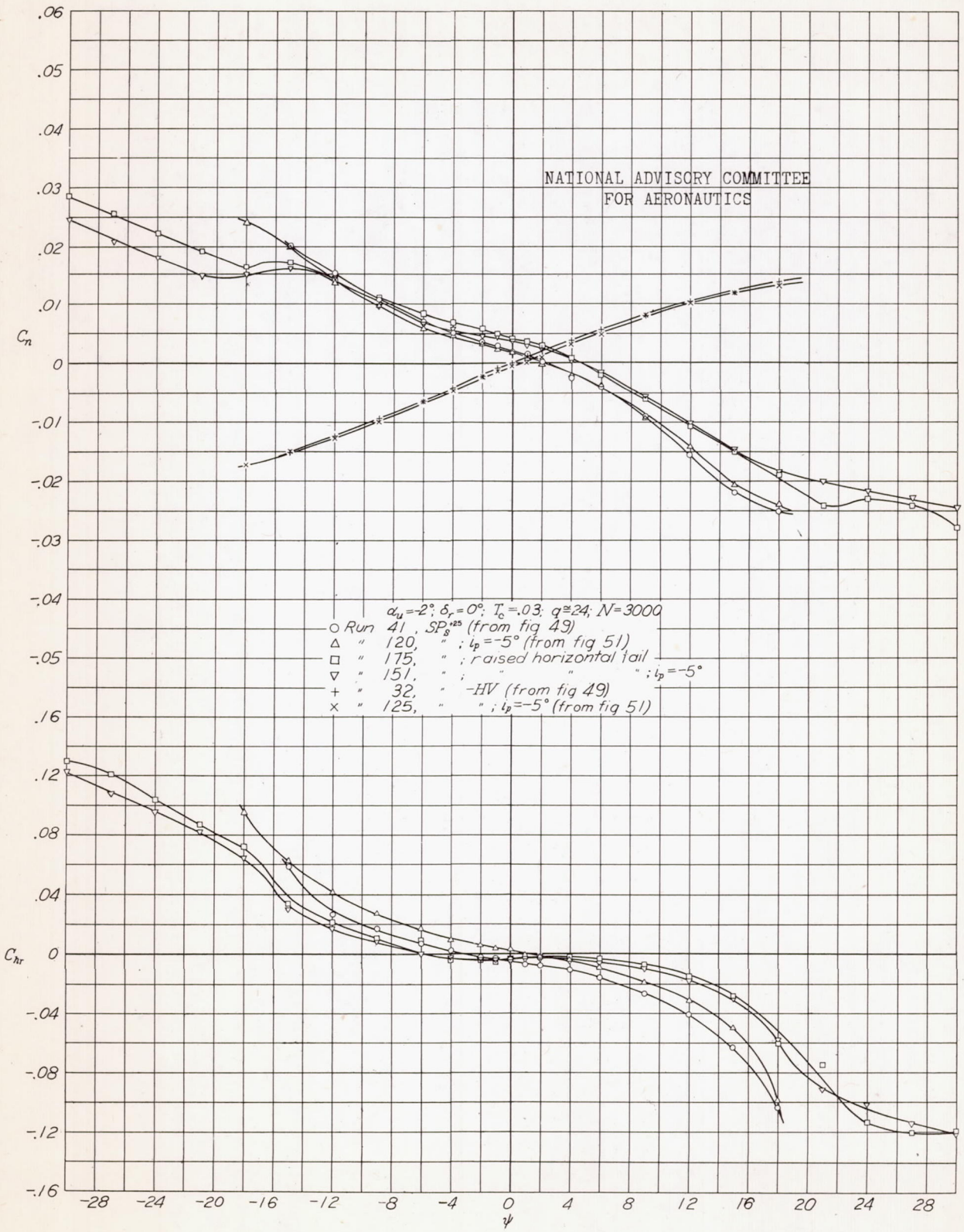

Figure 60.- Effect of configuration on characteristics of stability model in yaw, δ_r = 0°, α_u = -2°, T_c = .03, single rotation, β = 25°.

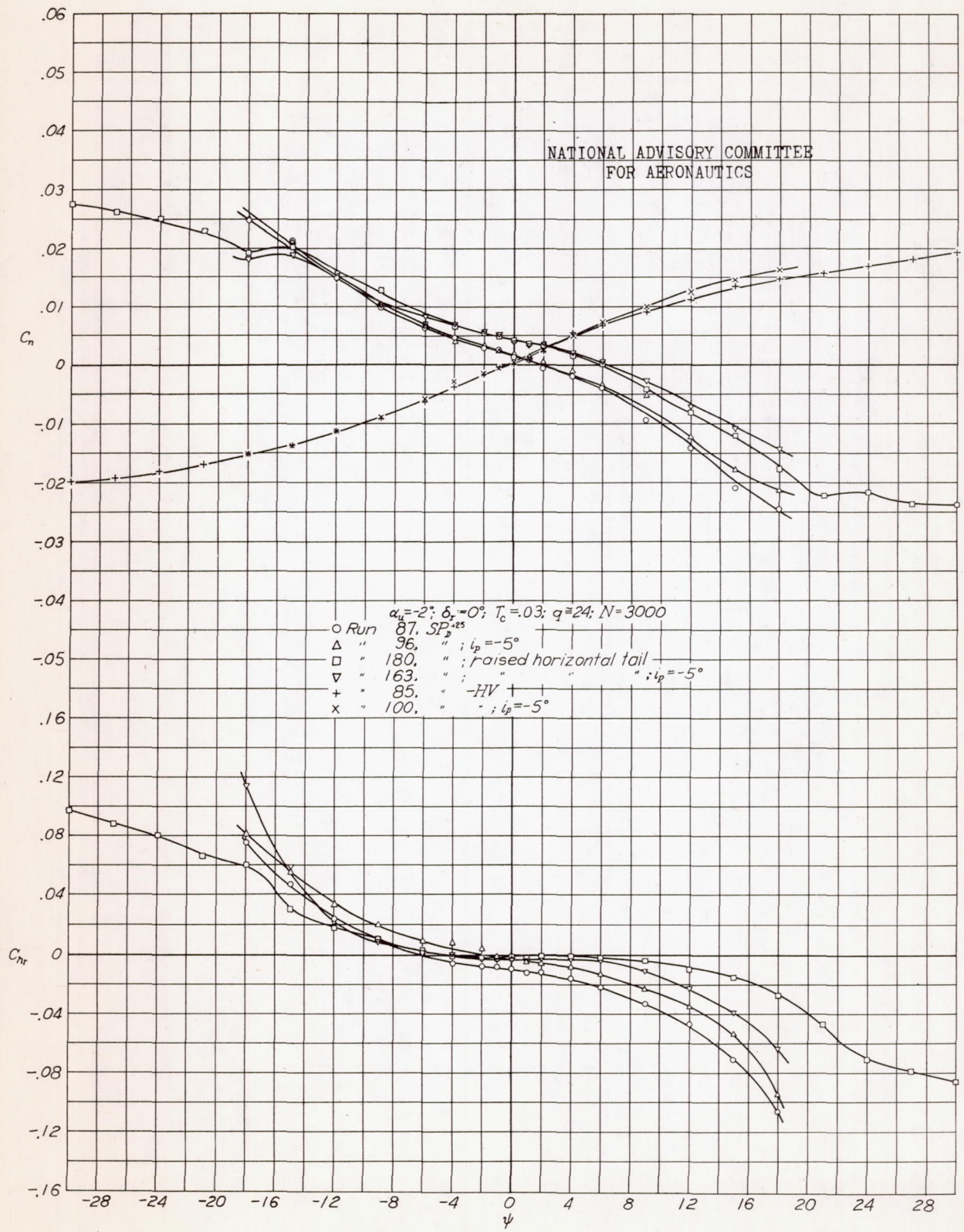

Figure 61.- Effect of configuration on characteristics of stability model in yaw, δ_r = 0°, α_u = -2°, T_c = .03, dual rotation, β = 25°.

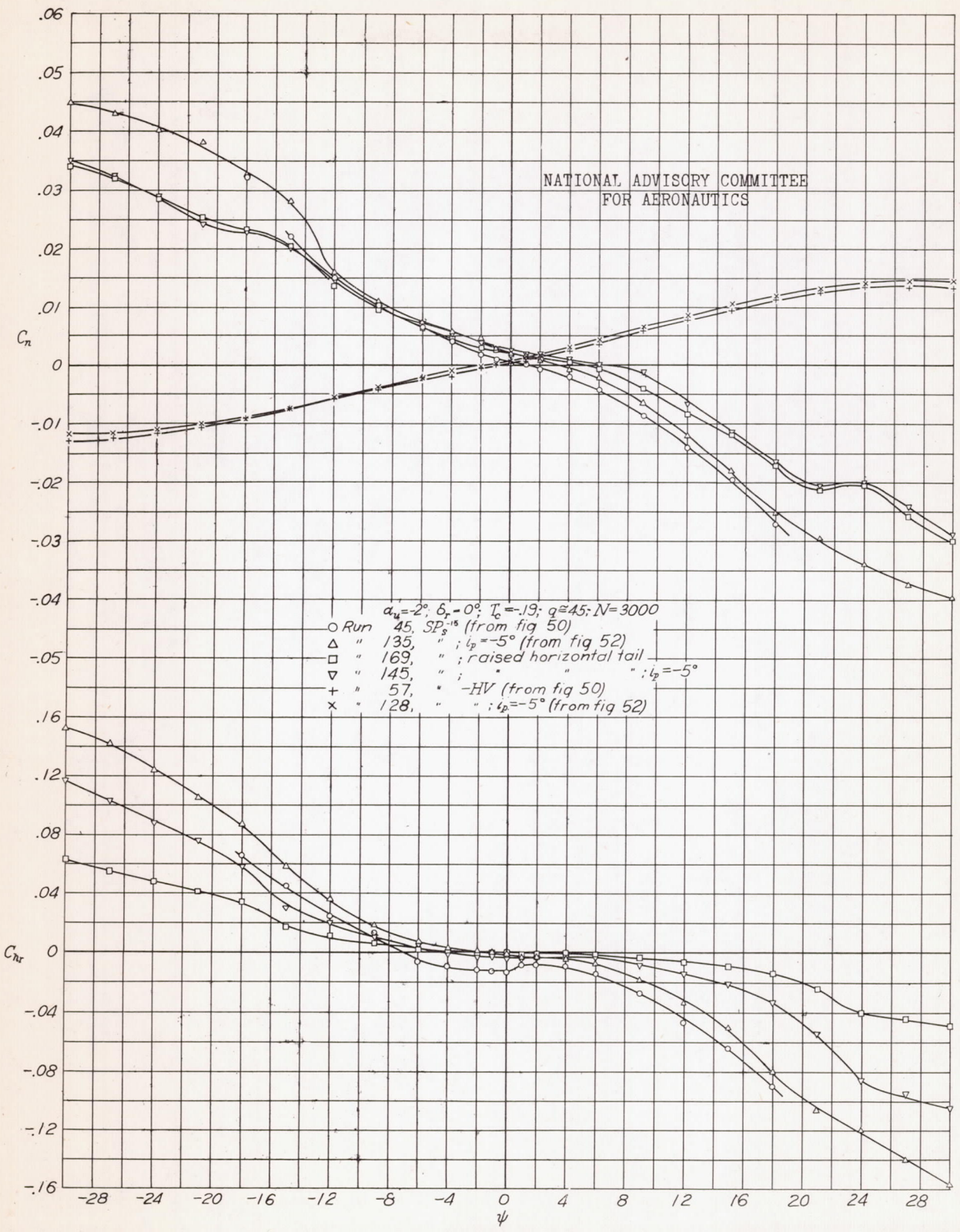

Figure 62.- Effect of configuration on characteristics of stability model in yaw, δ_r = 0°, α_u = -2°, T_c = -.19, single rotation, β = -15°.

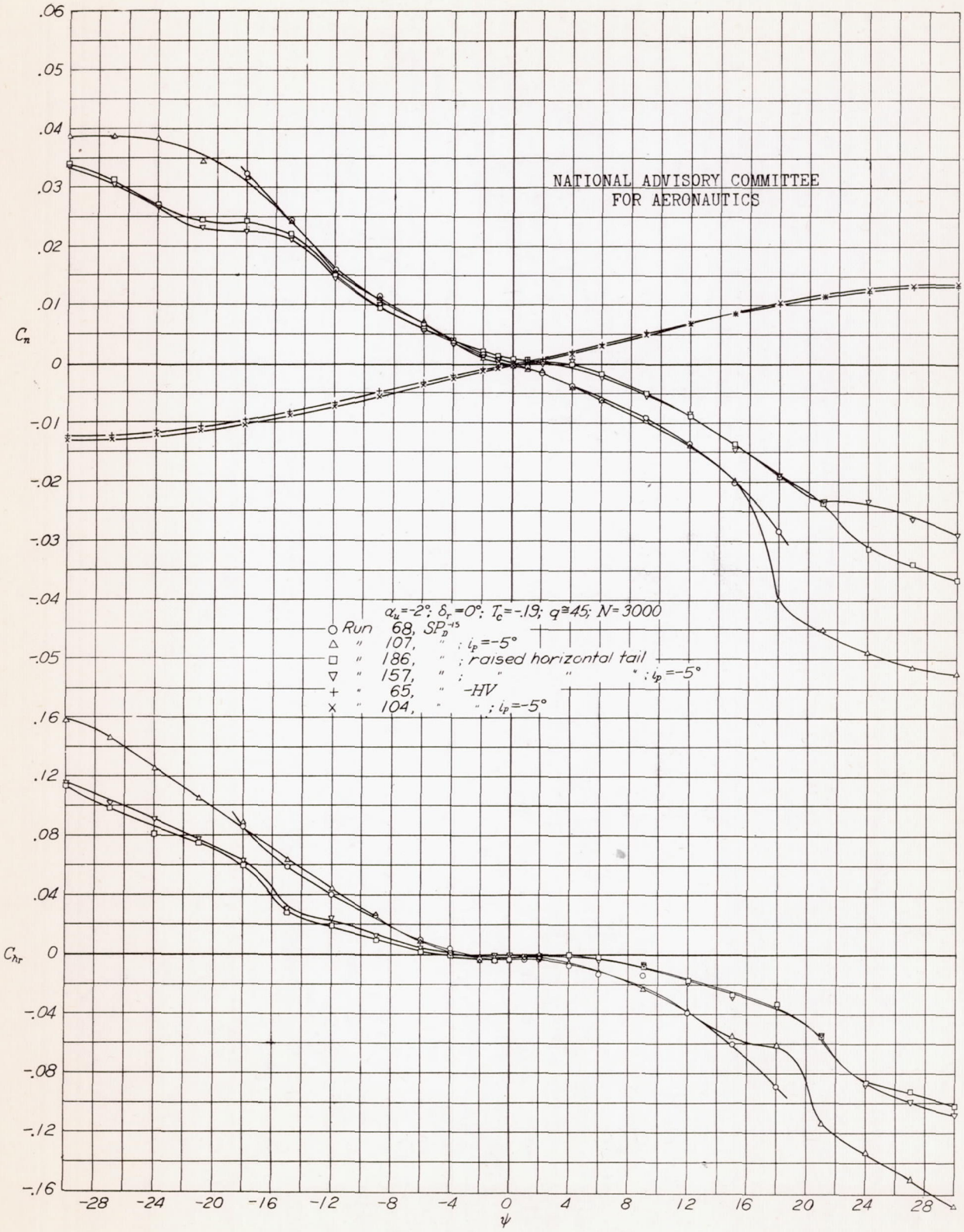

Figure 63.- Effect of configuration on characteristics of stability model in yaw, δ_r = 0°, α_u = -2°, T_c = -.19, dual rotation, β = -15°.

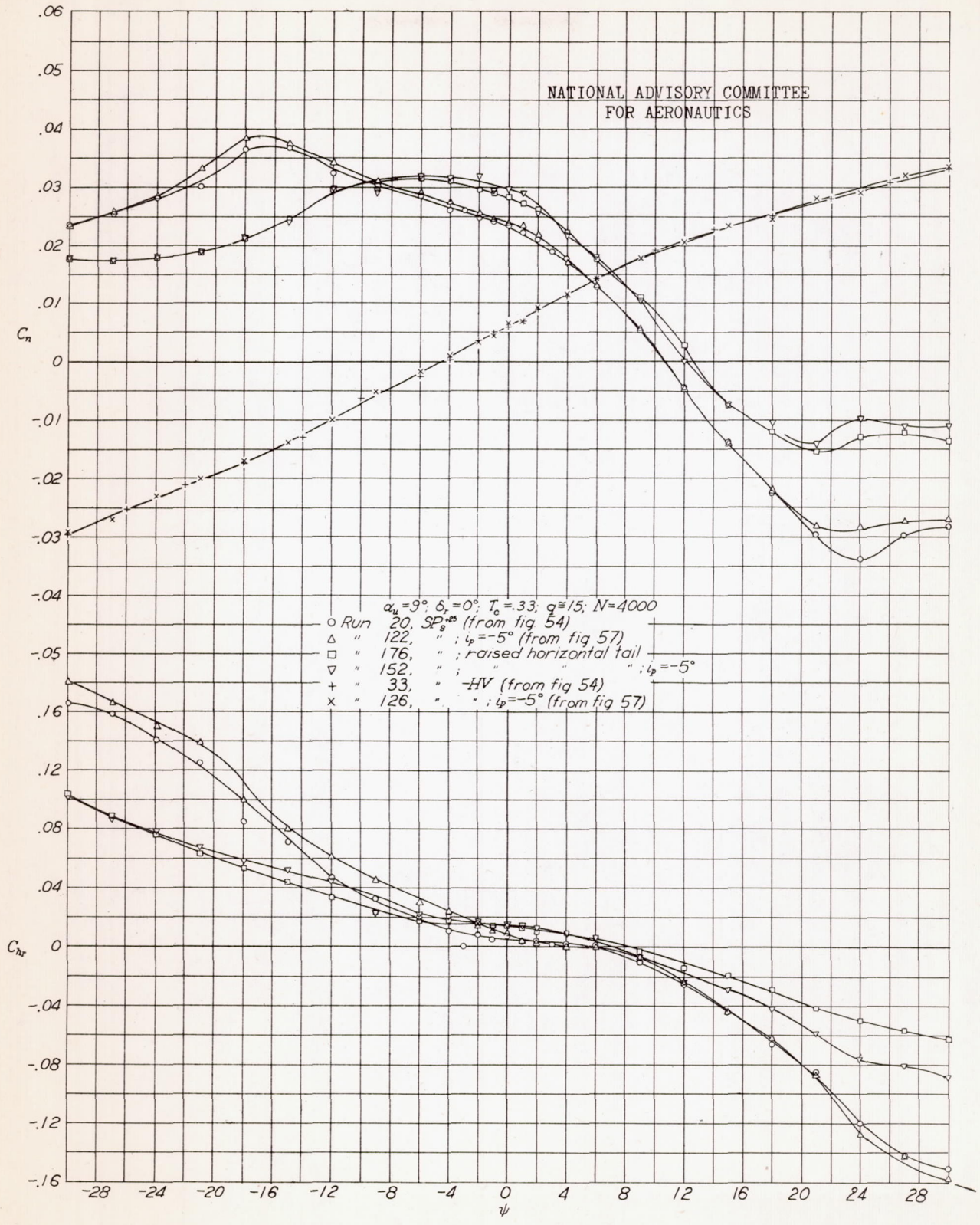

Figure 64.- Effect of configuration on characteristics of stability model in yaw, δ_r = 0°, α_u = 9°, T_c = .33, single rotation, β = 25°.

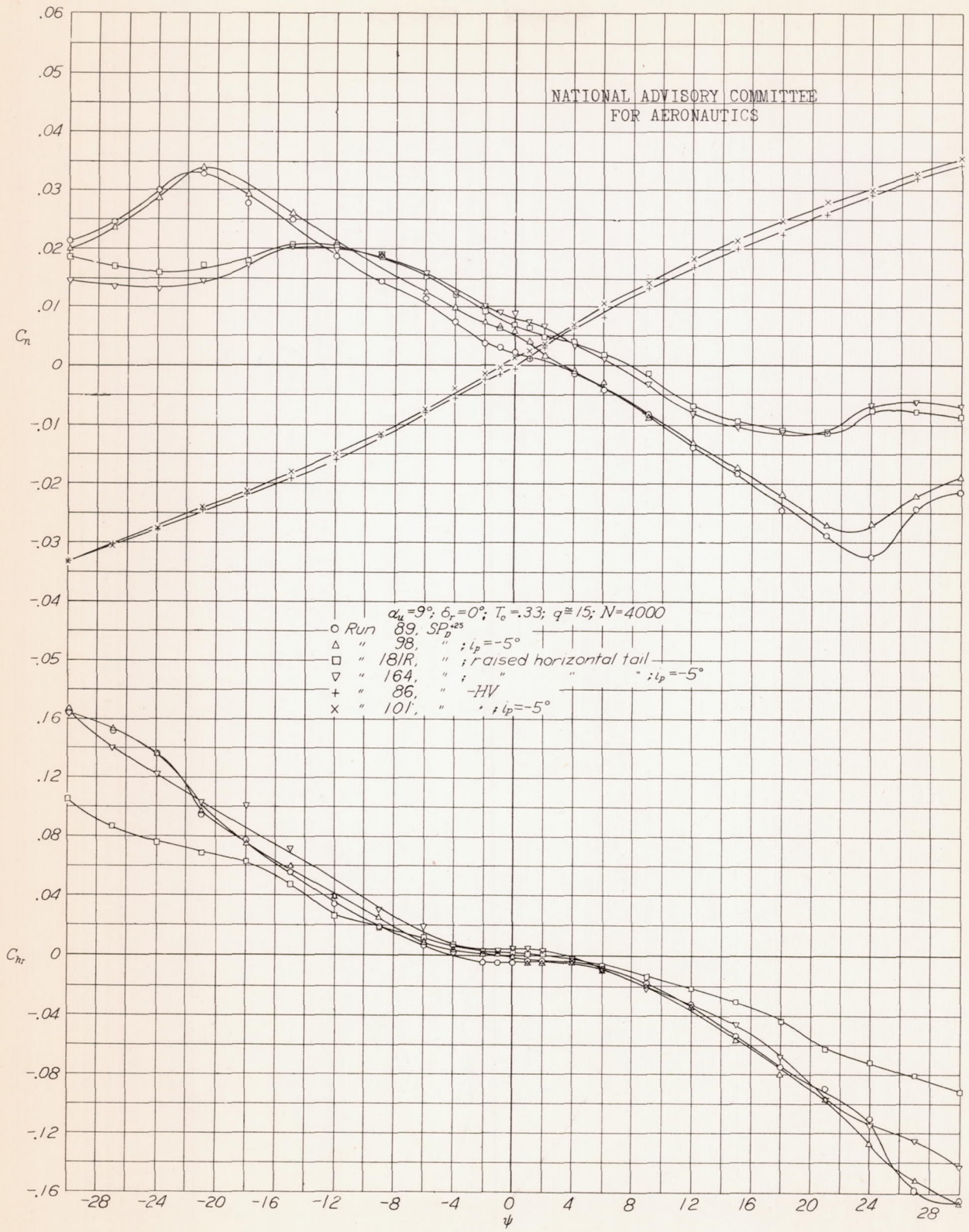

Figure 65.- Effect of configuration on characteristics of stability model in yaw, δ_r = 0°, α_u = 9°, T_c = .33, dual rotation, β = 25°.

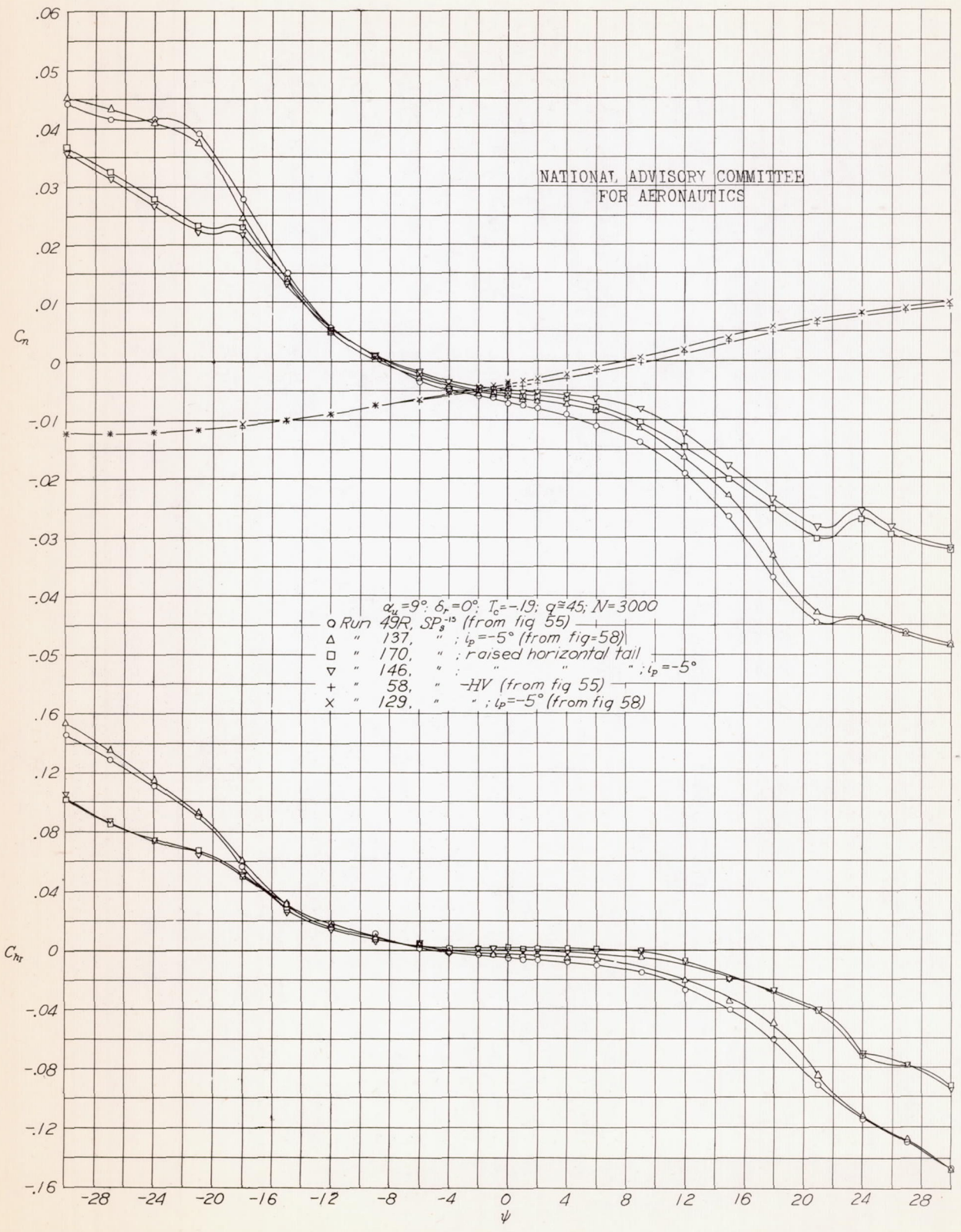

Figure 66.- Effect of configuration on characteristics of stability model in yaw, δ_r = 0°, α_u = 9°, T_c = -.19, single rotation, β = -15°.

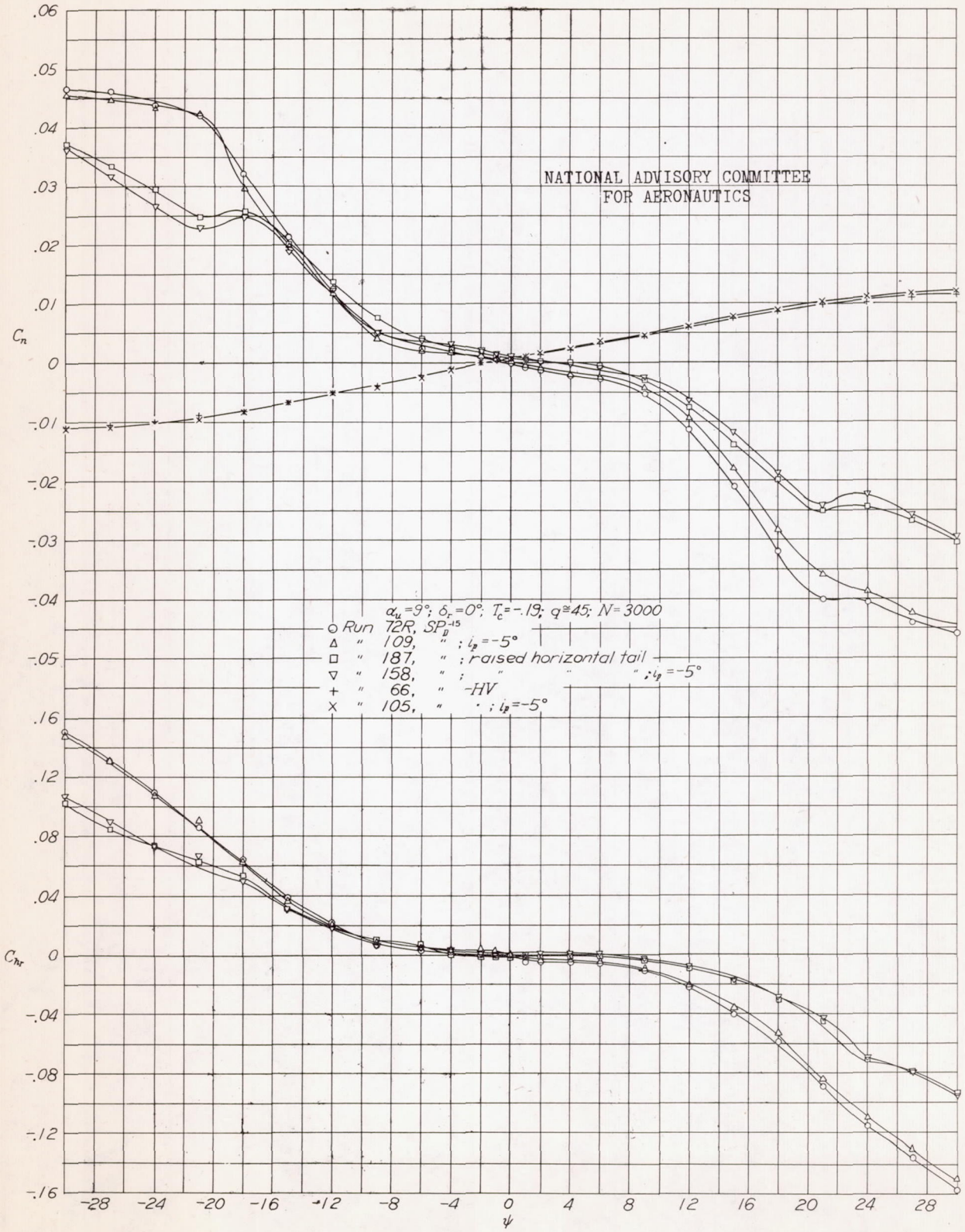

Figure 67.- Effect of configuration on characteristics of stability model in yaw, $\delta_r = 0^\circ$, $\alpha_u = 9^\circ$, $T_c = -.19$, dual rotation, $\beta = -15^\circ$.

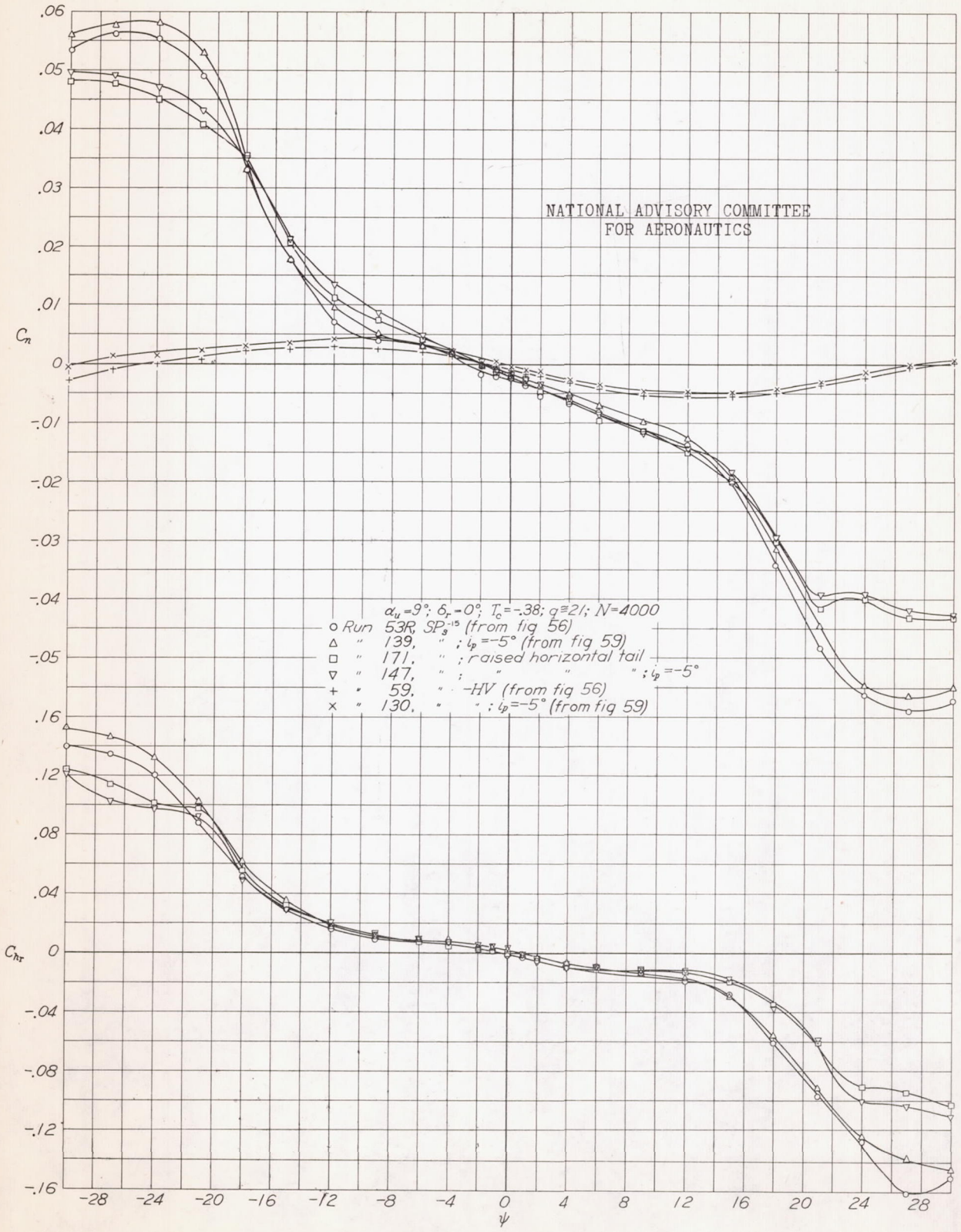

Figure 68.- Effect of configuration on characteristics of stability model in yaw, δ_r = 0°, α_u = 9°, T_c = -.38, single rotation, β = -15°.

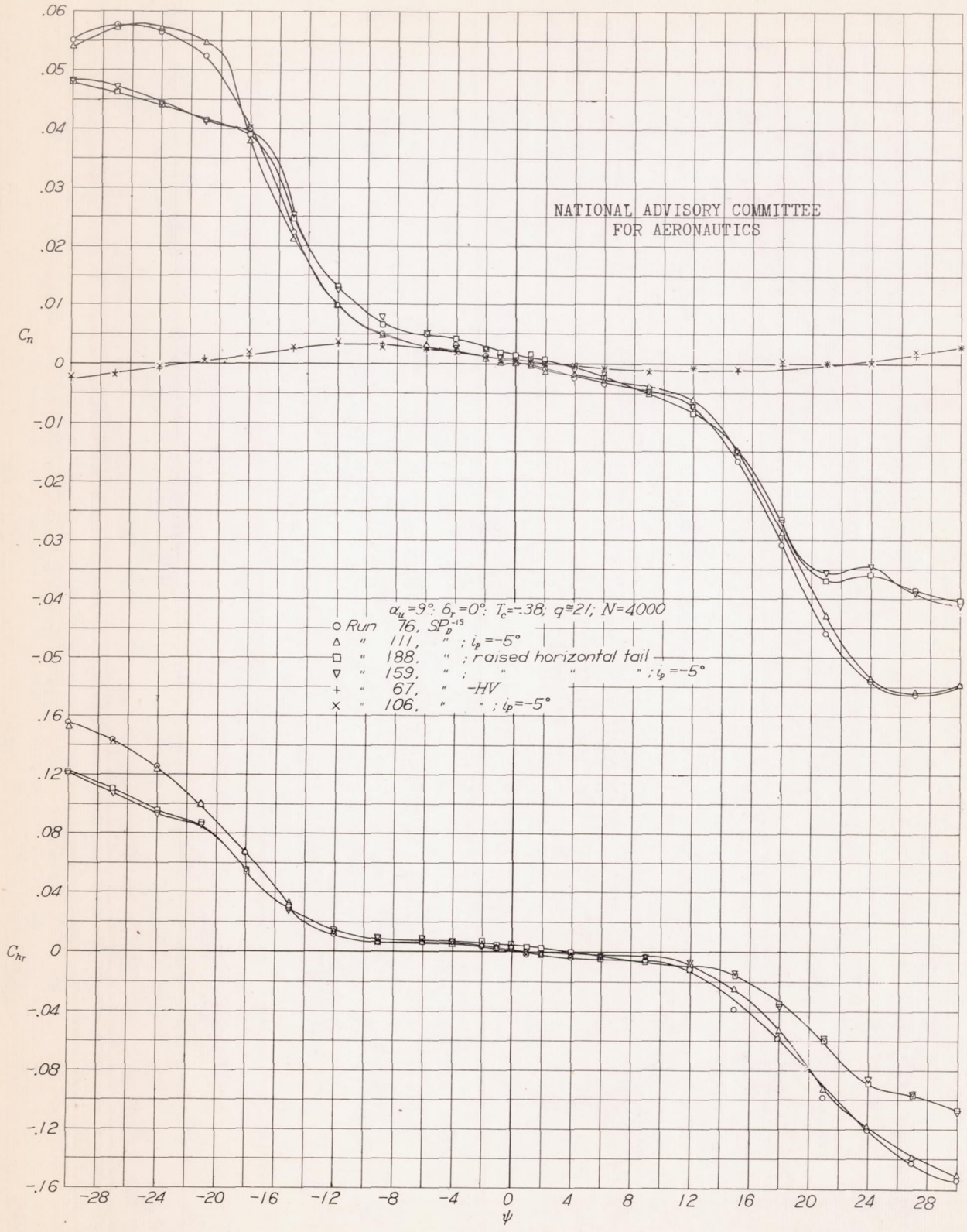

Figure 69.- Effect of configuration on characteristics of stability model in yaw, δ_r = 0°, α_u = 9°, T_c = -.38, dual rotation, β = -15°.

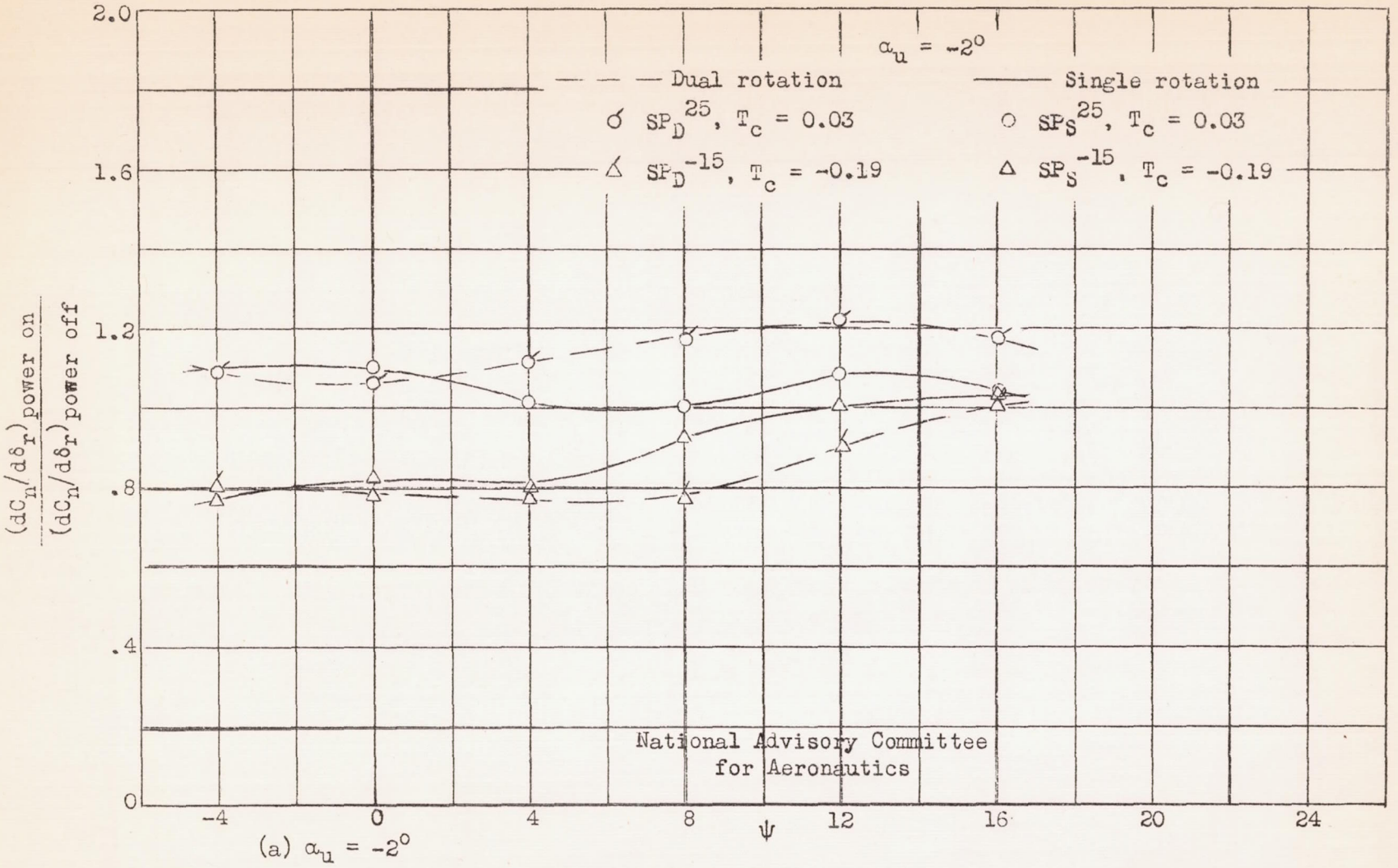

Figure 70.- Comparative effectiveness of the rudder for various power conditions. Stability model, basic configuration.

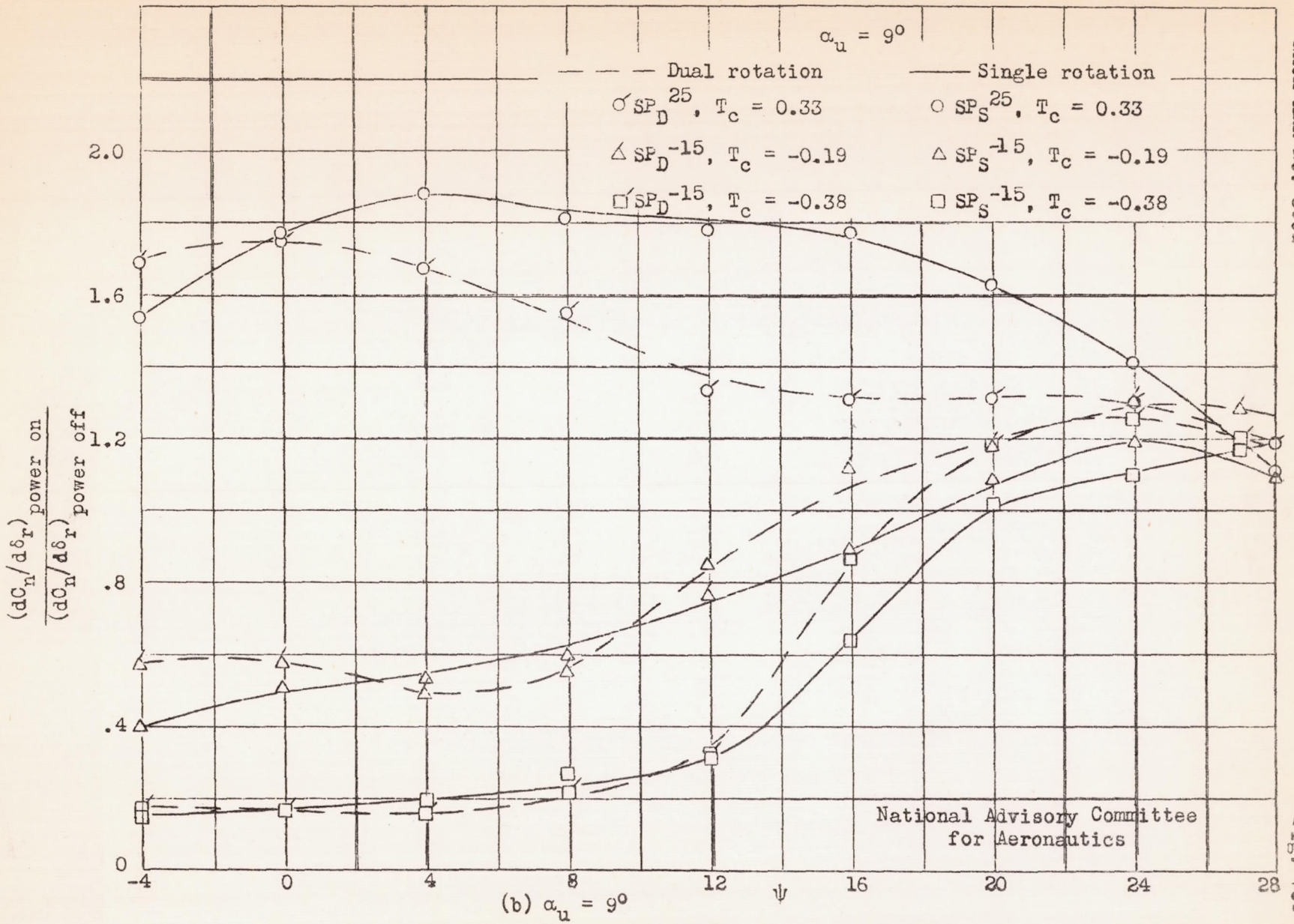

(b) α_u = 9°

Figure 70.- Concluded. Stability model.

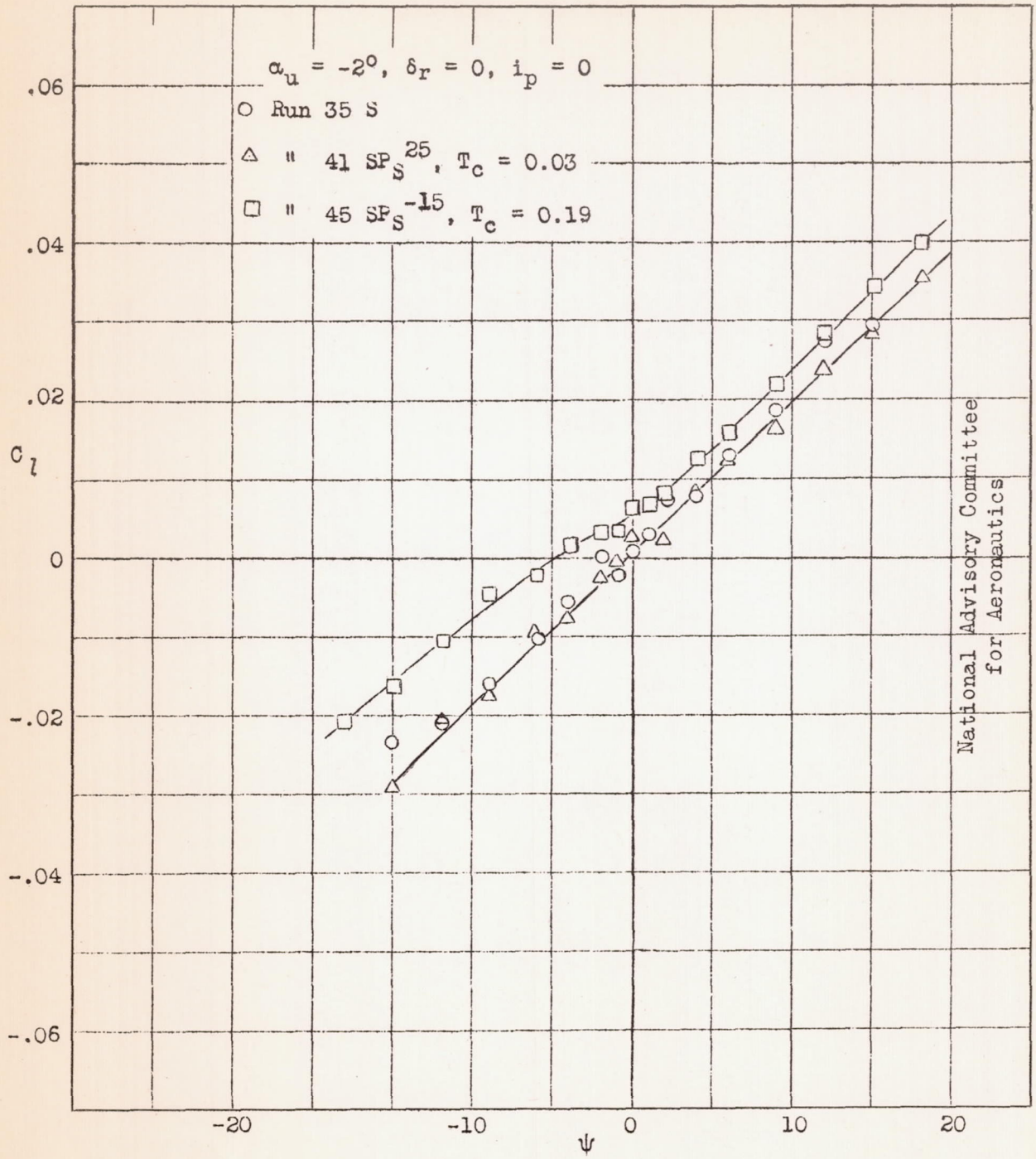

Figure 71.- Effect of power on the rolling moment of the stability model in yaw, $\alpha_u = -2^\circ$, $T_c = 0.03$ and -0.19, single rotation, $\beta = 25^\circ$ and -15°.

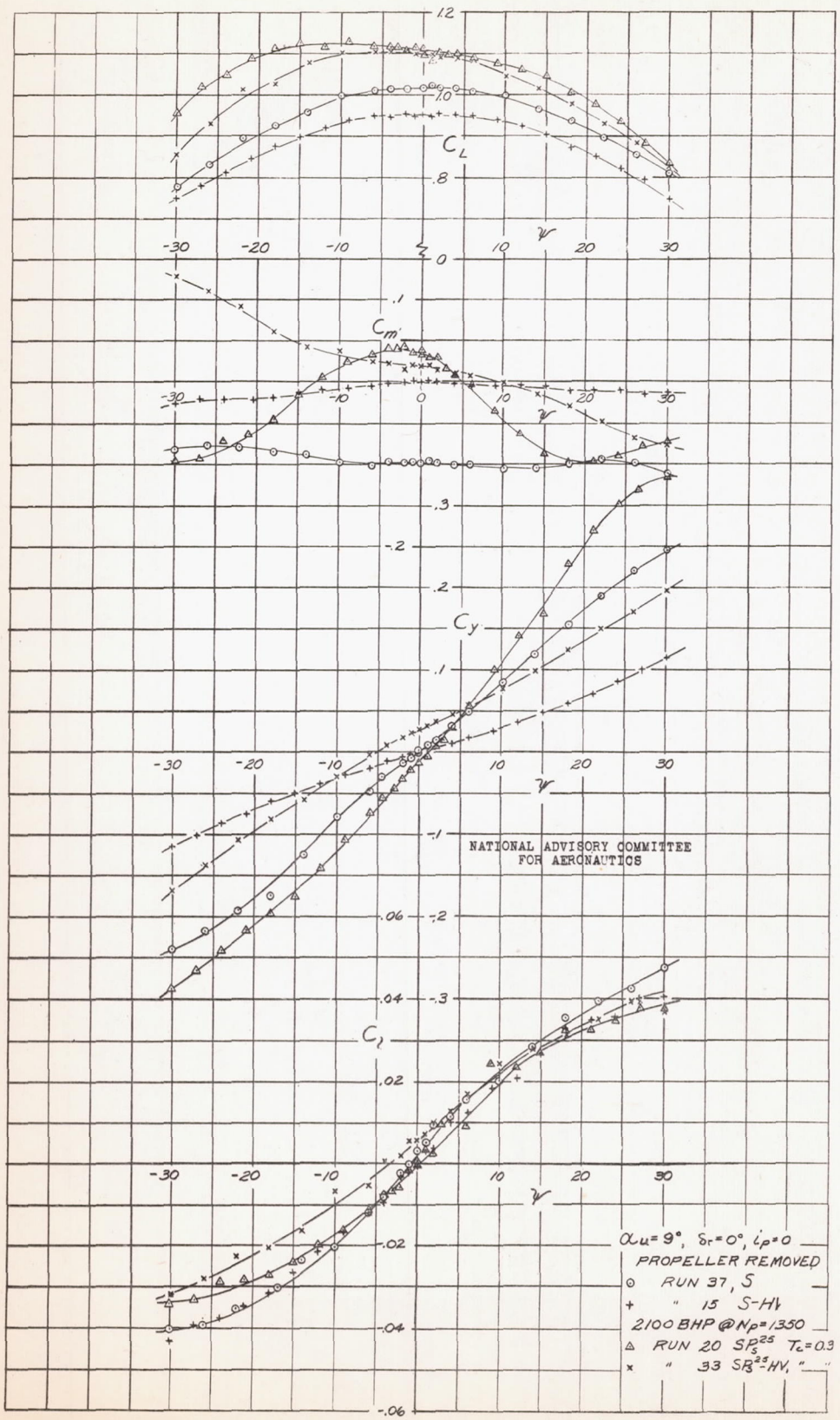

FIGURE 72.- EFFECT OF POWER ON THE CHARACTERISTICS OF THE STABILITY MODEL IN YAW. $\alpha_u = 9°$, $T_c = 0.33$, SINGLE ROTATION, $\beta = 25°$.

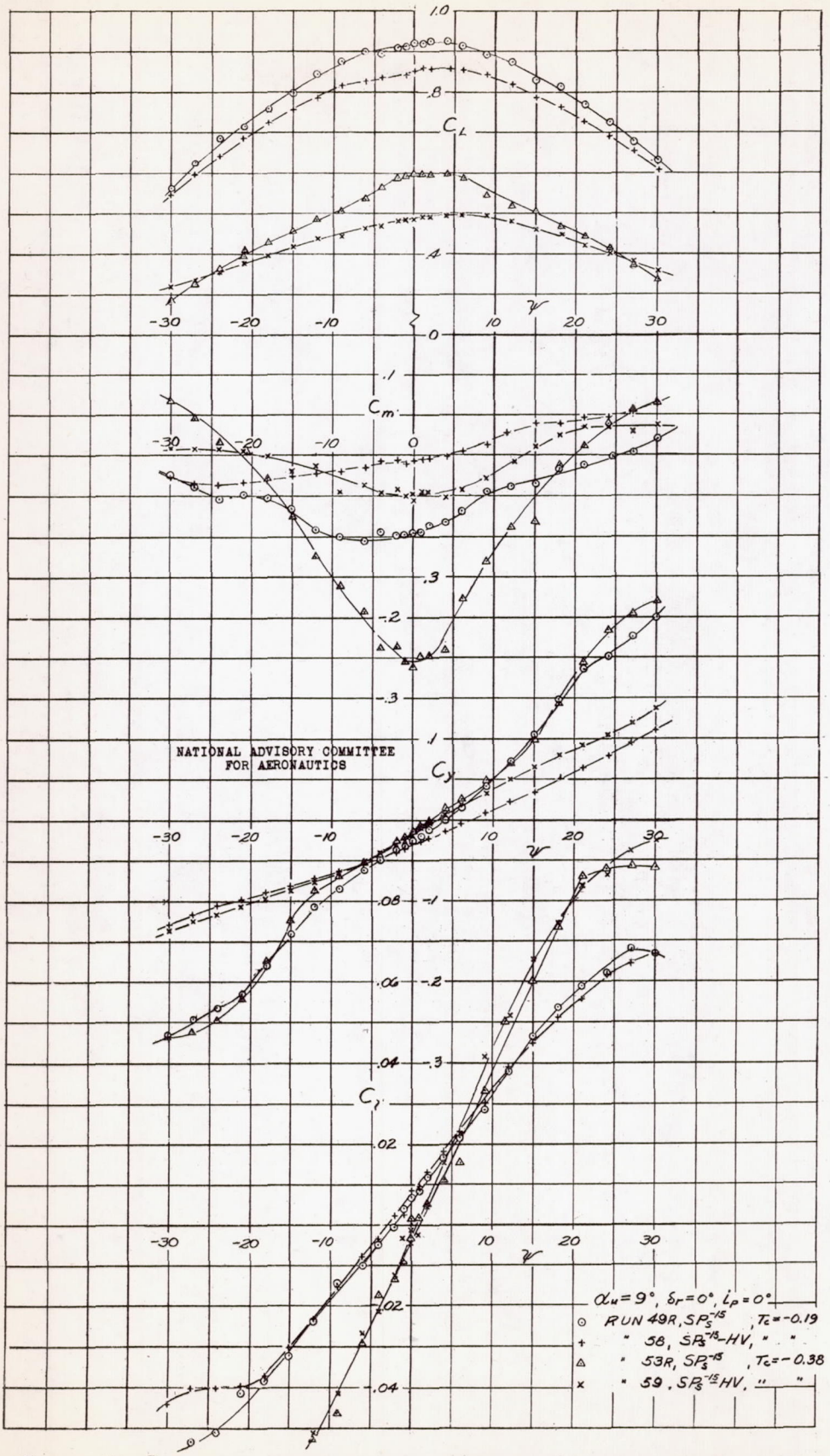

FIGURE 73.- EFFECT OF POWER ON THE CHARACTERISTICS OF THE STABILITY MODEL IN YAW. $\alpha_u = 9°$, $T_c = -0.19$ AND -0.38, SINGLE ROTATION, $\beta = -15°$.

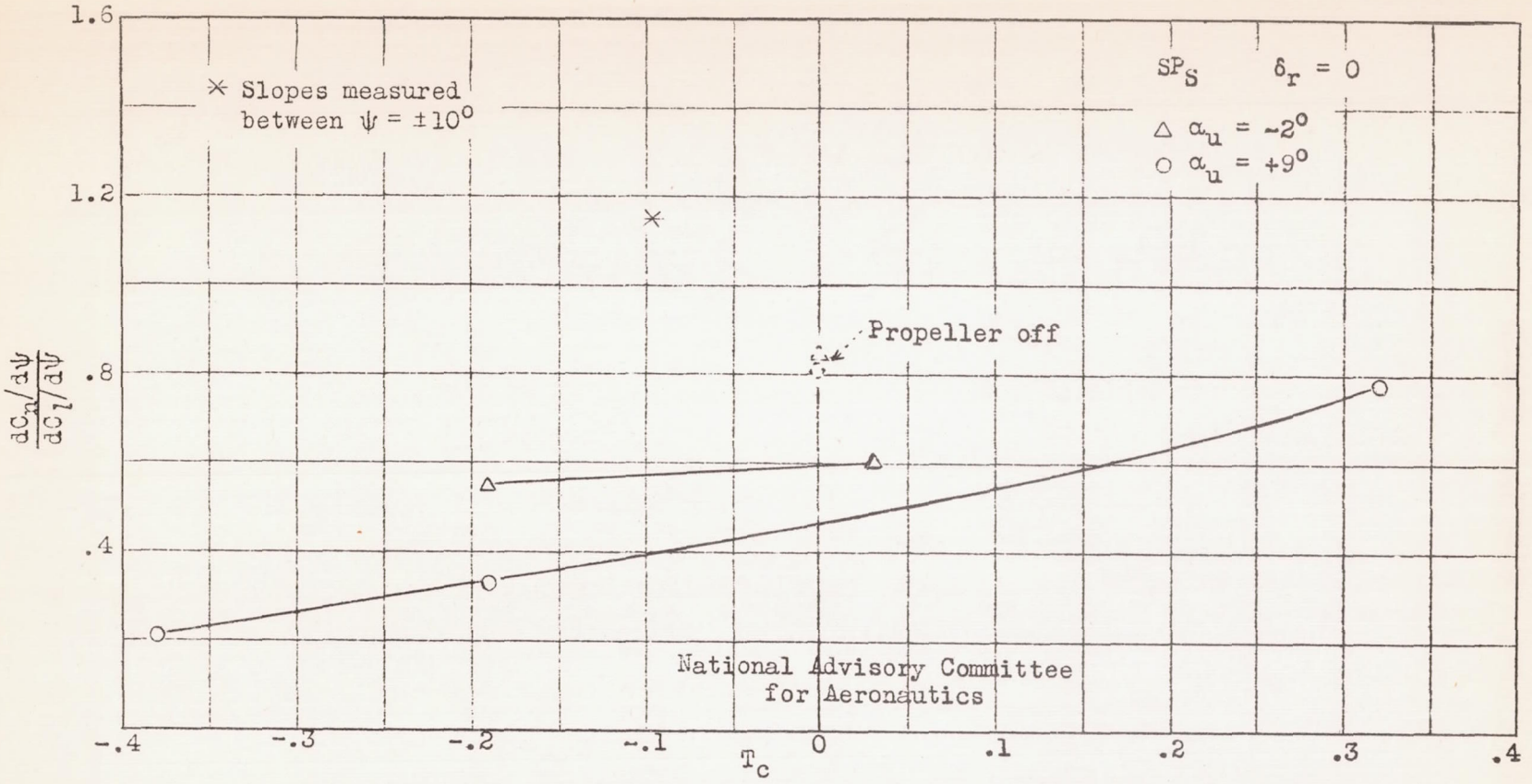

Figure 74.- Effect of thrust coefficient on the lateral-directional correspondence of the stability model in the basic configuration.